Feedback systems for the quality of chest compressions during cardiopulmonary resuscitation

by

Digna María González Otero

Supervisors:

Jesús Ruiz Ojeda

Sofía Ruiz de Gauna Gutiérrez

Submitted in partial fulfillment
of the requirements for the degree
of doctor of science

Universidad del País Vasco
Euskal Herriko Unibertsitatea

Department of Communications Engineering

Bilbao, October 2015

Dedicated to my parents, for their endless support.

To my little brother, who makes everything more fun.

Abstract

Sudden cardiac arrest is defined as the sudden cessation of the mechanical activity of the heart, confirmed by the absence of signs of circulation. Two actuations are key for patient survival after cardiac arrest: early cardiopulmonary resuscitation (CPR) and early defibrillation. CPR consists in applying chest compressions and ventilations to the patient to artificially maintain a minimal flow of oxygenated blood to the vital organs.

The quality of chest compressions is related to patient's survival. For that reason, resuscitation guidelines recommend the use of feedback devices that monitor CPR performance in real-time. These devices are usually placed between the chest of the patient and the rescuer's hands, and guide the rescuers towards the target compression depth and rate.

This thesis explores new alternatives to provide feedback on the quality of chest compressions during CPR. Two strategies were studied: the use of the transthoracic impedance (TTI) signal, which is acquired by current defibrillators through defibrillation pads, and the use of the chest acceleration, which could be acquired using an extra pad.

First we assessed the feasibility of using the TTI signal to provide feedback on chest compression depth and rate. Chest compressions induce fluctuations in the TTI signal. We studied the characteristics of the TTI fluctuations in out-of-hospital cardiac arrest episodes. In humans, these fluctuations vary widely between patients, and also depending on the rescuer along the resuscitation attempt. When a wide variety of patients and rescuers were included, TTI could not be used to estimate chest compression depth. However, we developed a new method which accurately calculates chest compression rate based on the analysis of the TTI signal. Three different databases of out-of-hospital cardiac arrest were used to ensure the generalizability of the results.

Second we developed three methods to provide feedback on chest compression depth and rate based solely on the chest acceleration signal. The accuracy of the methods was evaluated using episodes

of simulated cardiac arrest with a resuscitation manikin. One of the methods, based on the spectral analysis of the acceleration (SAA), presented a particularly high accuracy in a wide range of conditions. This method is very novel, and it does not infringe any existing patents.

Finally, we evaluated the behavior of the SAA method in three challenging scenarios: when CPR was performed on a soft surface such as a mattress; when the accelerometer was fixed to the rescuer's back of the hand, to the wrist, or to the forearm, instead of being placed on the chest of the patient; and when CPR was performed in a moving long-distance train. In this last scenario, for the first time, the performance of two commercial feedback devices, CPRmeter and TrueCPR, was also analyzed.

Resumen

Se define la parada cardiorrespiratoria como la detención súbita de la actividad mecánica del corazón, confirmada por la ausencia de signos de circulación. En caso de parada cardiorrespiratoria, dos actuaciones son clave para la supervivencia del paciente: la reanimación cardiopulmonar (RCP) precoz, y la desfibrilación precoz. La RCP consiste en proporcionar compresiones torácicas y ventilaciones al paciente para mantener un mínimo flujo de sangre oxigenada a los órganos vitales.

La calidad de las compresiones está relacionada con la supervivencia del paciente. Por esta razón las guías de resucitación recomiendan el uso de sistemas de *feedback* que monitorizan la calidad de la RCP en tiempo real. Estos dispositivos se sitúan generalmente entre el pecho del paciente y las manos del rescatador, y guían al rescatador para ayudarle a alcanzar la profundidad y frecuencia de compresión objetivo.

Esta tesis explora nuevas alternativas para monitorizar la calidad de las compresiones durante la RCP. Se han seguido dos estrategias: usar la señal de impedancia transtorácica (ITT), que es adquirida por los desfibriladores actuales a través de los parches de desfibrilación, y usar la aceleración del pecho, que podría ser registrada usando un dispositivo adicional.

En primer lugar se estudió la viabilidad del uso de la ITT para monitorizar la profundidad y frecuencia de las compresiones. Las compresiones torácicas inducen fluctuaciones en la señal de ITT. Tras analizar las características de estas fluctuaciones en episodios de parada cardiorrespiratoria extrahospitalaria, se concluyó que en humanos estas fluctuaciones varían mucho dependiendo del paciente, y también a lo largo de un mismo episodio de resucitación dependiendo del rescatador. Cuando se incluyeron una gran variedad de pacientes y rescatadores, la ITT no permitió estimar la profundidad de las compresiones de forma fiable. Sin embargo, sí se desarrolló un método para calcular la frecuencia de las compresiones mediante el análisis de la ITT. Para asegurar que

los resultados fueran generalizables, se usaron tres bases de datos de parada cardiorrespiratoria extrahospitalaria.

En segundo lugar desarrollamos tres métodos para monitorizar la profundidad y frecuencia de las compresiones basados únicamente en la señal de aceleración del pecho. La precisión de estos métodos se evaluó usando episodios de parada cardiorrespiratoria simulada con un maniquí de resucitación. Uno de los métodos, basado en el análisis espectral de la señal de aceleración (AEA), destacó por su alta precisión en una gran variedad de condiciones. Este método es muy novedoso, y no infringe ninguna patente existente.

Finalmente, evaluamos el comportamiento del método AEA en tres situaciones adversas: cuando se realiza la RCP en una superficie blanda, tal como un colchón; cuando el acelerómetro se sitúa en el dorso de la mano, en la muñeca o en el antebrazo del rescatador, en lugar de sobre el pecho del paciente; y cuando la RCP se realiza en un tren de larga distancia en movimiento. En este último escenario, se evaluó también por primera vez el rendimiento de dos sistemas de *feedback* comerciales, CPRmeter y TrueCPR.

Laburpena

Bat-bateko bihotz-geldiketa deritzo bihotzaren funtzio mekanikoa eteteari, zirkulazio zantzuen ezak baieztaturik. Bat-bateko bihotz-geldiketan, bi ekintza hauek ezinbestekoak dira pazienteen biziraupenerako: bihotz-biriketako berpizte (BBB) goiztiarra eta desfibrilazio goiztiarra. BBBa bularreko sakada eta aireztapenetan oinarritzen da, eta odol oxigenatuaren zirkulazio minimoa bermatzen du bizitzarako ezinbestekoak diren organoetan.

Bularreko sakaden kalitatea lotuta dago pazienteen biziraupenarekin. Horregatik, berpizte-gida internazionalek BBB-kalitatea denbora errealean neurtzen duten berrelikadura-gailuen erabilera gomendatzen dute. Gehienetan, gailu horiek pazientearen bularraren eta erreskatatzailearen eskuen artean jartzen dira, eta erreskatatzailea gidatzen dute, gomendatutako maiztasunean eta sakontasunean eman ditzan sakadak.

Tesi honetan, BBBko sakaden kalitatearen berrelikadura sistemetarako aukera berriak proposatzen dira. Bi estrategia aztertu dira: bularreko inpedantzia-seinalea (BI seinalea) erabiltzea, gaur egungo desfibrilagailuetan desbifrilazio elektrodoen bidez eskutatzen dena; eta bularreko azelerazio-seinalea erabiltzea, kuxin gehigarri bat erabiliz eskuratzen dena.

Hasteko, BI seinalea erabiltzearen bideragarritasuna aztertu da, sakaden maiztasun eta sakontasunaren berrelikadura emateko. BI seinalearen gorabeheren ezaugarriak aztertu dira ospitalez kanpoko bihotz-geldiketako kasuetan. Gizakietan gorabehera horiek oso aldakorrak dira paziente batetik bestera, baita erreskatatzaileen artean ere, berpizte-saiakeran zehar. Paziente eta erreskatatzaile asko aztertuta frogatu da BI seinaleak ez zuela balio sakontasunaren berrelikadura emateko. Bestetik, sakaden maiztasuna era fidagarrian neurtzeko, BI seinalean oinarrituta metodo berri bat garatu da. Emaitzak orokorrak direla bermatzeko, hiru ospitalez kanpoko bihotz-geldiketen datu-baseak erabili dira.

Ondoren, azelerazio-seinalean soilik oinarritutako hiru metodo garatu dira, sakaden maiztasunaren eta sakontasunaren berrelikadurako. Metodoen zehaztasuna aztertu da, BBB berpiztea maniki

batean simulatuz. Horietatik, azelerazioaren espektro-analisian (AEA) oinarritutakoa oso zehatza da lan-baldintza askotarako. Oso metodo berritzailea da, eta ez du gaur egungo patenterik hausten.

Bukatzeko, AEA metodoaren konportamoldea aztertu da hiru baldintza zailetan: BBBa gainazal bigun baten gainean egiten denean, koltxoi baten kasu; azelerometroa erreskatatzailearen esku gainean, eskumuturrean edo besaurrean jartzen denean, pazientearen bularrean jarri ordez; eta BBBa mugitzen ari den distantzia luzeko tren batean egiten denean. Azken egoera honetan, CPRmeter eta TrueCPR gailu komertzialen zehaztasuna aztertu da lehenengo aldiz.

Resumo

Defínese a parada cardiorrespiratoria como a detención repentina da actividade mecánica do corazón, confirmada pola ausencia de sinais de circulación. No caso de parada cardiorrespiratoria, dúas actuacións son clave para a supervivencia do doente: a reanimación cardiopulmonar (RCP) precoz e a desfibrilación precoz. A RCP consiste en proporcionar compresións torácicas e ventilacións ó doente para manter un mínimo fluir sanguíneo osixenado ós órganos vitais.

A calidade das compresións está relacionada coa supervivencia do doente. Por esta razón as guías de resucitación recomendan o uso de sistemas de *feedback* que monitorizan a calidade da RCP en tempo real. Estes dispositivos sitúanse xeralmente entre o peito do paciente e as mans do rescatador, e guían ó rescatador para axudarlle a acadar a profundidade e frecuencia de compresión obxectivo.

Esta tese explora novas alternativas para monitorizar a calidade das compresións durante a RCP. Seguíronse dúas estratexias: usar o sinal de impedancia transtorácica (ITT), que é adquirida polos desfibriladores actuais a través dos parches de desfibrilación, e usar a aceleración do peito, que podería ser rexistrada usando un dispositivo adicional.

En primeiro lugar estudouse a viabilidade do uso da ITT para monitorizar a profundidade e frecuencia das compresións. As compresións torácicas inducen fluctuacións no sinal de ITT. Despois de analizar as características destas fluctuacións en episodios de parada cardiorrespiratoria extrahospitalaria, concluíuse que en humanos estas fluctuacións varían moito dependendo do doente, e tamén ó longo dun mesmo episodio de resucitación dependendo do rescatador. Cando se incluíron unha gran variedade de doentes e rescatadores, a ITT non deixou estimar a profundidade das compresións de forma fiable. Con todo, si se desenvolveu un método para calcular a frecuencia das compresións mediante a análise da ITT. Para asegurar que os resultados fosen xeneralizables, usáronse tres bases de datos de parada cardiorrespiratoria extrahospitalaria.

En segundo lugar deseñamos tres métodos para monitorizar a profundidade e frecuencia das compresións baseados unicamente no sinal de aceleración do peito. A precisión destes métodos avaliouse usando episodios de parada cardiorrespiratoria simulada cun boneco de resucitación. Un dos métodos, baseado na análise espectral do sinal de aceleración (AEA), destacou pola súa alta precisión nunha gran variedade de condicións. Este método é moi novo, e non infrinxe ningunha patente existente.

Finalmente, avaliamos o comportamento do método AEA en tres situacións adversas: cando se realiza a RCP nunha superficie branda, tal coma un colchón; cando, no canto de poñer o acelerómetro sobre o peito do doente, este se sitúa no dorso da man, na boneca ou no antebrazo do rescatador; e cando a RCP se realíza nun tren de longa distancia en movemento. Neste último escenario, avaliouse tamén por primeira vez o rendemento de dous sistemas de feedback comerciais, CPRmeter e TrueCPR.

Acknowledgments

This thesis is the culmination of four years of work. I would like to thank all the people who inspired me to follow this path, those who helped me along the way, and those who brightened up the journey.

First of all I want to thank my supervisors, Jesus and Sofía. Words cannot express how I feel. Thanks for your commitment, for your tireless efforts, and for all the shared moments. With you, even the hard times were good times. Jesus, thanks for sharing your intuitive insight and perception, and for always taking the time to explain things in simple terms. Sofía, thanks for your hard work, always with that calm and reassuring attitude. Thanks for introducing me to the field of resuscitation so many years ago.

To all the members of the GSC group, thanks for the company and for the technical support. Thanks to Eli and Unai for all the shared work in the field of resuscitation. A special mention to Julio, who inspired me to start this journey, and whose cheerful character makes the laboratory a livelier working place. To Andoni; you will always live in our memories. To Unai and Erik, who already finished; to Izaskun and Koldo, who are almost there; and to Bea, who is just starting. It was a pleasure to share this experience with all of you.

I am grateful to the Basque Government for supporting me economically these four years, and to all the institutions that funded our research projects: the Ministry of Economy and Competitiveness, the Basque Government, the University of the Basque Country (UPV/EHU), and Osatu SCoop (Bexen cardio). Thanks to Félix from Osatu for giving us interesting problems to work on; to Silvia, for her energy and enthusiasm; and to Elena, for sharing the implementation process with me. Thanks for turning ideas into products.

I thank all the researchers who participated in the studies presented in this thesis: Jim Russell, Trygve Eftestøl, Jo Kramer-Johansen, Mohamud Daya, and Lars Wik. Thanks for your willingness to cooperate. Thanks to Riccardo Barbieri for kindly hosting me in his research lab in Boston.

Thanks to Jesus, Sofía, and Unai for the opportunity to teach with them, and to all the students who collaborated with our research group; you really enriched my experience. Thanks to all the volunteers who participated in the recording sessions with the manikin.

To my friends, for all the moments together. For the coffees, the concerts, the laughs, and for those few but wonderful days on the beach.

Dedicated to my parents, Carmen and José, who gave me everything. To Cristian, my little brother and best friend.

— *Digna González*

Contents

List of Figures

List of Tables

List of Acronyms

AED	Automated external defibrillator
AHA	American Heart Association
ALS	Advanced life support
AUC	Area under the curve
BLS	Basic life support
cpm	Compressions per minute
CPR	Cardiopulmonary resuscitation
ECG	Electrocardiogram
EMS	Emergency medical services
ERC	European Resuscitation Council
FFT	Fast Fourier transform
HSFC	Heart and Stroke Foundation of Canada
ILCOR	International Liaison Committee on Resuscitation
OHCA	Out-of-hospital cardiac arrest
PEA	Pulseless electrical activity
PPV	Positive predictive value
PR	Pulse-generating rhythm
RMSE	Root mean square error
ROC	Resuscitation Outcome Consortium
Se	Sensitivity
Sp	Specificity
TTI	Transthoracic impedance
TVF&R	Tualatin Valley Fire & Rescue
VF	Ventricular fibrillation
VT	Ventricular tachycardia

Albert grunted. "Do you know what happens to lads who ask too many questions?"
Mort thought for a moment. "No," he said eventually, "what?"
There was silence.
Then Albert straightened up and said, "Damned if I know. Probably they get answers, and serve 'em right."

— Terry Pratchett. Mort.

1 Introduction

Time is life itself, and life resides in the human heart.

— Michael Ende. *Momo.*

This chapter provides a description of the context in which this thesis work was developed. Section 1.1 presents the concept of cardiac arrest and the steps that should be followed to treat cardiac arrest victims. These steps are represented by the metaphor of the chain of survival, which is composed of four links. Emphasis is put on two of them, particularly determinant for survival: cardiopulmonary resuscitation (CPR), described in Section 1.2, and defibrillation, described in Section 1.3. Section 1.4 covers the transthoracic impedance (TTI) signal, acquired by most external defibrillators. Then, in Section 1.5 systems to monitor the quality of chest compressions during CPR and to provide feedback to the rescuers are presented. The chapter concludes with a description of the objectives of this thesis work.

1.1 Cardiac arrest

Sudden cardiac death is a dramatic event defined as the sudden, unexpected death caused by cardiopulmonary arrest in a person with functional vital organ systems.[128] Cardiac arrest usually results from an electrical disturbance in the heart that disrupts its mechanical action, stopping blood flow.

The heart is responsible for pumping blood rhythmically through the blood vessels. It comprises two upper low-pressure chambers called atria that pick-up the blood, and two lower high-pressure chambers called ventricles from which blood is pumped out. For an effective blood pumping function, the cardiac muscle must contract in an organized way. This contraction is triggered by an electric impulse generated in the heart and propagated through a complex conduction system. The electrical activity of the heart can be recorded by electrodes placed on the body surface. The acquired signal is called

electrocardiogram or ECG, and its analysis provides information about the cardiac function. Figure 1.1 shows a segment of an ECG of a healthy person with a normal sinus rhythm.

Figure 1.1: ECG of a healthy person with a normal sinus rhythm.

Most cardiac arrests occur in out-of-hospital settings,[29] and as a first clinical event of heart disease.[108] Four rhythms are associated with an absence of circulation: ventricular fibrillation (VF), pulseless ventricular tachycardia (VT), pulseless electrical activity (PEA), and asystole.[75] The mechanism for the majority of cardiac arrest is VT degenerating to VF.[37,39,160] During VF, the ventricular muscle is thrown into a state of irregular arrhythmic contraction, the ventricles rapidly depolarize and repolarize, and the heart stops pumping blood efficiently. The only effective way to terminate VF and to restore a perfusing cardiac rhythm is defibrillation, procured through the delivery of an electrical shock to the heart.[22] However, as time elapses, VF will gradually deteriorate into asystole, the absence of electrical activity of the heart, and the probability of a successful resuscitation will decrease.

The precise incidence of out-of-hospital cardiac arrest (OHCA) is unknown and estimates vary depending on the inclusion criteria,[112] but data obtained from 37 European countries indicate that it is around 38 per 100 000 population every year.[11] Taking into account European population records in 2015 (almost 507 000 000 persons[1]), this implies more than 190 000 cardiac arrests annually only in Europe.

Survival rates are about 10 % for all rhythms, but increase to about 20 % for VF cardiac arrest.[11,113] However, reported outcomes

1 Data source: European Commission, Eurostat.

vary widely depending on the study and on the geographic region, ranging from less than 2% in some rural and urban areas to more than 20% in certain cities with dedicated quality assurance programs.[20,48] This variation is caused in part by regional differences in the availability and quality of emergency protocols and cardiac care interventions.

Organizations such as the European Resuscitation Council (ERC), the American Heart Association (AHA), the Heart and Stroke Foundation of Canada (HSFC), and resuscitation councils in other parts of the world publish guidelines with recommendations for optimal treatment of cardiac arrest. In 1992 the International Liaison Committee on Resuscitation (ILCOR) was formed to allow cooperation between the different resuscitation councils worldwide. Since 2000, researchers from the ILCOR have identified and reviewed international science and knowledge in 5-year cycles to achieve a consensus on the science of resuscitation. This consensus permits the definition of similar evidence-based practices to be used all over the world, although local, regional and national adaptations may be required to account for differences in the availability of drugs, equipment, and personnel.

The ILCOR promulgates the concept of the *chain of survival*, (see Figure 1.2), a metaphor established by the American Heart Association (AHA) in the early 1990s to describe the sequence of actions linking the victim of OHCA with survival.[36] It consists of four independent links: early activation of the emergency medical services (EMS) system, early CPR, early defibrillation, and early advanced cardiac care.

- *Early access*: The first link of the chain comprises the early recognition of the symptoms either by the person suffering the cardiac arrest or by a witness and the call for help, that is, the activation of the emergency services so that they arrive to the scene as soon as possible.
- *Early cardiopulmonary resuscitation*: CPR consists of cycles of chest compressions and ventilations delivered to the patient to artificially maintain a minimal flow of oxygenated blood to the vital organs. This second link refers to bystander CPR, provided by laypeople before the arrival of the emergency

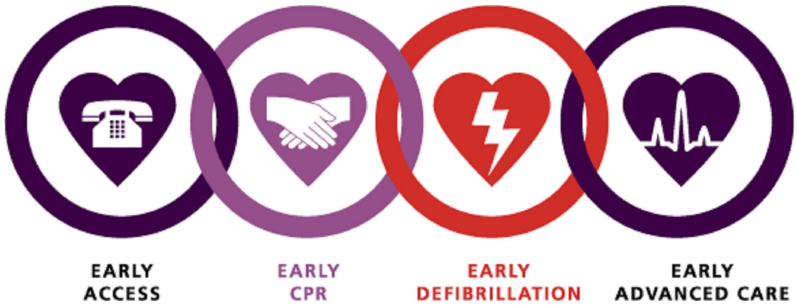

Figure 1.2: The chain of survival and its four links: early access, early CPR, early defibrillation, and early advanced care. Source: ERC guidelines 2010.[91]

services personnel. Early CPR reduces no-flow time, which improves neurological outcome. Immediate CPR has also shown to increase survival rates, sometimes even twofold or threefold.[76,77,156,167]

- *Early defibrillation*: Defibrillation consists in the passage of electrical current through the myocardium to terminate certain arrhythmias. It is indicated in case of pulseless VT or VF, which are called shockable rhythms.[86] In out-of-hospital settings, defibrillation is normally procured using an automated external defibrillator (AED). AEDs are portable simple-to-operate devices that analyze the victim's ECG to determine whether a shockable rhythm is present. When an AED detects a shockable rhythm, it charges the capacitors and then prompts the rescuer to press a shock button to deliver an electrical shock. If a non-shockable rhythm is detected, the device prompts the rescuer to continue CPR for another 2 min, after which another rhythm analysis will be performed.

- *Early advanced care*: The last critical link in the management of cardiac arrest is the treatment provided by qualified health care personnel, including medication and intubation. More recently, new interventions for postresuscitation care, such as therapeutic hypothermia, have been developed. These interventions are targeted at preserving brain and heart function, and have shown to improve patient outcomes.[111,149]

The four links of the chain of survival are important, but two of these interventions are pivotal for a successful outcome of the patient: early CPR and early defibrillation.[99,156] When no CPR is provided, for every minute delay in defibrillation, survival from witnessed VF decreases by 10–12 %.[124,156] On the contrary, if bystander CPR is provided, the decline is more gradual, and averages 3 % to 4 %.[99,159,160] The data shown in Table 1.1 summarize the importance of reducing the time intervals from collapse to CPR and from collapse to defibrillation. Without CPR starting within 5 min and defibrillation occurring within 10 min, the chances of survival of the patient are virtually null.

Table 1.1: Percentage of survival to hospital discharge in OHCA, showing the influence of early CPR and early defibrillation.[35]

	Collapse to defibrillation	
Collapse to CPR	<10 min	>10 min
<5 min	37 %	7 %
>5 min	20 %	0 %

1.2 Cardiopulmonary resuscitation

CPR has been taught to professionals since the late 1960s and to the lay public since the early 1970s.[146] It consists in applying chest compressions and ventilations to the patient to artificially maintain a minimal flow of oxygenated blood to the vital organs. Immediate CPR is important for two reasons: it maintains some degree of cerebral perfusion, necessary for the preservation of brain function and to prevent brain death, and it generates myocardial blood flow, which is related to the restoration of cardiac function after cardiac arrest and improves the heart's ability to regain a perfusing rhythm.

The mechanism by which external chest compressions generate blood flow is not clear. Three main hypothesis have been proposed:[71] direct cardiac compression (heart pump model), the increase of intrathoracic pressure (chest pump model), and a combination of both. In the *heart pump model*, it is postulated that chest compression

causes the ventricles to be compressed between the sternum and the vertebral column. It is assumed that during chest compression blood is squeezed from the heart into arterial circulation, and that with the release of the compression, the heart would expand and fill with blood. In the *chest pump model*, it is postulated that chest compression increases intrathoracic pressure, which is transmitted to intrathoracic vasculature. This high pressure would cause blood to flow out of the thorax with chest compression.

Resuscitation guidelines describe how CPR should be provided, both in basic life support (BLS) and in advanced life support (ALS) settings. BLS refers to the variety of non-invasive emergency procedures performed to assist in the immediate survival of a patient, and it is typically provided by first responders until the victim can be given full medical care.[31] ALS techniques comprise those interventions and procedures that would require physician's orders, if not the physicians themselves, to be delivered.[164]

Current resuscitation guidelines for BLS indicate that when a cardiac arrest is recognized in an adult, all rescuers, trained or not, should provide chest compressions.[91] The rescuer should kneel by the side of the victim, and compressions should be provided in the center of chest, applying the pressure with the heel of the hand, as illustrated in Figure 1.3. Trained rescuers should also provide ventilations (mouth-to-mouth rescue breaths), alternating series of 30 chest compressions with 2 ventilations. They should open the airway using head tilt and chin lift, pinch the soft part of the nose closed, and blow steadily into the mouth. CPR should be continuously administered until an AED is available. Then, the AED should be attached to the patient and, after an initial rhythm assessment, CPR should be provided in 2-min cycles, with pauses in between for rhythm analysis.

In ALS settings, personnel skilled in advanced airway management should attempt laryngoscopy and intubation, minimizing interruptions of chest compressions during the process. After intubation, the patient should be ventilated at 10 breaths per minute, and continuous chest compressions should be provided at a rate of 100 cpm, without pausing during ventilations. Rhythm should be assessed every 2 min.

Guidelines emphasize the importance of the quality of chest compressions. Optimal chest compression technique comprises:

Figure 1.3: Positioning of the rescuer to provide chest compressions during CPR. Source: ERC guidelines 2010.[91]

- Compressing the chest at a rate of at least 100 compressions per minute (cpm), but not more than 120 cpm,[2]
- achieving a depth of at least 5 cm (but not more than 6 cm),
- allowing a complete chest recoil between compressions,
- and minimizing interruptions in chest compressions.

There is strong evidence that the quality of chest compressions is related to the chance of successful defibrillation. Adequate rate[80], depth[45,95], chest recoil between compressions[12,168] and minimal interruptions[47] improve the effectiveness of CPR. However, studies on CPR quality have shown that delivering high quality chest compressions is difficult both for laypeople[57] and for well trained rescuers.[2,55,95,114,166] Pauses between compressions are very frequent, compressions are often too shallow, and there is a tendency to provide too fast chest compressions. Monitoring and feedback devices can improve skill acquisition and retention during training.[169] They can

2 AHA 2010 guidelines do not establish an upper limit for the rate of chest compressions.[75]

also improve CPR quality during resuscitation episodes[69,130,134], and their use is encouraged by resuscitation guidelines.[91]

1.3 Defibrillation

CPR artificially maintains blood flow and extends the window of opportunity to perform more advanced live-saving procedures, but it cannot by itself restore a perfusing rhythm in the majority of victims of cardiac arrest; it is also necessary to defibrillate.

Defibrillation consists in delivering an electrical current to the cardiac muscle to terminate certain life-threatening arrhythmias. It is the single most important factor in surviving cardiac arrest due to VF. To be effective, the electrical shock should have enough magnitude to depolarize a critical mass of the myocardium and restore the coordinated electrical activity of the heart.

The probability of successful defibrillation decreases with time. When untreated, VF gradually deteriorates,[161,162] going from an electric phase ($<$4 min) in which defibrillation is very effective, into a circulatory phase (4–10 min), in which it is recommended to provide artificial circulation before attempting defibrillation. Then, VF goes to a metabolic phase ($>$10 min), and it finally leads to asystole, the absence of electrical activity of the heart.

In ALS settings, that is, in hospitals or ALS ambulances, professional healthcare providers generally use **monitor/defibrillators**. These are sophisticated devices that have the ability to monitor different signals such as the ECG, transthoracic impedance (TTI), capnography (concentration of CO_2 in the respiratory gases), or pulse oximetry (oxygen saturation of arterial blood). They can also measure CPR quality parameters though CPR aid pads. Additionally, these devices can deliver external cardiac pacing and defibrillation. They are commonly used in manual mode, in which healthcare providers analyze the rhythm every 2 min and, using their medical knowledge, decide if an electrical shock is required. Most monitor/defibrillators can also function like AEDs. Figure 1.4 shows four monitor/defibrillators from different commercial brands. From left to right and from top to bottom, the first device is a Heartstart MRx (Philips Healthcare, Andover, MA), and in the picture it is connected to the defibrillation pads (left) and to a CPR aid

Figure 1.4: Monitor/defibrillators from different commercial brands. From left to right and from top to bottom: Heartstart MRx (Philips), Lifepak 15 (PhysioControl), R Series ALS (Zoll), Reanibex 800 (Bexen cardio).

pad for CPR feedback (right); the second device is a Lifepak 15 (PhysioControl, Redmond, WA); the third one is an R Series ALS defibrillator (Zoll Medical Corporation, Chelmsford, MA), and it is connected to the defibrillation pads and to a single-use CPR aid pad; the last device is a Reanibex 800 (Bexen cardio, Ermua, Spain), and it is connected to defibrillation paddles (not adhesive defibrillation pads) in the picture.

Most cardiac arrests occur out of hospital. The mean time until the arrival of the ambulances after activation of the emergency services varies widely between areas, but it is in many cases above the critical first 4 min.[128] It is thus necessary to implement programs for early defibrillation in the community. In 1995, the AHA promoted the concept of public access defibrillation.[163] They recommended to

make defibrillation accessible to the general public through the use of **AEDs**. AEDs are lighter and simpler to use than monitors, and they reliably guide the resuscitation procedure. Figure 1.5 shows some AED models from different companies: Philips, PhysioControl, Zoll, and Cardiac Science (Copenhagen, Denmark).

Figure 1.5: AEDs from different commercial brands. From left to right and from top to bottom: Heartstart OnSite HS1 (Philips), Lifepak CR Plus (PhysioControl), AED Plus (Zoll), Powerheart G3 Plus (Cardiac Science).

AEDs operate following four universal steps:

1. *Power on the AED:* This initiates voice (and in some cases visual) prompts that guide the user through subsequent steps.
2. *Attach defibrillation pads:* AEDs come with disposable self-adhesive defibrillation pads. They must be attached to the chest of the patient, preferably in the antero-lateral position. The correct position of the pads is often illustrated on the pads themselves or on another part of the AED. The pads are used to

continuously monitor the ECG signal, to acquire the TTI signal, and to deliver the electrical shock when required.

3. *Analyze the rhythm:* Once the pads are correctly attached, the AED automatically initiates the rhythm analysis. During this process, the rescuer should not touch the patient to avoid inducing motion artifacts on the ECG. The rhythm is analyzed by a shock advice algorithm that automatically detects if the victim presents a VF or a pulseless VT.
4. *Shock advised:* When the shock advice algorithm detects a lethal ventricular arrhythmia, the device prompts the user to provide an electrical shock. In case that other rhythms are detected, the device will ask the rescuer to resume CPR for another 2-min cycle, after which the cardiac rhythm will be reassessed.

Placement of AEDs in selected public settings for immediate use by trained laypersons has been a success. They are being used in casinos,[157] airports,[25] bus and railway stations,[26] shopping malls, sports facilities, and schools and universities. AEDs continue to be increasingly deployed in places with high risk of incidence (usually high-density public areas) or remote from any chance of conventional treatment, such as commercial aviation,[66,123,125] ships,[38,122] or long-distance trains.

Another strategy to reduce time to defibrillation consists in defining lay first-responder schemes. In this case, instead of using the AED close to where it is kept, it is transported to the emergency. Response times will generally be longer than for on-site defibrillation, but shorter than those achieved by conventional emergency services.[83,92] Responders can be volunteers from the community with training in AED use or, more frequently, non-healthcare professionals with a duty to respond, such as fire service or police forces.[165]

AEDs are also used by some healthcare professionals. They are particularly useful for BLS personnel or for physicians not routinely treating life-threatening emergencies, such as general practitioners. The main advantage of these devices is their simplicity and the minimal training required for an adequate use, as the clinical diagnosis of the cardiac rhythm is made by the AED itself. For this group of intended users **intermediate devices**, such as the ones

showed in Figure 1.6, are also available. These defibrillators can work in manual or AED mode and are usually compact and intuitive, but provide more functionality than AEDs. They can monitor and display several signals in the screen, which allows rescuers to adapt the therapy to the necessities of the patient without the complexity of monitor/defibrillators.

Figure 1.6: Intermediate defibrillators from different commercial brands. From left to right and from top to bottom: Lifepak 1000 (PhysioControl), AED Pro (Zoll), Powerheart AED G3 Pro (Cardiac Science), Reanibex 300 (Bexen cardio).

1.4 Transthoracic impedance

Defibrillators measure the ECG and the TTI signal through defibrillation pads. TTI represents the resistance of the thorax to current flow. It can be measured by passing an alternate current (I), usually 2–3 mA at 20–30 kHz, through the tissue and measuring the

voltage drop (V). Applying Ohm's law the impedance value (Z) can be computed: $Z = V / I$.

TTI is measured by defibrillators to check that the defibrillation pads are correctly attached to the chest of the patient. Figure 1.7 shows the recommended anterior-lateral position, with one pad placed below the right clavicle and the other one below the left axilla. An adequate skin-electrode contact is critical for two reasons: for a safe delivery of the electrical shock, and for a correct ECG acquisition, essential for a reliable rhythm analysis. Additionally, some devices use the TTI measurement to adjust the energy of the defibrillation pulse (impedance compensation).[90,100] The determining factor for successful defibrillation is energy with respect to impedance, and not energy alone. In order to minimize myocardial damage, shocks should be provided with the lowest amount of energy that will achieve defibrillation.

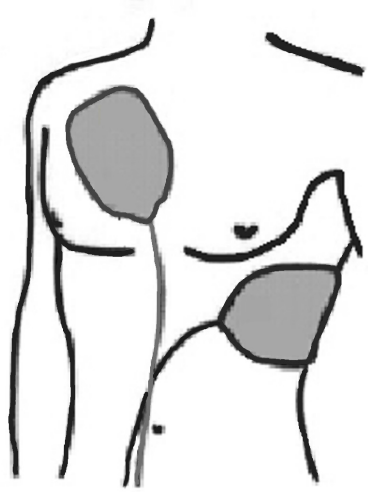

Figure 1.7: Antero-lateral position for self-adhesive defibrillation pads. Adapted from Krasteva et al.[97]

TTI is approximately 70–80 Ω in adults, but it varies considerably between subjects, with a range of 15 Ω to 150 Ω.[88,89] Baseline TTI is affected by several factors, summarized in Table 1.2. The most important one is chest size (patient dependent) and interelectrode distance. Electrode size also plays a determinant role; larger pads have lower impedance, but too large electrodes may reduce

transmyocardial current flow, as a greater proportion of the current may traverse extracardiac pathways.[40] Another element that influences TTI is the interface between the electrodes and the chest wall. In order to minimize impedance at the electrode-skin interface, low-resistance couplants should be used. Self-adhesive pads incorporate a conductive gel between the electrode and skin surface, so no additional couplant is required. Electrode-skin interface can also be affected by chest hair, which causes poor electrode contact and air trapping. Thus, it is recommended to shave the chest prior to defibrillation.[21]

Table 1.2: Factors affecting human transthoracic impedance. Adapted from Kerber et al.[87]

Factor	Effect on TTI
Chest size or interelectrode distance	Larger chest → higher impedance
Electrode size	Larger electrodes → lower impedance
Electrode and chest wall interface	Low resistivity couplant → lower impedance Shaved chest → lower impedance
Shock energy	Higher energy → lower impedance
Multiple shocks	Successive shocks → lower impedance

Changes in tissue composition due to redistribution and movement of fluids induce fluctuations in the TTI. During the cardiac cycle, the distribution and amount of blood in the thorax varies, causing small changes in the conductivity of the tissue that are reflected in the TTI waveform, with amplitudes ranging from 0 to 200 mΩ.[84,98] Respiration (or ventilation of the patient) also affects TTI; impedance increases about 0.2–3 Ω during inspiration, and decreases again during expiration.[4,101]

Figure 1.8 shows a segment of the TTI signal acquired through defibrillation pads for a patient with a pulse-generating rhythm. Fluctuations induced by circulation and by respiration of the patient can be identified in the second panel. The baseline impedance of the patient is about 103 Ω, and four respirations can be distinguished. During inspiration the impedance increases between 1 and 2 Ω, and during expiration it returns to its baseline value. There are also some

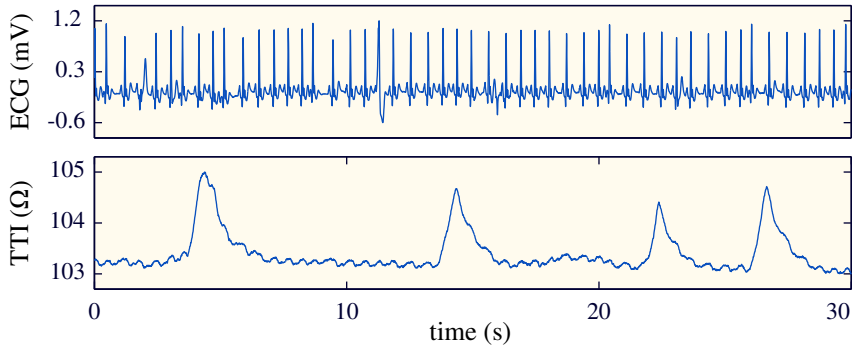

Figure 1.8: Segment of TTI signal with circulatory and ventilation-related components.

faster low-amplitude fluctuations (approximately 0.2 Ω), correlated with the ECG; this is the circulatory component of the TTI.

During CPR, chest compressions cause a disturbance in the electrode-skin interface, inducing artifacts on the ECG and on the TTI signal.[53,148] With each compression the TTI fluctuates around the patient's baseline impedance with an amplitude ranging from 0.15 to several ohms. Figure 1.9 shows a segment of the compression depth and the TTI signals recorded during a resuscitation episode. The compression depth was recorded using a CPR assist pad. In this segment, two series of 15 compressions are provided to the patient, with pauses in between for ventilation. Each compression induces a fluctuation in the TTI, with a peak-to-peak amplitude of almost 4 Ω in this case. During each pause the patient is ventilated twice, and slow fluctuations are induced in the TTI. The waveform of the fluctuations induced by chest compression is very variable between episodes and even along each episode.[6,65]

1.5 Monitoring and feedback systems

Both animal and clinical studies demonstrate that the quality of CPR delivered is critical to maximize survival from cardiac arrest. Current resuscitation guidelines recommend monitoring CPR quality and using feedback systems to guide rescuers during resuscitation attempts. According to a consensus statement from the AHA,[105]

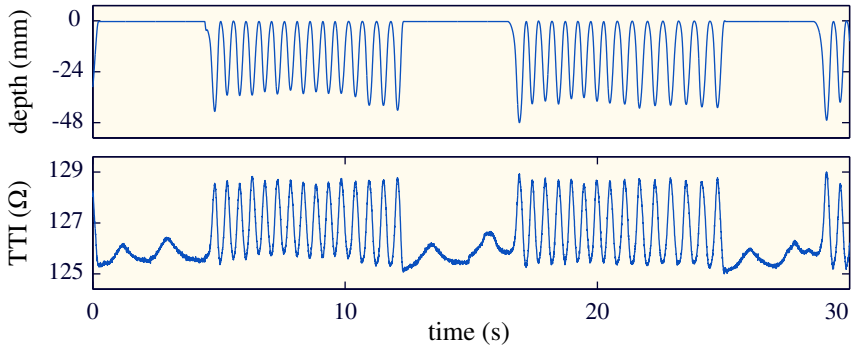

Figure 1.9: Segment of TTI signal with artifact induced by chest compressions and fluctuations induced by ventilations.

> *Monitoring of CPR quality is arguably one of the most significant advances in resuscitation practice in the past* 20 *years and one that should be incorporated into every resuscitation and every professional rescuer program.*

Chest compression quality monitoring allows providing real-time feedback to the rescuers during resuscitative efforts and the subsequent analysis of the resuscitation episode during debriefing sessions or in retrospective quality improvement programs. The main components for the quality of chest compressions are, by order of priority:[105] compression fraction (that is, percentage of time during which chest compressions are provided), compression rate, compression depth, and full chest recoil between compressions. Chest compression fraction is measured a posteriori, while the other components can be measured online during the cardiac arrest event.

The first devices developed to provide feedback on chest compression quality appeared in the 1990s, and they measured the force exerted on the chest of the patient during resuscitation attempts.[69] However, studies showed that the relationship between force and depth achieved is not linear, and it varies between subjects depending on chest stiffness.[120,153] Thus, most current devices are based on accelerometers, small and cheap electronic components that provide an accurate acceleration measurement. They are placed between the rescuer's hands and the chest of the patient, and measure the acceleration to which the chest is subjected during

compressions. The displacement of the chest can be computed by applying double integration to the acceleration signal. However, the integration process is intrinsically unstable, and even a very small DC component in the acceleration signal leads to large errors in the displacement estimation after a few seconds.

Owing to the commercial impact of solving this problem, several companies have tried to address it following different strategies. These approaches are usually industrially protected and published in the form of patents rather than in scientific articles. The most important standalone solutions currently in use for clinical practice are PocketCPR (Zoll Medical, Chelmsford, MA) and CPRmeter (Laerdal Medical, Stavanger, Norway), shown in Figure 1.10. PocketCPR is cheaper (about US$150), but it has limited capabilities and a very basic interface based on LEDs. CPRmeter provides a more sophisticated and attractive interface and a more precise estimation of the compression depth. This improvement in accuracy is achieved by incorporating a pressure sensor, which increases the complexity and the price of the device (about $650). Despite this, all the

Figure 1.10: CPR quality feedback devices based on accelerometers: PocketCPR (Zoll) and CPRmeter (Laerdal), from left to right.

systems based on accelerometers share two limitations: first, if CPR is performed on a soft surface (such as a mattress), the compression depth is overestimated leading to erroneous feedback;[115,132] second, they should not be used in moving vehicles, in which they would be subjected to accelerations other than the ones induced by chest compressions.

A new commercial solution overcomes these limitations: TrueCPR (PhysioControl). This system is based on triaxial magnetic field induction, and works both in soft surfaces and in moving vehicles.

It consists of a chest pad that should be positioned between the rescuer's hands and the chest, and a back pad, as shown in Figure 1.11. The compression depth is estimated from the changes in magnetic field between both pads. This alternative is bulkier than the ones based on accelerometers, and more expensive (about $1700).

Figure 1.11: TrueCPR feedback device (PhysioControl).

The deployment of these devices is still very limited, particularly in public access defibrillation and BLS settings.

1.6 Objectives of the thesis

Several studies have shown that the quality of chest compressions is suboptimal both for laypeople and for professional rescuers. This affects survival rates and outcomes of cardiac arrest victims. In order to improve CPR quality, resuscitation guidelines recommend the use of monitoring and feedback devices during resuscitation episodes.

A straightforward solution would be using the signals already available in current defibrillators to provide feedback. The simplest devices acquire only the ECG and the TTI signal through the defibrillation pads. Chest compressions induce fluctuations in the TTI signal. At the beginning of this thesis work, the relationship between the amplitude of these fluctuations and the compression depth had not been established yet. The use of the TTI signal to provide online feedback on chest compression rate to the rescuers had not been proposed either. The development of a feedback system

based solely on the TTI could have an important impact on CPR quality, as it could be universally available.

The systems that were being commercialized and in use to provide feedback during CPR were external devices based on accelerometers. These devices are placed below the rescuer's hands during chest compressions. Displacement of the chest (and thus, compression depth) is computed by doubly integrating the acceleration. The integration process is intrinsically unstable, and devices require reference signals to compensate for this instability. The development of methods to provide reliable feedback using exclusively the acceleration signal would reduce costs, simplify the devices, and support the widespread deployment of these systems.

On this context, the main objective of this thesis work was **to develop new strategies to provide feedback on the quality of chest compressions during cardiopulmonary resuscitation based on the TTI and on the acceleration signal**. In order to accomplish this objective, the following intermediate goals were defined:

- *Feasibility analysis of using the TTI to provide feedback on the rate and depth of chest compressions:* The relationship between fluctuations induced in the TTI and compression depth, and the ability of these fluctuations to discriminate chest compressions with inadequate depth will be analyzed using human data. The accuracy and reliability of the TTI signal to compute the chest compression rate will also be studied.

- *Estimation of the chest compression rate and depth using exclusively the acceleration signal:* Novel methods to provide feedback on the rate and depth of chest compressions using only the acceleration signal will be developed. Their accuracy will be characterized using manikin data, in which a reliable reference compression depth signal is available to be used as a gold standard and a wide range of situations can be tested.

- *Feasibility analysis of providing feedback using exclusively the acceleration signal under adverse conditions:* The accuracy of the chest compression rate and depth estimation will be evaluated when CPR is provided on a soft surface; when the accelerometer is positioned on the rescuer's back of the hand, or fixed to the

wrist or to the forearm; and when CPR in provided in a moving long-distance train.

The accomplishment of the objectives of this thesis work would have practical applications. Methods based on the TTI could be integrated into current defibrillators with just some minimum requirements for TTI acquisition, potentially not requiring hardware modifications. Alternatives based only on the acceleration signal would require dedicated devices, but cheaper and simpler than the ones comprising additional sensors. Both options would contribute to the widespread of CPR feedback systems.

2 Background

Once you do know what the question actually is,
you'll know what the answer means.

— Douglas Adams. *The Hitchhiker's Guide to the Galaxy.*

This chapter describes the context in which this thesis work was developed. It provides an account of the previous studies in the field regarding clinical uses of the thoracic impedance and existing feedback systems for chest compression quality. Section 2.1 covers the applications of the thoracic impedance signal, particularly when the signal is acquired through defibrillation pads. Emphasis is put on chest compression detection, which has attracted the attention of the scientific community during the last few years because of its potential as a CPR quality indicator. Section 2.2 presents a historical review of the technologies used to provide real-time feedback and describes the drawbacks of the existing solutions. The chapter concludes with a brief description of the pending challenges in this area.

2.1 Uses of the thoracic impedance

Impedance plethysmography is a well-established non-invasive method to determine changing tissue volumes in the body based on the measurement of electric impedance at the body surface. It has several applications, including the diagnosis of deep venous thrombosis, the measurement of lung water content, and the determination of cardiac stroke volume, that is, the volume of blood pumped by the left ventricle with each heartbeat. Stroke volume is measured by monitoring the impedance of the thorax and its changes with time. This technique is known as impedance cardiography, and it is based on the fact that circulation modifies the thorax conductivity as a function of the heart cycle. These modifications are reflected in the waveform of the first derivative of the impedance with respect to time.[98] Analyzing this signal, stroke volume and other cardiodynamic parameters such as cardiac output

or ventricular ejection time can be determined. The first publications concerning this technique date back to the 1930s and 1940s, but the method did not reach clinical value until the 1960s.[16,59,104] Figure 2.1 shows the electrode configuration for impedance cardiography measurement, with two band electrodes placed on the neck and another two on the chest. The impedance plethysmography has also been used to quantify myocardial contractility and to measure total peripheral resistance. Apart from measuring blood volume changes, this technique can also be used to evaluate the pulmonary function by detecting ventilation and computing air volume.[4,72]

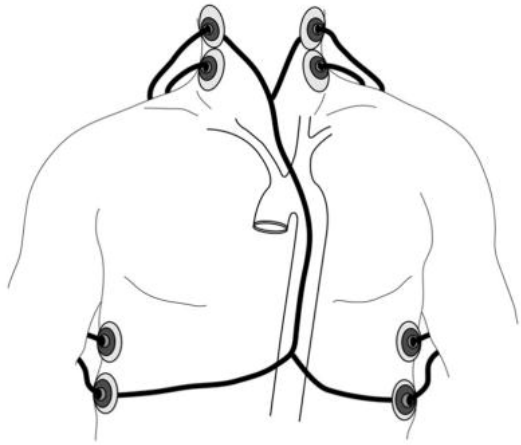

Figure 2.1: Electrode configuration for impedance cardiography measurement. Adapted from Tang et al.[150]

In the field of resuscitation, TTI is recorded by AEDs to check that the defibrillation pads are properly connected to the chest of the patient and to adjust the energy of the electrical shock. Defibrillators inject an alternate current, usually 2–3 mA at 20–30 kHz, and measure the resulting voltage between the pads to compute TTI. This signal is available during any resuscitation attempt in which adhesive defibrillation pads are used, without requiring additional instrumentation. As with impedance plethysmography, changes in tissue volumes and fluid distributions (such as blood and air) are reflected in the TTI measured by defibrillators. In addition, chest compressions disturb the electrode-skin interface and induce motion artifacts in the acquired TTI signal. Several studies have been

performed to detect circulation, ventilation, and chest compressions by analyzing TTI waveform. The main studies are summarized in the sections to follow.

2.1.1 Circulation detection

Assessment of carotid pulse has proved to be time-consuming and inaccurate both for rescuers with basic CPR training[15,44] and for healthcare professionals,[152] and it was removed from BLS resuscitation guidelines in 2000. However, reliable identification of pulse-generating rhythms is useful to distinguish between cardiac arrest and other collapse states, and to detect the return of spontaneous circulation during resuscitation attempts.

Circulation induces fluctuations in the TTI, as mentioned in Section 1.4. Figure 2.2 shows an example of the fluctuations induced with each heartbeat for a patient with a pulse-generating rhythm.

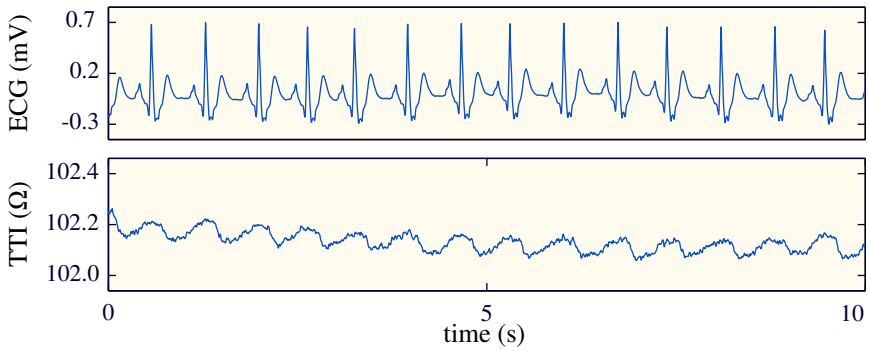

Figure 2.2: Fluctuations induced by circulation in the TTI.

In 1998, Johnston and colleagues[84] showed that the TTI recorded by defibrillators could potentially be used to discriminate between pulse-generating rhythms and those associated with haemodynamic collapse. Their aim was to increase the sensitivity (Se) of shock advice algorithms. They extracted four features from the TTI signal and evaluated their ability to identify pulse-generating rhythms using recordings acquired during cardiac arrest episodes, with promising results. This was the first study to report the effects of cardiac arrest on the TTI. Four years later, Pellis et al. (2002)[129] showed in an experimental study with swine that for each cardiac contraction

and for each respiration, fluctuations appeared on the TTI signal. These fluctuations ceased after inducing VF to the animals. The authors suggested equipping AEDs with cardiac and respiratory arrest detectors based on the analysis of the TTI signal.

Losert et al.[102] proposed in 2007 a classifier based on neural networks using several features extracted from the circulatory-related waveform of the TTI. Their aim was to detect the return of spontaneous circulation during resuscitation attempts. The method was evaluated using records from 32 haemodynamically stable and 37 cardiac arrest patients. Despite the low correlation obtained between blood pressure and impedance features, they could classify patients with an arterial pressure above or below 80 mmHg with a Se of 90 % and a specificity (Sp) of 82 %. The following year, Risdal et al.[135] introduced a new classifier based on pattern recognition to discriminate between PEA and pulse-generating rhythms (PR). The method was tested with clinical data, and when using an analysis window as short as 3 s, it correctly identified PEA and PR with a Se of 90 % and 91 %, respectively. That same year, Cromie et al.[33] showed in a swine study that the Fast Fourier Transform (FFT) of the impedance cardiogram recorded through defibrillation pads was a potential clinical marker of circulatory collapse. In a later clinical study[32] they refined the method and evaluated its performance with 132 cardiac arrest patients and 97 controls. They obtained a Se of 81 % and a Sp of 97 % for cardiac arrest detection in the validation set. More recently, Ruiz and colleagues[138] proposed an adaptive system based on a least mean square algorithm to extract the circulation component of the TTI. They obtained three features from the circulation component and its first derivative. When trying to discriminate between PEA and PR in cardiac arrest victims, all the features showed an area under the curve (AUC) higher than 0.96.

2.1.2 Ventilation detection

The relationship between respiration and electrical resistive impedance of the chest has been studied for decades.[4] During the last few years, with the widespread of external defibrillators, there has been an increasing interest in extracting information about CPR performance from the TTI signal acquired through defibrillation electrodes, including ventilation-related parameters.

During inspiration, the gas volume of the chest increases in relation to the fluid volume, causing chest conductivity to decrease. This effect, along with the expansion of the chest and the consequent enlargement of interelectrode distance, causes the measured TTI to rise.[70] During exhalation the TTI gradually returns to its baseline value. Figure 2.3 illustrates the changes in TTI with respiration or with artificial ventilation. The first panel shows the capnography signal, that is, the concentration of CO_2 in the respiratory gases. During inhalation the level of CO_2 is almost null, and it slowly increases during exhalation. The second panel shows the TTI signal, which increases with inhalation and decreases with exhalation.

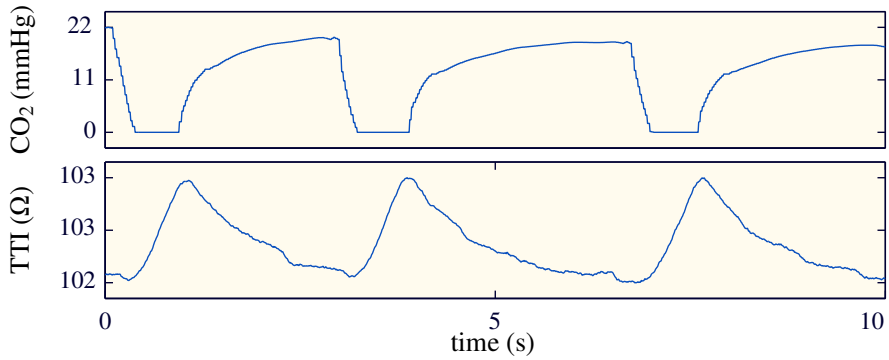

Figure 2.3: Fluctuations induced by respiration (or ventilation) in the TTI.

In a clinical study performed in 2006 by Losert et al.[101] the correlation between TTI change and tidal volume was calculated for mechanical ventilated patients, cardiac arrest patients, and patients after restoration of spontaneous circulation. Mean correlation coefficients above 0.96 were obtained for the three populations. The authors concluded that TTI can be used to quantify ventilation rates, inspiration times, and to calculate tidal volumes when chest compressions are interrupted. The following year, Risdal et al.[136] proposed a system based on pattern recognition that, using reference channels correlated with the chest compression artifacts, allowed detection of ventilations even during chest compressions.

Kramer-Johansen et al.[96] used the TTI signal to annotate ventilations in a clinical study about CPR quality before and after tracheal intubation. In 3 % of the cases, the changes induced by

ventilations in the TTI signal disappeared after placement of the tracheal tube. The authors suspected this was due to undesired accidental esophageal intubation, and hypothesized that online analysis of the TTI could be used to identify incorrect tube placement. Two years later in a prospective study,[94] they showed that changes in TTI could be used to detect malpositioned tubes with a Se of 99 % and a Sp of 97 %.

In 2010, Edelson et al.[46] assessed the accuracy of two methods to compute ventilation rate during CPR, one based on TTI and the other on capnography. They compared their algorithms to a manually annotated reference rate, but they did not have any independent signal to be used as gold standard. No significant differences in Se and positive predictive value (PPV) were found between the methods. All these studies used data from adults. Roberts et al.[137] analyzed whether changes in TTI could also be used to detect and guide rescue ventilations in children. They enrolled 28 mechanically-ventilated subjects in the study, from 6 months to 17 years of age. The algorithm detected more than 95 % of the ventilations with volumes higher than 7 ml/kg for two pad positions: anterior-apical and anterior-posterior.

Apart from these scientific studies, some commercial devices implement the estimation of ventilation rate from the TTI signal. This is the case of the Heartstart MRx monitor/defibrillator (Philips Medical Systems, Andover, MA), which detects changes in TTI induced by ventilations and provides audible and visual feedback to the rescuer on ventilation volume and rate.

2.1.3 Chest compression quality assessment

Compression of the chest during CPR induces both true TTI variations due to the thoracic volume change, and motion artifacts in the TTI and the ECG signals due to movements on the electrode-skin interface. Several researchers have investigated the feasibility of using the TTI signal acquired by defibrillators for chest compression quality assessment. Some studies have focused on quality parameters related to the instants of the chest compressions, such as chest compression rate. Others have studied the relationship between chest compression depth and the amplitude of the fluctuations.

Chest compression identification

The commercial program Codestat data review software (PhysioControl, Redmond, WA), incorporates an automated chest compression detector based primarily on the TTI. The program identifies fluctuations induced by chest compressions and annotates their position. These annotations are then used to compute CPR quality metrics such as chest compression rate and chest compression fraction. It also detects slower fluctuations induced by ventilations of the patient and computes ventilation rate. The program allows users to visualize the signals acquired by the defibrillator and to manually correct the marks if necessary. It has filtering options to emphasize either chest compressions (high-pass filter with a cut-off frequency of 1.5 Hz) or ventilations (low-pass filter with a cut-off frequency of 0.5 Hz). Figure 2.4 shows a segment of a record for a patient in asystole as visualized by Codestat. The ECG is plotted in black and the TTI in green. Each detected compression is depicted with a red arrow and the code <C>.

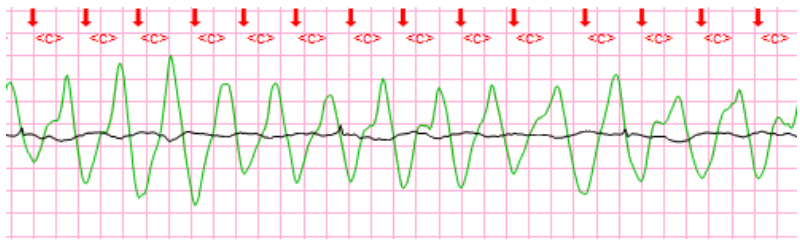

Figure 2.4: Automatic annotation of chest compressions from the TTI and ECG signals on Codestat Data Review Software (PhysioControl).

In 2012, Aramendi et al.[10] used the TTI signal to automatically detect chest compressions and estimate the instantaneous chest compression rate. They used a fixed threshold to identify compressions on the TTI. The computed compression rate was compared with that obtained from the compression depth signal acquired by an external CPR aid pad. Their objective was to use the instantaneous rate of the compressions in an adaptive filtering scheme designed to suppress the artifact induced by chest compressions in the ECG. Ideally, this would allow rhythm

analysis by the shock advice algorithm without interrupting chest compressions. The correlation coefficient between the instantaneous rate computed from TTI and from the compression depth signal was 0.91, consistent with the value they had previously reported in a short communication.[9] Although the correlation was high, they acknowledged that a fixed threshold could be inadequate as a result of the amplitude variation of the TTI fluctuations along an episode, and that more elaborated methods could improve the results and reduce the number of outliers. That same year, Firoozabadi et al.[52] reported in a short communication a mean error in rate of 2 cpm, also comparing the rate obtained from the TTI with that computed from the compression signal recorded by an external CPR aid pad. Unfortunately, details on the chest compression detection method were not provided.

González-Otero et al.[62] proposed in 2012 an automatic method to identify pauses in chest compressions by analyzing the TTI. First, the signal was filtered to isolate the fluctuations induced by chest compressions. Then, its squared slope was computed to emphasize chest compressions. The resulting signal was then smoothed using a low-pass filter. Finally, an adaptive threshold was applied to identify the pauses. The method was tested in episodes of OHCA, and it provided a Se of 94 % and a PPV of 96 % in the almost 1800 pauses analyzed. The main objective of this method was to allow rhythm analysis by an AED during ventilation pauses, as proposed by Ruiz de Gauna et al.[144] Chest compressions induce artifact in the ECG, and thus interruptions in chest compressions are required for reliable rhythm analysis. Current resuscitation guidelines recommend providing CPR for 2 min, and then pausing to assess the rhythm. In BLS, CPR should be delivered alternating series of 30 compressions and 2 ventilations. In this work, authors proposed to use pauses in chest compressions, particularly those for ventilation, to analyze the rhythm. This would eliminate the need for interrupting chest compressions after each 2-min cycle. Although the method for pauses detection has not been used to evaluate CPR quality, it could be useful to compute presence-related parameters, such as chest compression fraction.

At the beginning of this thesis work in 2012 no scientific publication had proposed methods to automatically compute the

chest compression rate from TTI in real time. This would allow providing feedback on compression rate to the rescuers without requiring additional devices besides the defibrillator.

Chest compression depth

Contradictory results have been presented in short communications regarding the relationship between chest compression depth and the amplitude of the fluctuations induced in the TTI. In 2011, Brody et al.[24] presented an experimental study with swine in which chest compressions were provided with different depths using a mechanical resuscitator. They recorded the TTI through defibrillation pads, and observed fluctuations of higher amplitude for higher compression depths. Figure 2.5 shows an example of the fluctuations induced in the TTI for compression depths of 2 cm, 4 cm, and 5 cm. Another experimental study using porcine models[78] reported a correlation coefficient of about 0.85 between TTI and four physiological parameters related to chest compression efficacy: systolic blood pressure, end-tidal CO_2, cardiac output, and carotid flow. This coefficient was very similar to that obtained when correlating the parameters with the compression depth instead of with TTI fluctuation. In another study, a correlation coefficient of 0.86 was reported between TTI and the compression depth measured using a commercial CPR feedback device.[41]

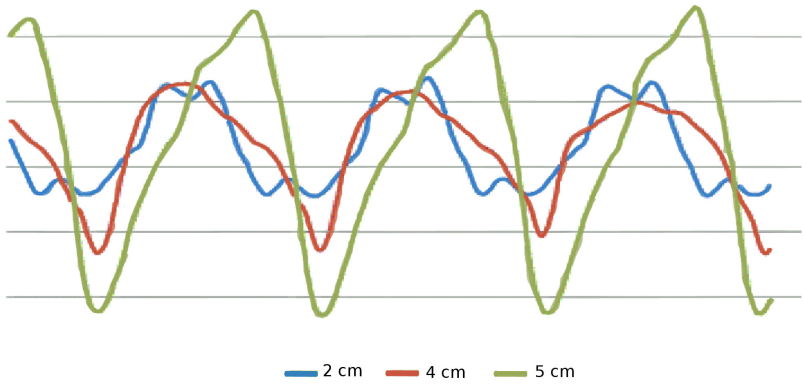

Figure 2.5: Fluctuations induced in the TTI for different compression depths in swine. Source: Brody et al.[24]

In two clinical studies, Di Maio et al.[43] and Navarro et al.[110] suggested the potential of TTI to identify adequate compression depth in patients in cardiac arrest. However, none of them included any objective measurement of the actual compression depth, and thus they did not have an independent gold standard. In a later study[42] using a commercial CPR feedback device to provide a reference chest compression depth, a correlation coefficient of 0.75 between the amplitude of the TTI fluctuations and the compression depth was reported. This contradicts the results of another analysis that also included a reference compression depth signal,[9] in which a correlation coefficient of 0.32 was obtained. All the described analyses were published in short communications, and limited details are available on the methods and the data analyzed. This makes it difficult to objectively compare the results.

In the first months of this thesis work, a prospective, experimental study by Zhang et al.[171] reported strong correlation between TTI fluctuations and both the compression depth and the coronary perfusion pressure during CPR in a swine model of cardiac arrest. They used 14 male domestic pigs weighing between 28 and 34 kg. The animals were anesthetized and mechanically ventilated with a volume-controlled ventilator. Aortic pressure, right atrial pressure, and pulmonary arterial pressure were monitored. TTI was recorded by applying a sinusoidal excitation current of 2 mA and 30 kHz between the adhesive defibrillation pads, which were attached in the anterior-lateral position. During chest compressions, an accelerometer-based CPR feedback device (CPR-D-Padz, Zoll Medical Corporation) was positioned between the chest of the animal, just above the heart, and the rescuer's hands. This device recorded the chest compression acceleration, which was used to compute the chest compression depth signal by double integration. Cardiac output was measured by the thermo-dilution technique. Cardiac arrest was electrically induced with a 2 mA alternating current delivered to the endocardium of the right ventricle. Then mechanical ventilation was discontinued and cardiac arrest was untreated for 6 min. Animals were randomized to one of the following groups: *optimal CPR* or *suboptimal CPR*. In the optimal group, manual chest compressions were performed by an emergency medical doctor instructed to compress the chest at a rate of 100 cpm and a depth of approximately

50 mm. In the suboptimal group, another emergency medical doctor provided manual chest compressions at the same rate but with a target depth of about 35 mm. In both groups compressions were given with a compression/ventilation ratio of 30:2. Compression depth, peak-to-peak amplitude change of TTI, and coronary perfusion pressure were obtained from each identifiable compression and averaged within a 5 s window. As anticipated, compression depth and coronary perfusion pressure were significantly higher in the optimal group. Amplitude of TTI fluctuations also presented significant differences between groups, with a mean $\pm$ standard deviation of $(1.45 \pm 0.37)\,\Omega$ vs. $(0.47 \pm 0.12)\,\Omega$ for optimal and suboptimal, respectively. Correlation coefficient was 0.89 between TTI amplitude and compression depth, and 0.83 between TTI amplitude and coronary perfusion pressure. Figure 2.6 shows the linear regression and correlation results between TTI and compression depth. In view of the strong correlations obtained, the authors concluded that changes in TTI have the potential to serve as an indicator of the quality of chest compressions and are associated with physiological changes produced by compressions. However, they acknowledged that further research was needed to clarify whether TTI could provide a self-referenced measurement of depth in different subjects.

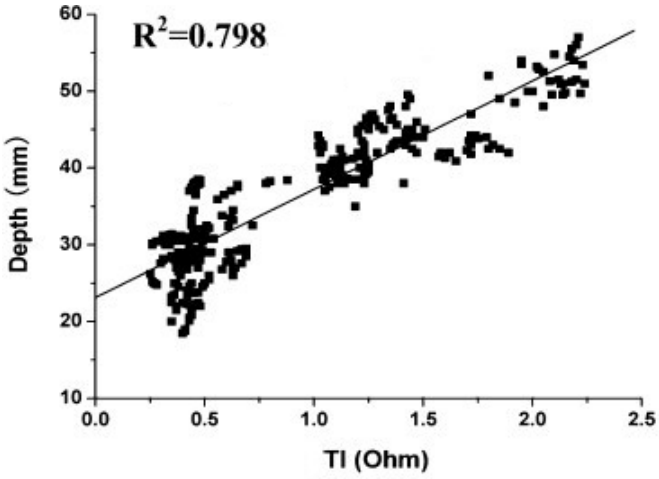

Figure 2.6: Linear regression and correlation between fluctuations induced by chest compressions in the TTI and compression depth. Adapted from Zhang et al.[171]

2.2 Feedback systems

Effective CPR after sudden cardiac arrest artificially provides some perfusion to the myocardium and brain and can double or triple a victim's chances of survival. Resuscitation guidelines define how CPR should be performed to achieve optimal results. These recommendations are updated periodically to incorporate the latest scientific evidence. However, in many cases CPR fails to meet the recommendations. Studies have shown that both professionals and laypeople often apply CPR at an improper rate and depth.[57,166]

The use of metronomes and real-time feedback systems increases adherence to CPR quality guidelines.[130,134,169] Metronomes generate regular audible beats that help rescuers to follow a rhythm, for example compression or ventilation rate. Feedback systems are more sophisticated devices that are placed on the chest of the patient to measure CPR performance. A processing unit evaluates CPR quality in real time, and the device reacts providing audiovisual messages that help rescuers to maintain target rates and depths. They can be standalone devices or work connected to defibrillators.

The clinical studies conducted to date had an insufficient power to establish a significant relationship between the use of feedback devices and an increased chance of survival,[69] although some of them showed non statistically significant improvements in patient outcome.[3,95] Large clinical trials[107] are being performed to evaluate whether or not real-time feedback increases survival. There is, however, strong evidence that feedback improves chest compression quality,[95,169] which has been linked to survival from cardiac arrest.[57,95] For these reasons, according to current consensus on science, the use of monitoring and feedback systems is recommended during resuscitation attempts.[91,105]

The development of CPR feedback systems is a topic of great commercial interest. Since the idea was first conceived, several companies started working on different alternatives to provide feedback and protecting their inventions via industrial property rights. There are few scientific publications on this subject, but various commercial devices have been developed.

The first CPR feedback systems were based on force or pressure sensors. Then, electronic devices based on the acceleration signal

were developed. Most of the devices currently in use rely on this technology, and derive mainly from two multinational companies: Philips (Laerdal) and Zoll. More recently, in 2013, PhysioControl entered the market with a new device based on magnetic field induction.

2.2.1 Systems based on force or pressure sensors

The first CPR feedback systems were mechanical devices that used force or pressure sensors to provide feedback on chest compression depth. They measured the force applied with each chest compression, but they did not assess chest compression rate. Devices in this category include CPRplus (Kelly Medical Products, Princeton, NJ), CPREzy (Health Affairs, London, England), and the more recent Cardio First Angel (Schiller, Baar, Switzerland), shown in Figure 2.7, from left to right.

Figure 2.7: CPR quality feedback devices based on force or pressure sensors: CPRplus (Kelly Medical Products), CPREzy (Health Affairs) and Cardio First Angel (Schiller).

CPRplus, shown in Figure 2.7 (left), was the first CPR device to be analyzed in any scientific study, and it is no longer available.[69] It was based on a pressure sensor with an analog display that showed compression force and recommended a force range depending on the characteristics of the patient (child, small adult, or average adult). In 1995, Thomas et al.[151] demonstrated that the proportion of correct

chest compressions provided in a manikin scenario in a helicopter increased significantly when using this device. Three years later, another study confirmed the potential of the device to increase chest compression quality, also in a simulated cardiac arrest scenario.[49]

CPRezy is a battery-powered device that shows using indicator lights the kind of patient for which the applied force would be adequate: child (activated when applying at least 23 kg of force), small adult (at least 32 kg), average adult (41 kg), large adult (50 kg), or extra large adult (54 kg).[23] It also incorporates a metronome to guide adequate compression rate. Since 2002, several studies have shown that the use of this device can improve effectiveness of chest compressions in simulated cardiac arrest,[19,23,116,130] and it can also increase skill acquisition and retention during training.[19] The use of the device does not require applying additional force to achieve the target depth, but it does require additional effort. This is due to the need to compress the device in addition to the chest of the patient. The work required to achieve the target compression depth increases in about 25 %, which causes a subjective feeling of increased rescuer fatigue.[158]

Cardio First Angel is a single-use mechanical device presented by Schiller in 2012. It consists of a hard plastic disk on which the rescuer has to apply the pressure, mounted over a water-repellent foam surface that helps to ensure even pressure distribution while it keeps the device in place. The disk contains multiple coil springs that produce an audible clicking sound when a force of about 41 kg is applied, indicating that the pressure is correct. In an unpublished practical test performed in 2013, the use of the device improved compression rate and depth achieved by laypeople in a simulated scenario.

All these systems measure the force applied for each compression to guide the rescuer to achieve the target depth. However, the chest has a non-linear stiffness[17,67,154] that varies among individuals.[120,153] Tomlinson et al.[153] simultaneously measured compression force and depth in 91 adult OHCA patients. Figure 2.8 shows the obtained relationship between force and depth for each patient. The force required to achieve 38 mm varied from 10 to 54 kg in the studied population. Additionally, they detected a decrease in chest stiffness along time.

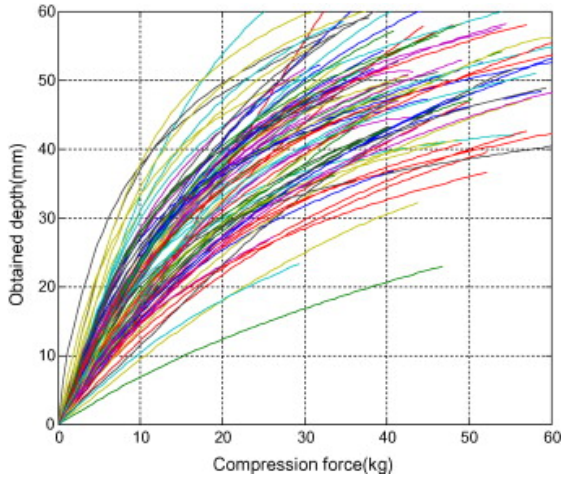

Figure 2.8: Relationship between compression force and compression depth for 91 cardiac arrest patients. Source: Tomlinson et al.[153]

Even if some of the previously described devices take into account the approximate size of the patient, the wide variation in chest wall elasticity and its changes with time impede an accurate estimation of compression depth from compression force only.

2.2.2 Systems based on accelerometers

To overcome the limitations of force and pressure sensors, electronic systems based on accelerometers were developed. These devices sense the acceleration of the patient's chest during CPR, and they process it in real time to obtain compression depth. For that purpose, a processing unit performs double integration numerically. Then, the computed compression depth signal is analyzed to calculate compression rate and depth. In base of these values, audiovisual feedback is provided to the rescuer.

The problem of double integration

Displacement can be obtained from acceleration by applying double integration. By definition, acceleration is the first derivative of velocity with respect to time, and velocity is the first derivative of displacement with respect to time. Conversely, chest acceleration $a(t)$

can be integrated once to obtain velocity, $v(t)$, and again to obtain displacement, $s(t)$:

$$v(t) = v(0) + \int_0^t a(\tau)\,\mathrm{d}\tau \tag{2.1}$$

$$s(t) = s(0) + \int_0^t v(\tau)\,\mathrm{d}\tau \tag{2.2}$$

The terms $v(0)$ and $s(0)$ represent the initial conditions, that is, the velocity and the displacement at the instant $t = 0$, respectively. Every system that performs an integration is intrinsically unstable, as not every bounded input results in a bounded output.

When acceleration is measured and digitized, integration has to be performed numerically. There are a number of discrete integration algorithms available, the most common ones being rectangular integration, the trapezoidal rule, and Simpson's method. Because of its trade-off between simplicity and accuracy, the trapezoidal rule is the most widespread. This rule can be implemented as a discrete linear filter in which the output is the integrated signal (in this case, the velocity), with the following difference equation:

$$v[i] = v[i-1] + \frac{a[i] + a[i-1]}{2} \cdot T_\mathrm{s}, \tag{2.3}$$

where T_s represents the sampling period in seconds, i.e., the inverse of the sampling frequency for the acquisition of the acceleration signal. Likewise, displacement can be computed filtering the velocity:

$$s[i] = s[i-1] + \frac{v[i] + v[i-1]}{2} \cdot T_\mathrm{s} \tag{2.4}$$

Note that even for the first point of the dataset an $i - 1$ term is required, which corresponds to the initial condition for the integration. The transfer function of this system is given by the following expression:

$$H_\mathrm{TR}(z) = \frac{T_s}{2} \cdot \frac{1 + z^{-1}}{1 - z^{-1}} = \frac{T_s}{2} \cdot \frac{z+1}{z-1} \tag{2.5}$$

This filter presents a pole in the unit circle for $z = 1$. In the frequency domain, this means that the magnitude of the frequency response $|H_{\mathrm{TR}}(f)|$, shown in Figure 2.9, becomes infinite for $f = 0$, and thus the output will tend to infinity when the input contains a DC component.

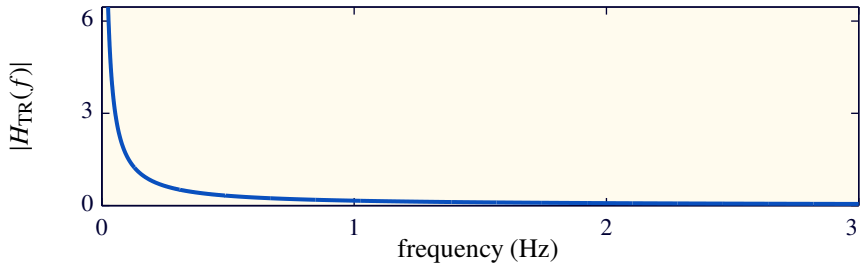

Figure 2.9: Magnitude of the frequency response of the filter that implements the trapezoidal rule.

Real-world acceleration recordings usually comprise baseline offsets: small errors in the reference level of motion that may be caused by several reasons, including instrumental instability, background noise, or calibration errors. Any offset of the acceleration signal (constant or with a slow variation), when double integrated, will cause an error in the estimation of displacement that grows quadratically with time. Additionally, inaccuracies in the acceleration signal may result in a drift in the response, particularly in the regions where noise is unbalanced, acting as a small DC offset.

Figure 2.10 illustrates the problem of the double integration using a record acquired while chest compressions were provided to a manikin. The acceleration signal (top panel) and the reference compression depth signal obtained from a displacement sensor (bottom panel, blue line) were registered. The second panel shows the velocity signal computed applying the trapezoidal rule to the acceleration signal (red), and the reference velocity signal, computed differentiating the reference compression depth signal (blue). As can be seen in the figure integration errors accumulate, and during the last seconds the computed velocity presents a noticeable offset with respect to the reference signal. When the trapezoidal rule is applied again, these inaccuracies lead to big errors in the computed

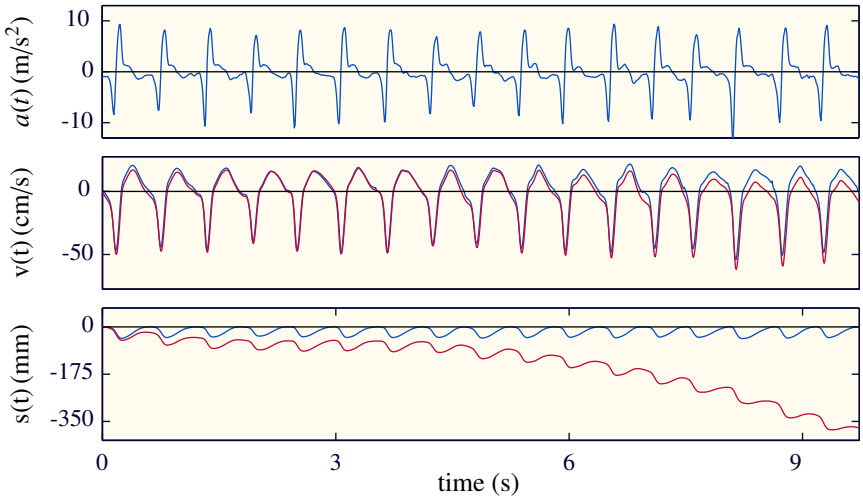

Figure 2.10: Integration errors that appear in the displacement signal when applying direct double integration to the acceleration signal.

displacement (third panel, red line), of more than 35 cm after only 10 s in this case.

One strategy to reduce integration errors would be to suppress baseline offsets. When the DC component of the acceleration signal (its mean value) is suppressed before the integration, Figure 2.11, the computed velocity signal better replicates the reference one (there is no discernible offset in the last seconds of the record), but there is still a drift in the computed depth of more than 15 cm after nine seconds. This is because for each compression cycle velocities are not perfectly balanced.

In order to reduce the accumulation of integration errors, the integration could be performed for small signal segments, for example for each compression cycle. For this purpose, it is necessary to identify the onset/offset of each compression and to reset the integration applying boundary conditions after each cycle. Figure 2.12 shows the result of the integration when the onset/offset of each compression, depicted by a vertical gray line, is identified in the reference compression depth signal recorded by the manikin, and when the initial conditions for the velocity and for the displacement at these points are set to $v(t) = 0$ and $s(t) = 0$, respectively. In this

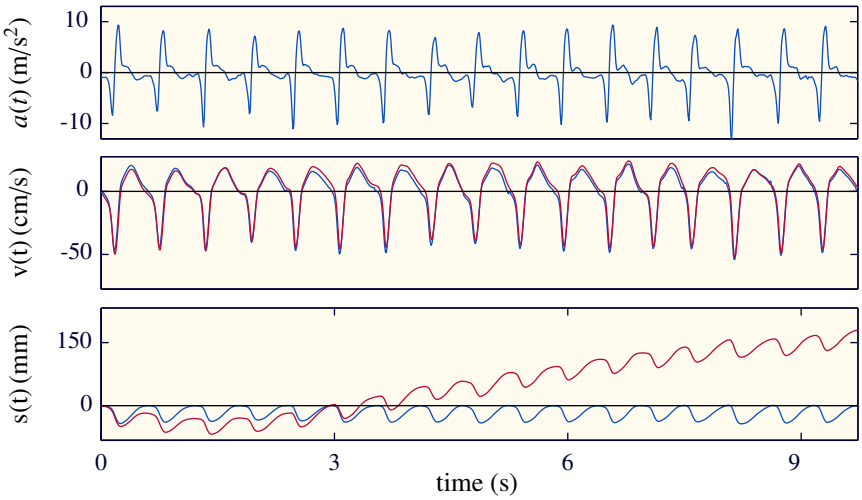

Figure 2.11: Integration errors that appear in the displacement signal when suppressing the DC component prior to integrating the acceleration signal.

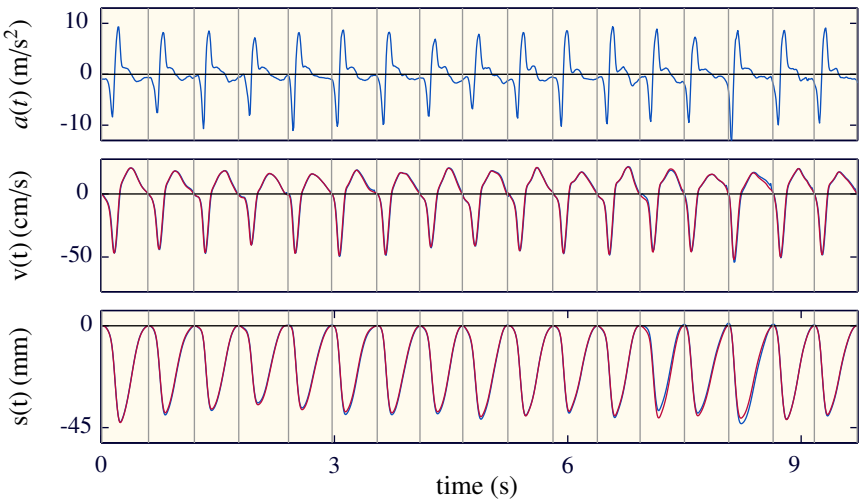

Figure 2.12: Double integration with reset of the initial conditions both for the velocity and for the displacement after each compression.

case integration errors are no longer accumulated and there is no drift in the estimated compression depth signal.

Proposed solutions

In 1990, Gruben et al.[68] developed a system to measure several signals related to CPR performance. A cylindrical module placed between the rescuer's hands and the patient's chest acquired the acceleration and the force applied at the sternum. A 5 degree-of-freedom arm connected to this device measured three-dimensional position and orientation of the module. This information was used to calculate chest compression depth (vertical displacement) and the component of the applied force perpendicular to the sternum. Additionally, the central venous and aortic pressures were measured. They tested the device during manual CPR on humans, and provided real-time feedback on external force and displacement to the rescue team. The authors found that the accurate calculation of chest displacement from acceleration alone was not easily accomplished because of offset drifts. To compensate this effect, they used information related to the displacement and orientation of the device with respect to gravity measured by the position-sensing arm.

In 2002, Aase and Myklebust[1] described and evaluated another solution to the acceleration drift problem. They designed a chest compression sensor comprised by an accelerometer and a membrane switch. For each chest compression, the switch was activated by the pressure of the rescuer's hands. Compression depth was computed by double integrating the acceleration signal. Each time the switch was activated, the integration started with zero initial conditions, and releasing the switch stopped the integration process. This limited the accumulation of integration errors to a single compression cycle. This solution was tested on a manikin equipped with a resistive displacement sensor that provided a reference compression depth signal. The 95% confidence interval for the estimation error was ± 4.3 mm when testing the method both in harsh environments (boat, car, sensor/patient misalignment), and in a regular, flat-floor controlled environment, and ± 1.6 mm when taking into account only the measurements performed on flat-floor. This strategy, that is, the use of a force-activated switch to reset the initial conditions for the integration of the acceleration, is patented both in the United

States[109] and in Europe,[54] in patents assigned to Laerdal Medical (Stavanger, Norway).

Other proposed approaches are based on applying signal processing techniques to compensate the integration drift with or without using reference signals. Palazzolo et al., in patents assigned to Zoll Medical (Chelmsford, MA),[126,127] describe a method of filtering and integrating acceleration to compute compression depth. They use a moving average model to estimate the starting point and the peak of each compression. Optionally, a reference signal such as the ECG may be used to identify the starting points of chest compressions. Babbs et al. (2008)[14] and Oh et al. (2012)[121] use exclusively the acceleration signal to estimate compression depth and apply filtering techniques and peak detection to minimize integration errors caused by double integration. Nysaether et al.[118,119] patented a method to compensate the computed compression depth signal for the distortion caused by the filters. They acquire the compression force (although other reference signals could be used) and adjust it so it has an amplitude, phase, and shape similar to those of the compression depth. This adjusted signal is then filtered and used to calculate a compensation signal. The compression depth signal is calculated by adding the double integrated filtered acceleration and the compensation signal. These patents are assigned to Laerdal Medical.

Commercial devices

Zoll and Laerdal (in collaboration with its partner Philips Healthcare) provide accelerometer-based commercial feedback solutions that can be used both in training and during the clinical practice. They market their feedback systems as Real CPR Help and Q-CPR, respectively. Both systems are available as standalone devices (PocketCPR and CPRmeter) and in some defibrillators with built-in feedback technology.

PocketCPR (Zoll), shown in Figure 1.10 in Chapter 1, is a small, reusable device that provides feedback on chest compression rate and depth by means of audible messages and LEDs. It incorporates an audiovisual metronome (lights flashing and a beeping sound) to guide adequate chest compression rate. If good compressions are delivered, the device responds flashing four LED lights. Otherwise, if

the compressions are too shallow, PocketCPR prompts the rescuer to push harder. This device is based on accelerometers only; integration drift is compensated by applying signal processing techniques, without the use of additional sensors. The signal is filtered before each integration process to suppress low-frequency components. These filtering stages distort the compression depth signal waveform, causing errors in the estimation of chest compression depth. There are no studies reporting the accuracy of PocketCPR. However, an study reported an improvement in the quality of chest compressions provided by experienced hospital nurses in a simulated setting when using this device.[134] Unlike with mechanical devices, no increase in fatigue was perceived or measured.

CPRmeter (Laerdal), shown in Figure 1.10 in Chapter 1, has two embedded sensors: an accelerometer and a force sensor. The force is used to increase the accuracy of compression depth estimation and to identify leaning, that is, to detect if the chest is being adequately released after each compression. Feedback information is presented in a colored display, as shown in Figure 2.13. Each compression is represented on the display by a moving white indicator bar. The bar moves up and down between the target area for adequate chest release (top) and the target area for adequate compression depth (bottom). If the device detects that a compression meets the requirements for release or depth, the corresponding target briefly

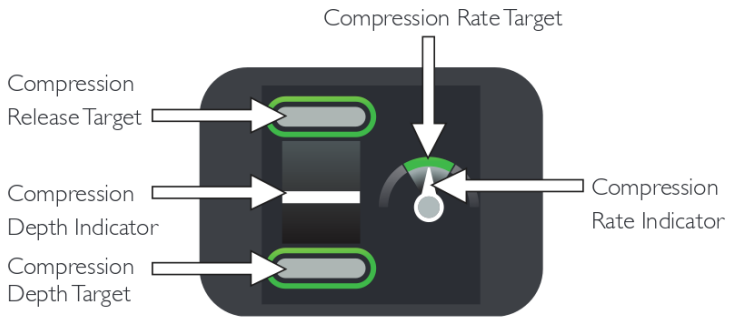

Figure 2.13: Display of the CPRmeter to provide real-time feedback on chest compression depth, rate, and chest release. Source: Laerdal.

illuminates. Feedback on the rate of chest compressions is provided by a speedometer. The target range for chest compression rate is indicated in green. Apart from providing real-time feedback, the device records the acquired signals for a later review. A simulation study using this device showed that it improved chest compression rate, depth, and reduced leaning. Users did not report an increase in perceived fatigue.[147]

Zoll defibrillators come with real-time feedback on the rate and depth of chest compressions. For that purpose, special single-use defibrillation pads are required: OneStep Complete, OneStep CPR, or CPR-D-padz (see Figure 2.14). The pads cost between $90 and $160, depending on the model, and integrate an accelerometer to monitor chest displacement. The defibrillator processes the acquired acceleration to provide feedback to the rescuers. Studies that examined the quality of CPR with this technology found contradictory effects on compression depth and no-flow time, while compression rate tended to improve. Some studies criticized the design of the one-piece CPR-D-padz electrodes, which hindered pad handling and made CPR uncomfortable.[69]

Figure 2.14: Zoll AED plus defibrillator with CPR-D-padz for CPR feedback.

Philips Heartstart MRx monitor/defibrillator is equipped with Q-CPR technology for CPR feedback. A CPR aid pad is placed beneath the heel of the rescuer's hand during chest compressions. The device, shown in Figure 2.15 (bottom right), is a wired version of the standalone CPRmeter. Additionally, the defibrillator uses the thoracic impedance signal acquired through defibrillation pads to provide feedback on ventilation rate. Clinical trials and simulation studies have yielded contradictory results concerning compression depth, rate, and chest release, with some of them showing improvements with the use of feedback and others showing no effect.[69]

Figure 2.15: Heartstart MRx with Q-CPR for CPR feedback.

Other companies may establish agreements with Zoll or Laerdal to provide feedback solutions using their technology. For example, GS GmbH (Kaufering, Germany) reached in 2012 an agreement with Zoll to incorporate Real CPR Help technology in Corpuls defibrillators. Corpuls provides a single-use pad (corPatch CPR sensor), shown in Figure 2.16, that measures chest acceleration. The acceleration is sent to the defibrillator, which gives audiovisual feedback on compression rate and depth.

Figure 2.16: CorPatch CPR sensor (Corpuls) for CPR feedback.

2.2.3 Systems based on magnetic field

In 2012 PhysioControl presented TrueCPR, a novel system for feedback on chest compression rate, depth, and chest release based on triaxial magnetic field induction. The device comprises two pads; the chest pad should be placed on the center of the chest, beneath the rescuer's hands during CPR. It contains the colored screen in which feedback is shown. The reference pad is longer and flatter, and should be placed beneath the patient's back. Figure 2.17 shows TrueCPR and its two pads.

Figure 2.17: TrueCPR (PhysioControl) feedback device. The chest pad contains the user interface, and the back pad acts as a reference.

The device uses three-dimensional magnetic fields to measure the distance between the two pads,[18] even if they are not perfectly aligned. During a resuscitation attempt, an in-built metronome guides chest compression rate, and feedback on chest compression rate, depth, and chest release is shown on the screen. Additionally, the device stores information related to CPR performance for a later review and debriefing. The disadvantage of this device compared to accelerometer-based solutions is that it is more complex, bulkier, and more expensive, which limits its spread, particularly in BLS settings.

2.2.4 Limitations of current feedback systems

Current commercial feedback devices present three main limitations:

- *Use on soft surfaces.* When the patient is lying on a mattress or on another soft surface, feedback devices based on accelerometers will overestimate chest compression depth, even if a backboard is being used.[115,132] This would lead to erroneous feedback, which could contribute to the delivery of shallow chest compressions. The depth calculated by the device corresponds to the total displacement of the chest. If the patient is lying on a soft surface, the total displacement will correspond to the chest compression depth (sternal-spinal displacement) plus the mattress compression depth. Feedback systems based on magnetic fields, however, overcome this limitation. TrueCPR measures the displacement between the back and the chest pad, independently of the displacement of the supporting surface.
- *Placement of the feedback device.* Current feedback devices are designed to be placed between the chest of the patient and the rescuer's hands. The prolonged pressure of the device may cause skin and soft-tissue damage to the patient.[27] Additionally, some rescuers refer discomfort in the heels of their hands and wrists associated with the use of feedback systems.[69,130] Some cases of injuries due to the use of feedback devices have also been reported.[130,170] Devices comprising force sensors bear an additional risk, as the skin could be trapped between mobile parts. Figure 2.18 illustrates the kind of soft tissue injuries that could be suffered by the patient (A) and by the rescuer (B) when a CPR feedback device is used in the standard position.

Figure 2.18: Photographs showing soft tissue injury caused by the use of CPR feedback devices. (A) shows a depressed anterior chest wound after prolonged CPR. Source: Cho.[27] (B) shows tissue injury sustained by a rescuer whose hand became trapped between mobile parts of a feedback device. Source: Perkins et al.[130]

- *Moving vehicles:* Depending on the country and area, different vehicles can be used for patient transportation, such as ambulances, helicopters, and boats. Moreover, according to the concept of public access defibrillation, CPR and defibrillation should be provided as soon as possible whenever the cardiac arrest occurs. This applies also to public transportation, and is particularly important in long-distance trains, in which the distance between consecutive stations may be of tenths of minutes. However, in moving environments accelerometer-based CPR feedback devices would register the accelerations of the vehicle along with the accelerations due to chest compressions. This could lead to errors in the estimated depth and potentially cause erroneous feedback. In fact, CPRmeter's user manual warns of possible inaccurate feedback if the device is used during patient transportation. TrueCPR is not affected by the accelerations of moving environments, as it is based on electromagnetic fields. Conversely, its performance could be affected by possible electrical interferences caused by equipment emitting electromagnetic or radio frequency fields.

2.3 Challenges for this thesis work

Defibrillators, including AEDs, measure TTI through adhesive defibrillation pads to check if they are correctly connected. At the beginning of this thesis work, the TTI signal had been used to identify circulation and to measure ventilation rate. In addition, a commercial software program operating offline identified fluctuations induced by chest compressions in the TTI to calculate some CPR quality parameters of recorded resuscitation episodes. However, no online system to provide feedback on CPR quality during resuscitation attempts was available. Moreover, an animal study suggested that the amplitude of the fluctuations induced in the TTI was strongly related to the amplitude of the chest compressions, but this relationship had not been confirmed with human data. This thesis work tried to answer two questions regarding the TTI signal and its applications to provide feedback on chest compression quality:

- Is there a relationship between chest compression depth and TTI on humans that allows providing feedback on chest compression depth during CPR?
- Can the TTI signal be used to provide reliable feedback on chest compression rate?

Chapter 3 addresses these questions. The first part of the chapter studies the relationship between chest compression depth and three morphologic features of the fluctuations induced in the TTI signal. The second part presents a novel frequency domain method to estimate chest compression rate in order to provide feedback to the rescuers during CPR.

Most commercial devices are based on accelerometers. Chest displacement can be obtained by double integrating the acceleration signal, with or without using additional signals to minimize integration errors. This is a very competitive market, and most solutions are protected by intellectual property rights, limiting the development of new products based on the acceleration. Moreover, the use of additional signals leads to complex devices and increases

their cost. In this context we wanted to answer the following questions:

- Is it possible to develop a method to provide feedback on chest compression rate and depth using exclusively the acceleration signal without infringing current patents?
- If the answer was affirmative, how would this method perform in different challenging real-life situations, such as on a soft surface, when the device is not positioned on the chest of the patient, or in a public transportation system?

Chapter 4 presents three new methods to estimate chest compression rate and depth using exclusively the acceleration signal. In Chapter 5 one of these methods is further analyzed in different challenging scenarios: when CPR is performed on a mattress, when the accelerometer is placed on the back of the hand, on the wrist, or fixed to the forearm of the rescuer, and when CPR is performed in a moving long-distance train.

3 TTI signal for chest compression quality

From dreams I proceed to facts.

— Edwin Abbott Abbott. *Flatland: A Romance of Many Dimensions.*

This chapter is a compilation of two studies[6,65] on the feasibility of using the TTI signal acquired through defibrillation pads to provide feedback on chest compression depth and rate. Both works were carried out by retrospectively analyzing OHCA data. Section 3.1 describes the characteristics of the different databases used and how they were collected. Then, in Section 3.2, the relationship between the depth of the chest compressions and the fluctuations induced in the TTI signal is analyzed. Three morphologic features of the fluctuations are computed, and their power to classify chest compressions as too shallow or adequate is evaluated. This study was published in 2014.[6] Chest compression rate is another important CPR quality parameter. Section 3.3 describes a novel algorithm, published in 2015,[65] to compute and provide feedback on compression rate during CPR.

3.1 Databases

The studies described in this chapter use datasets extracted from three original databases: the Sister database, compiled between 2002 and 2004 in three European cities; the Tualatin Valley Fire & Rescue (TVF&R) database, gathered between 2006 and 2009 in Oregon, USA; and the Oslo EMS database, acquired between 2012 and 2013 in Oslo, Norway.

The GSC research group gained access to the Sister and Oslo EMS databases as a result of its cooperation with Prof. Trygve Eftestøl from the University of Stavanger (Norway), and Dr. Jo Kramer-Johansen from the Oslo University Hospital and Oslo University (Norway). Access to the TVF&R database was achieved thanks to a

collaboration with Dr. Mohamud Daya from the Oregon Health & Science University (USA), and with James K. Russell from Philips Healthcare (USA). All data were provided anonymous and use of the data was approved by the local institutional review board or ethics committees.

The following sections briefly describe the studies from which the data were derived, the contents of each database, and the characteristics of the signals of interest.

3.1.1 Sister database

The Sister study was a research project conducted between March 2002 and September 2004 by Dr. Lars Wik from the Institute for Experimental Medical Research in the Ulleval University Hospital (Oslo, Norway).[166,95] The aim of the study was to measure adherence to CPR guidelines during ALS in adult OHCA and to compare quality of CPR with and without automated feedback. CPR quality was measured in three European locations: Stockholm (Sweden), London (England), and Akershus (Norway). In each of these regions, six ambulances with historically high rates of cardiac arrest at their sites participated in the study. The project was conducted in two phases. During phase I,[166] between March 2002 and October 2003, the paramedics were instructed to follow the 2000 resuscitation guidelines.[74] Quality of CPR was recorded from the defibrillators without providing feedback to the rescuers. In phase II,[95] between October 2003 and September 2004, audiovisual feedback on CPR quality via the defibrillators was activated.

Recording system

Prototype defibrillators based on Heartstart 4000 (Philips Medical System, Andover) were installed in the ambulances. The defibrillators were equipped with an extra chest pad that incorporated an accelerometer (ADXL202e, Analog Devices, Norwood, MA), and a pressure sensor (22PCCFBG6, Honeywell International, Morristown, NJ). The chest pad was mounted on the lower part of the sternum of the patient, beneath the heel of the rescuer's hand. A second accelerometer was fitted within the defibrillator to compensate for possible vertical motion of the entire supporting surface. Compression depth signal was calculated by double integrating the

difference between the two accelerometers over a compression cycle, defined by a 2 kg threshold in the signal acquired by the pressure sensor.[1]

Defibrillators acquired and stored in data cards the following signals:

1. *ECG signal:* Differential ECG recorded between defibrillation pads.
2. *ECG common mode:* Voltage common to both pads with respect to ground in the instrumentation amplifier.
3. *TTI signal:* Measured by injecting a sinusoidal current (32 kHz, 3 mA peak-to-peak) through the defibrillation pads. It was recorded with a resolution of 0.74 mΩ per least significant bit and a bandwidth of 0–80 Hz.
4. *Pad pressure or force signal:* Obtained from the pressure sensor with a bandwidth of 0–50 Hz.
5. *Acceleration signal:* Computed as the difference of the signals acquired by the two accelerometers, acquired with a bandwidth of 0–50 Hz.
6. *Compression depth signal:* Calculated from the acceleration and the pad pressure signals using the algorithm described in Aase and Myklebust.[1]

All the signals were recorded with a sampling frequency of 500 Hz and a resolution of 16 bit. In addition, the device stored events such as intervals in which the cardiac rhythm was analyzed or when an electrical shock was administered. Figure 3.1 shows an example of the signals acquired by the defibrillators.

Data collection and annotation

For each resuscitation episode, the signals acquired by the defibrillator along with adapted versions of Utstein style forms for uniform reporting of cardiac arrest data[34] were collected. All cardiac rhythms occurring during the episode were manually annotated by consensus between an experienced anesthesiologist and a biomedical engineer, both specialized in resuscitation. Chest compressions were identified using the compression depth signal and coded as too

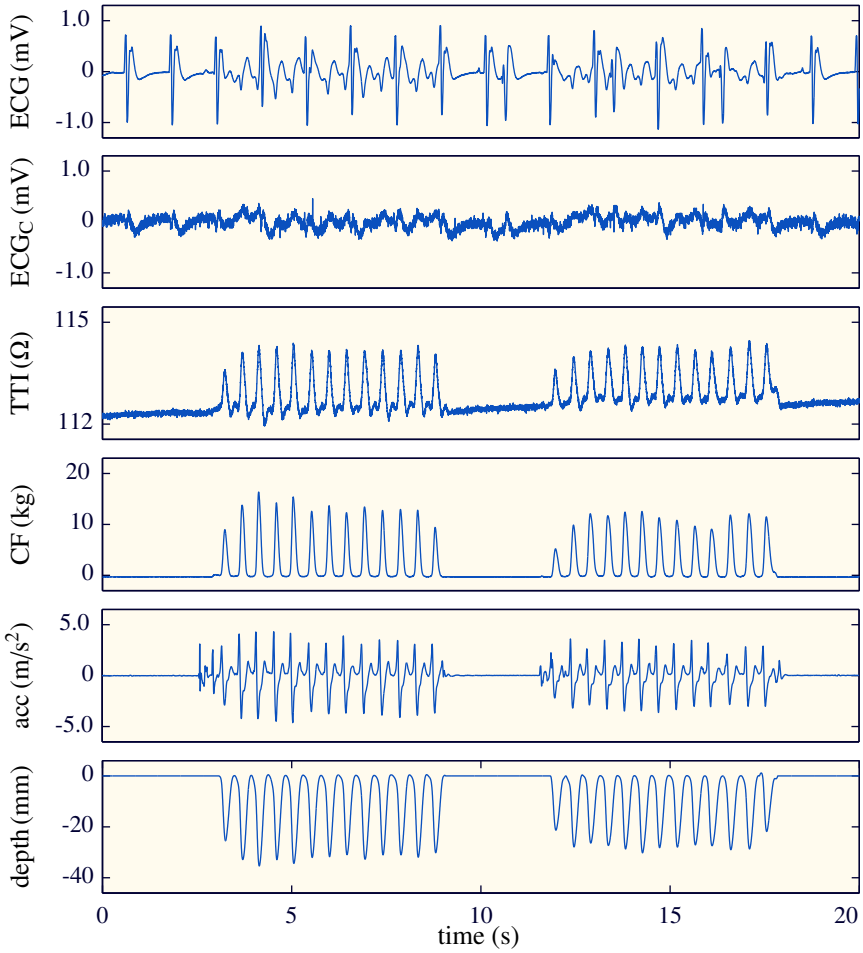

Figure 3.1: A 20 s extract from an episode in the Sister database showing the recorded signals. Chest compressions are visible in the reference channels acquired using the chest pad: compression force (CF), acceleration (acc), and compression depth. They are also identifiable in the TTI signal, in which they induce fluctuations. During compressions, artifact is also induced in the ECG (top panel).

deep, too shallow, or acceptable according to 2000 resuscitation guidelines.[74] Intervals of at least 1.5 s without compressions were considered pauses in chest compressions. Incomplete chest release was identified when residual force between compressions exceeded

4 kg. Ventilations were automatically annotated using the TTI signal. Intervals with and without chest compressions, ventilation, and rhythm annotations, and data from the defibrillators were integrated to form the annotated database.

Database summary

The Sister study database comprises 364 annotated episodes of adult OHCA of all causes (cardiac and non-cardiac), with a total duration of over 160 hours. The median duration of the episodes and the first and third quartiles (Q1, Q3) are 26 (17, 24) min.

When feedback was provided to the rescuer (phase II), CPR quality improved[95]. However, even with real-time feedback, almost half of the time chest compressions were not delivered and most of the compressions were too shallow according to 2000 guidelines (depth below 38 mm). Mean ventilation and compression rates were in accordance with guideline recommendations.

During phase I, 2.9 % patients survived to hospital discharge, and 4.3 % during phase II. This increase in survival with CPR feedback was not statistically significant.

3.1.2 TVF&R database

TVF&R is a first response ALS fire agency that serves nine incorporated cities in Oregon, USA. All of TVF&R's firefighters are certified emergency medical technicians, and approximately two thirds of the line personnel are paramedics. They provide patient care and treatment under the supervision of Dr. Mohamud Daya, the district's EMS medical director and EMS fellowship director in the Department of Emergency Medicine at Oregon Health & Science University (OHSU). Dr. Daya is also the link between TVF&R and the Resuscitation Outcome Consortium (ROC), a clinical trial network focused on research in prehospital cardiopulmonary arrest and severe traumatic injury.

Since 2005, TVF&R has been consistently recording CPR performance data and providing real time feedback to EMS crews during OHCA. That same year they signed an agreement with the cardiac products research division within Philips Healthcare. Under that agreement, the company gained access to CPR data collected

from their monitor/defibrillators to improve product safety and performance.

Recording system and data collection

Every unit of the TVF&R is equipped with a Heartstart MRx monitor/defibrillator (Philips Medical System, Andover, MA), with integrated Q-CPR technology for CPR feedback. A compression sensor placed on the patient's chest gathers data and transmits it to the defibrillator, which delivers feedback on chest compression depth, rate, and full chest release. The compression sensor (Q-CPR meter) is a marketed version of the chest pad used in the Sister study.

For each resuscitation episode, the following signals[1] were stored in data cards of the defibrillators, when available:

1. *ECG signals:* ECG acquired through defibrillation pads, or through limb or precordial leads. More than one channel may be available. Sampling rate was 250 Hz.
2. *TTI signal:* Measured by injecting a sinusoidal excitation current (32 kHz, 3 mA peak-to-peak) through the defibrillation pads. Recorded with a sampling rate of 200 Hz, a resolution of 2.5 mΩ per least significant bit, and a bandwidth of 0–20 Hz.
3. *Pad pressure or force signal:* Obtained from the pressure sensor in the Q-CPR meter, with a sampling rate of 100 Hz and a bandwidth of 0–50 Hz.
4. *Acceleration signal:* Acquired by the accelerometer fitted in the Q-CPR meter with a sampling rate of 100 Hz and a bandwidth of 0–50 Hz.
5. *Compression depth signal:* Calculated from the acceleration and the pad pressure signals using the algorithm described in Aase and Myklebust.[1]
6. *Capnography signal:* Level of carbon dioxide in exhaled breath acquired using Microstream, with a sampling rate of 125 Hz.

Cardiac rhythms were not annotated in this database, but Utstein style templates were available. Figure 3.2 shows an example of the signals acquired by the defibrillators.

1 Specification for the acquisition of the signals are nominal, as of the time of production of the units used for data collection.

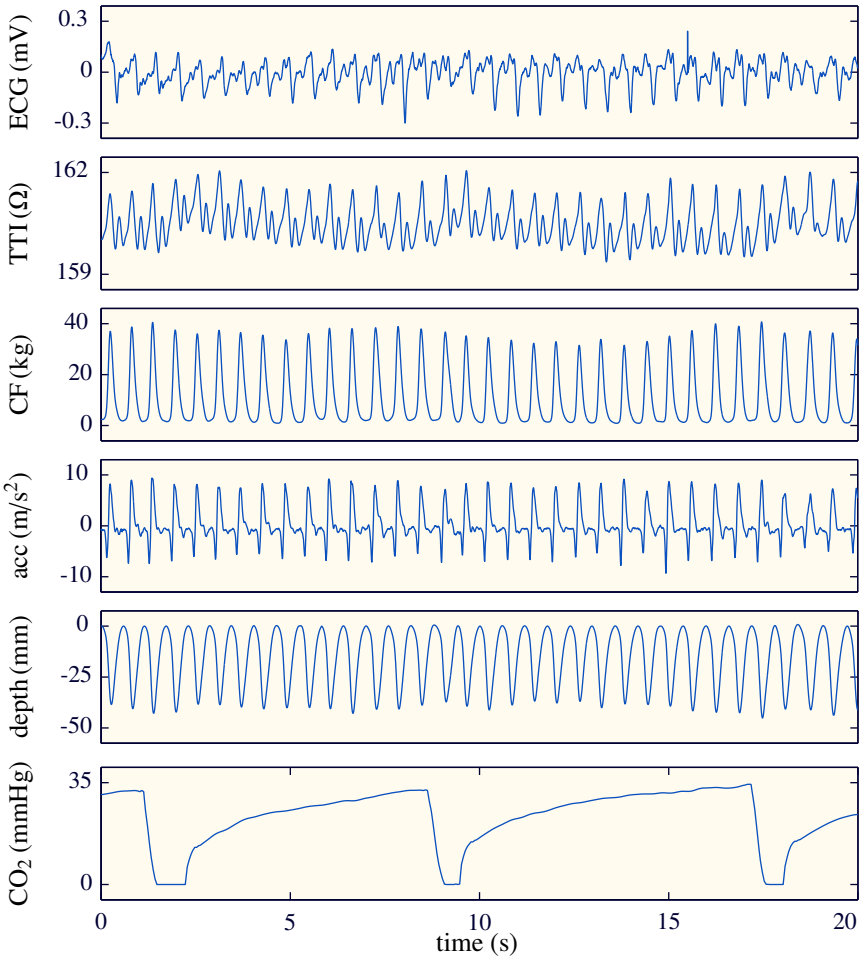

Figure 3.2: A 20 s extract from an episode in the TVF&R database showing the recorded signals. During this interval the patient is intubated, and thus chest compressions are continuously provided, without interruptions for ventilation. Three ventilations can be identified in the TTI and in the capnography signals.

Database summary

For the studies presented in this chapter, the GSC research group had access to 623 cardiac arrest episodes recorded between 2006 and 2009, while CPR was performed according to 2005 resuscitation guidelines.[73] CPR quality metrics of this database have not been published yet, but information regarding episode length, median compression depth, rate, and chest compression fraction were computed from the signals in the database. Values are presented as median (Q1, Q3). Aggregate duration of the episodes exceeded 195 hours, with a median duration per episode of 17 (7, 28) min. Median compression depth and rate per episode were 41 (36, 44) mm and 110 (104, 119) cpm, respectively. Median chest compression fraction was 68 (48, 77) %.

3.1.3 Oslo EMS database

The Oslo EMS study is an ongoing research project led by Dr. Jo Kramer-Johansen in Oslo (Norway). The aim of the project is to quantify differences in preshock pause duration when the defibrillators are used in manual and in semi-automatic mode. During phase I (July 2012 – June 2013) paramedics were instructed to visually assess the rhythm using the defibrillators in manual mode. In phase II (July 2013 – June 2014) defibrillators were used in semi-automatic mode and the rhythm analysis was automatically performed by the defibrillators.

Recording system and data collection

Episodes were recorded using Lifepak 12/15 defibrillators (PhysioControl, Redmond, WA). Each episode comprised the following signals:

1. *ECG signal:* Recorded through defibrillation pads with a sampling frequency of 125 Hz and a bandwidth of 1.3–30 Hz.
2. *TTI signal:* Acquired with a resolution of 1.2 mΩ, a sampling frequency of 61 Hz and a bandwidth of 0.3–30 Hz.

Figure 3.3 shows a segment of an episode in the Oslo database, containing the ECG and TTI recorded by the defibrillator.

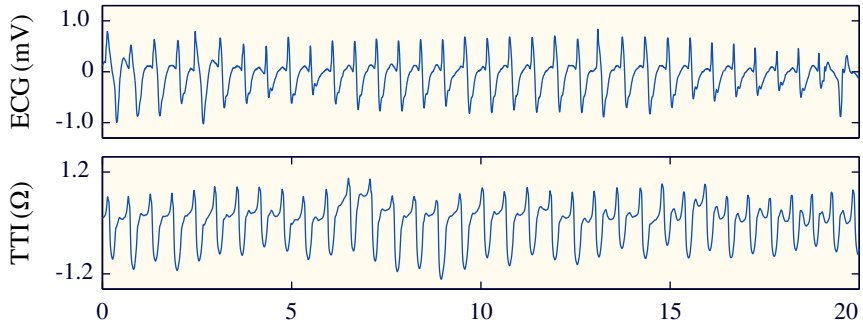

Figure 3.3: A 20 s extract from an episode in the Oslo EMS database showing the recorded signals: ECG and TTI.

The initial rhythm and each subsequent change in rhythm were annotated for each episode by consensus between an experienced anesthesiologist and a member of the GSC group, both specialized in resuscitation. Chest compressions were automatically marked by Codestat 9.0 data review software (PhysioControl) using the TTI and the ECG signals, and manually corrected by members of the GSC group.

Database characteristics

The GSC research group gained access to data from Phase I of the study. The database contains 370 episodes of OHCA in which CPR was provided according to 2010 guidelines. In most of the cases chest compressions were delivered manually, but in some of them LUCAS2 (PhysioControl) mechanical device was used. Total duration of the episodes is over 153 hours.

3.2 Estimation of chest compression depth from TTI signal

Resuscitation guidelines recommend providing chest compressions of at least 5 cm during CPR. However, this target depth is not easily achieved. Rescuer fatigue causes a decrease in depth over time, and shallow chest compressions are common. Current technology for feedback on compression depth requires the use of an accessory device that is placed on the chest of the patient to monitor CPR performance. This adds complexity to the equipment and limits the widespread of feedback systems, particularly in BLS settings.

Chest compressions induce fluctuations in the TTI signal acquired through defibrillation pads. However, the relationship between TTI fluctuations and the compression depth has not been established yet. In this context, the aim of this study was to analyze the relationship between TTI fluctuations and compression depth during OHCA episodes. This analysis was performed in collaboration with Erik Alonso, and is also part of his thesis work.[5] First, the correlation between three morphologic features of the TTI and compression depth was analyzed for the whole population. Second, the influence of the patient was evaluated by computing the correlation independently for each episode (one per patient). Third, to study the influence of the rescuer, this process was repeated with series of continuous chest compressions. Each series corresponded to a unique rescuer-patient pair. Then, we tried to replicate the experiments by Zhang et al.[171] by studying the correlation when only series of optimal or suboptimal chest compressions (no intermediate values) were included. Finally, we analyzed the power of the TTI features to discriminate between shallow and non-shallow chest compressions.

3.2.1 Materials and methods

Data collection

The dataset used in this study was a subset of the TVF&R database, which comprises 623 OHCA episodes recorded while CPR was provided according to 2005 guidelines (see Section 3.1.2). The compression depth and the TTI signal were available for 189 of the 623 episodes. We extracted 60 episodes containing both signals uninterruptedly recorded along the whole episode and with a minimum of 1000 chest compressions. For the analysis, only chest compressions that were part of a series with a minimum of 10 chest compressions were considered, which yielded a total of 116 679 chest compressions. Median (Q1,Q3) duration of the 60 episodes was 34 (25, 41) min, and they included 1852 (1362, 2556) chest compressions per episode.

Every episode of the dataset reflected the efforts of multiple rescuers. Crews composed by two to six rescuers performed 2-min chest compression series with pauses in-between to look at the

rhythm and rotate between them. We wanted to study the effect of the rescuer in the relationship between TTI and compression depth. For that purpose, we extracted intervals (series) where the single-rescuer-single-patient pattern was guaranteed. We defined series as epochs of chest compressions performed without interruptions by a single rescuer on a patient. Interruptions in chest compressions longer than 1.5 s were identified as a possible change of rescuer.[93] Only series with a minimum duration of 2 min were considered for the analysis. We extracted 75 series with a median duration of 149 (133, 187) s and 277 (243, 347) chest compressions per series. Median compression depth was 42 (37, 48) mm.

Signal processing and feature extraction

Compression depth and TTI signals were processed to compute for each chest compression its maximum depth and three features of the fluctuation induced in the TTI waveform. First, the instant of maximum depth of each chest compression, $D_{\mathrm{max}i}$, was automatically detected using a negative peak detector with a static threshold of 15 mm. Taking into account that instant, the cycle of each chest compression was identified in both the compression depth and the TTI signals, as shown in Figure 3.4, in which each compression cycle is delimited with vertical gray lines. Then, the TTI signal was downsampled to 100 Hz and band-pass filtered to remove the baseline drift, fluctuations caused by ventilations, and high frequency noise. We applied an order 6 Chebyshev filter with 0.1 dB of peak-to-peak ripple and 0.6–7 Hz passband to obtain $z_{\mathrm{p}}[n]$. The processed TTI signal during the ith chest compression cycle was denoted $z_{\mathrm{p}i}[n]$.

To characterize the fluctuations induced by chest compressions in the TTI signal, three different waveform features were computed for each chest compression:

- **Peak-to-peak amplitude, $Z_{\mathbf{pp}i}$:** Difference between the maximum and the minimum value of $z_{\mathrm{p}i}[n]$.
- **Area, A_i:** Area of the TTI during the ith chest compression cycle:

$$A_i = \sum_{n=1}^{N} \left| z_{\mathrm{p}i}[n] \right|, \tag{3.1}$$

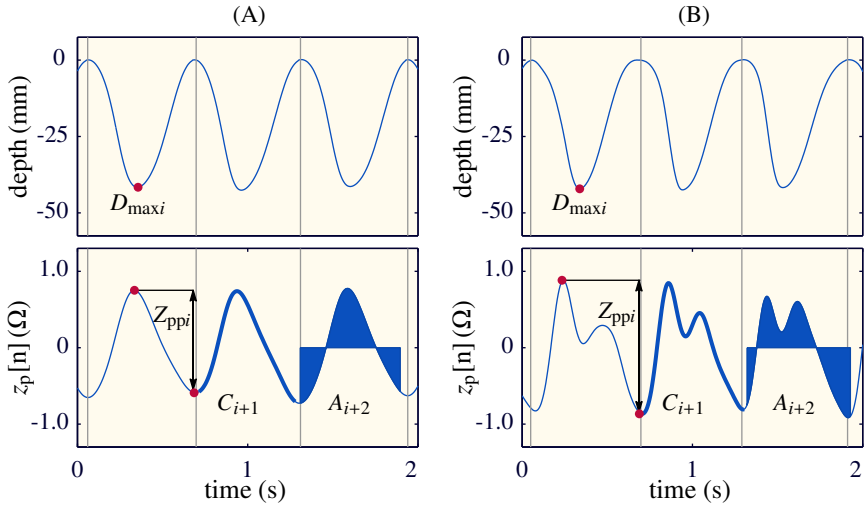

Figure 3.4: Example of the features extracted for two signal segments. The maximum depth D_{maxi} is represented on the compression depth signal (upper panels), and the three TTI features on $z_p[n]$ (lower panels). Compression cycles are delimited by vertical gray lines.

where n is the time sample number and N the length of the chest compression cycle $z_{pi}[n]$ in samples.

- **Curve length, C_i:** Length of the curve $z_{pi}[n]$, computed as follows:

$$C_i = \|z_{pi}[n]\| = \sum_{n=2}^{N} \sqrt{\left(\frac{1}{f_s}\right)^2 + \left(z_{pi}[n] - z_{pi}[n-1]\right)^2}, \quad (3.2)$$

where f_s is the sampling frequency of the TTI signal.

Figure 3.4 illustrates two examples where the extracted features are depicted on the compression depth signal (top) and on the processed TTI signal (bottom). Panel A shows an example where the TTI fluctuations caused by chest compressions are quite sinusoidal, while in panel B the fluctuations are more irregular. A_i and C_i were computed because Z_{ppi} was not able to characterize irregular TTI fluctuations. Examples in Figure 3.4 present similar Z_{ppi} but quite different A_i and C_i values.

In order to smooth the values of the features, the mean values for the compression depth maxima, D_{max}, and for the three TTI features (Z_{pp}, A, and C) were computed every 5 s.

Analysis of the linear relationship

The linear relationship between D_{max} and the TTI features was tested for the whole population, for each patient independently, and for series of compressions provided by a single rescuer. Spearman's rank correlation coefficient and Pearson's correlation coefficient (r) performed similarly in our analyses, so r values are reported, as they permit comparison with previous studies. Univariate linear regression was used to model the relationship between D_{max} and the different features.

Scatterplots of the D_{max} with respect to the different features were plotted for the whole population and for each patient independently, along with the corresponding fitted model and r value.

In order to avoid potential variability introduced by the rescuer, we analyzed the linear relationship between D_{max} and Z_{pp} in a single-rescuer-single-patient pattern. Series with a minimum standard deviation of 7 mm in the D_{max} were considered. This allowed adjusting the model to a considerable range of D_{max} values. To avoid bias, a single series per patient was selected, the one with the highest standard deviation. Selecting all series per patient did not significantly change our results. A total of nine series were extracted. Univariate linear regression was used to predict D_{max} using Z_{pp}, and r was computed independently for each series and jointly for the complete set of series.

Then, aiming to replicate the procedure that Zhang et al.[171] used with animals, series with optimal and suboptimal chest compressions were selected. A series was considered suboptimal when at least 75 % of its chest compressions were below 38 mm, and optimal when at least 75 % of its compressions were above 50 mm. One series per patient was selected, the one with the largest number of chest compressions above (optimal group) or below (suboptimal group) the threshold. A total of twelve series were selected. They were jointly analyzed by computing r and fitting a model through univariate linear regression.

Discrimination power of the TTI features

The power of the three TTI features to classify each 5-s window as shallow or non-shallow was evaluated in the context of 2005 resuscitation guidelines,[73] thinking of a possible feedback system that could be incorporated into an AED and alarm the rescuer if the compressions were too shallow. According to the guidelines, windows with an average chest compression depth $\overline{D}_{\max}$ below 38 mm were classified as shallow. To enlarge the difference between shallow and non-shallow chest compressions and to take into consideration possible measurement errors, a tolerance band of 5 mm was defined. Windows with $\overline{D}_{\max} \geq 43$ mm were classified as non-shallow, and those with $38 \leq \overline{D}_{\max} \leq 43$ mm were regarded as borderline and not considered for the evaluation of the classifier.

A multivariate logistic regression model based on a three feature vector was applied for the classification. The regression model assigned to each 5-s window a probability of non-shallow depth given by:

$$P_{\text{non-shallow}}(z) = \frac{1}{1+e^{-z}}, \tag{3.3}$$

with $z = \beta_0 + \beta_1 \cdot Z_{\text{pp}} + \beta_2 \cdot A + \beta_3 \cdot C$.

The 60 episodes were split into training (40) and test (20) sets. The regression coefficients (β_i) were calculated for the training set using the Waikato Environment for Knowledge Analysis (WEKA) software. The power of the classifier was evaluated in terms of area under the curve (AUC), Se, and Sp for the training and test sets. Se was defined as the capacity to correctly identify shallow chest compressions, and Sp as the capacity to correctly identify non-shallow chest compressions. The weight of the classes was set to maximize Sp while ensuring a Se above 90 %, in order to minimize the number of erroneous alerts. $P_{\text{non-shallow}} > 0.5$ were classified as non-shallow.

3.2.2 Results

Results did not pass the one-sample Kolmogorov-Smirnov normality test, so they are presented as median (Q1, Q3).

Figure 3.5 shows the scatterplot of $D_{\max}$ against each of the TTI features for the whole population and the model fitted in each case.

A total of 14 424 values with a depth of 42 (37, 48) mm were analyzed. The three features presented a high dispersion around the regression model. The value of r was 0.34, 0.36, and 0.37 for Z_{pp}, A, and C, respectively.

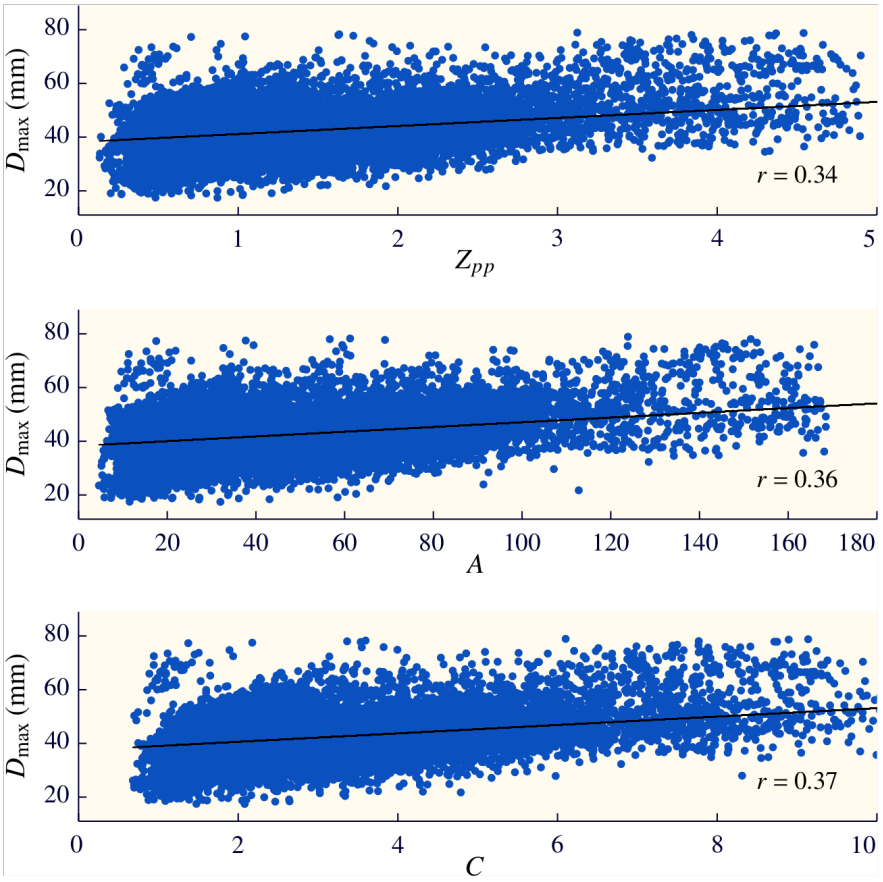

Figure 3.5: Scatterplots of the D_{max} with respect to the TTI features Z_{pp}, A, and C (from top to bottom) for the whole population. For each figure, the fitted regression line is depicted in the plot, and the value of r is shown.

The analysis within patients yielded a correlation coefficient r of 0.40 (0.24, 0.66) for Z_{pp}, 0.43 (0.26, 0.66) for A, and 0.47 (0.25, 0.68) for C. Figure 3.6 shows the scatterplot and the model fitted for the Z_{pp} in six representative patients. The cases depicted in panels A and B show a high r (0.92 for both cases), although the slopes of their

regression lines differ. Panels C and D show data from two patients with a low r and a high dispersion around the regression line. Finally, in the cases depicted in panels E and F two patterns can be observed, and a single model does not adequately adjust to all the values.

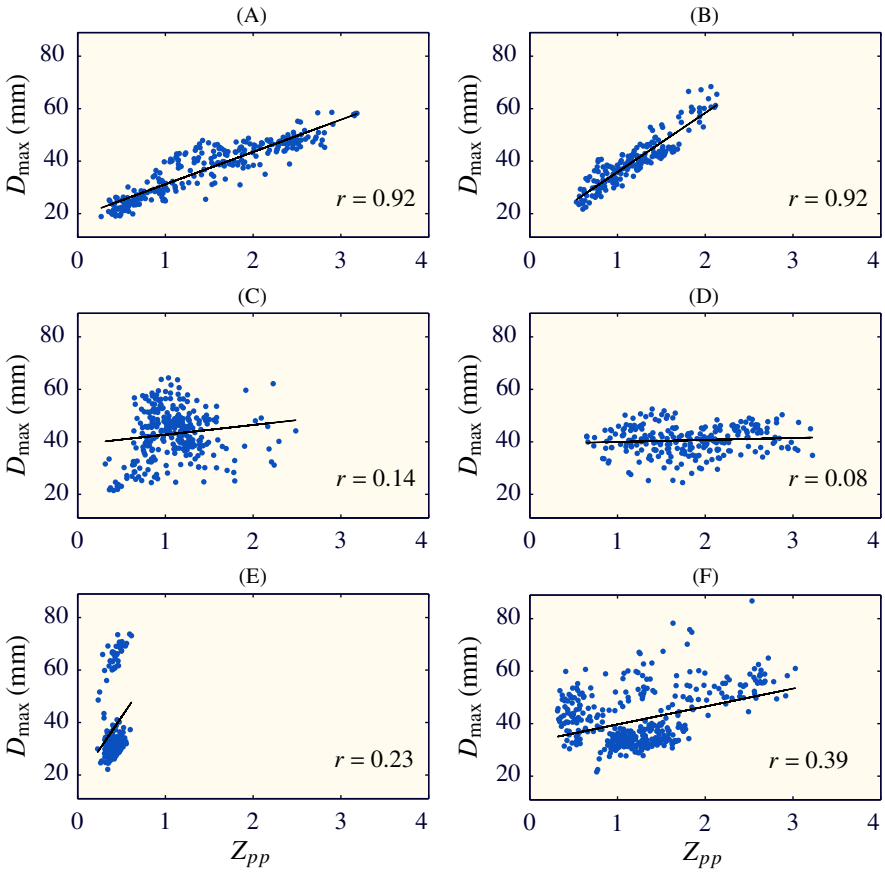

Figure 3.6: Scatterplot and linear model adjusted to Z_{pp} in six patients. Panels A and B represent cases where the model fits the data well and the correlation coefficient is high. For cases shown in panels C and D, the high dispersion of the data causes poor fitting and poor correlation. Finally, in panels E and F two different patterns may be identified.

Figure 3.7 shows the scatterplot for the nine series, in which the single-patient-single-rescuer pattern was maintained. Values for each series, a median of 28 (26, 40) data points per series, are

depicted in a different color along with the corresponding fitted model. The black line represents the model fitted to all the series when considered jointly: 320 values with a $D_{\max}$ of 48 (40, 56) mm. The individual analysis of each of the nine series yielded a median r of 0.81 (0.51, 0.83). However, when all of them were considered jointly, r decreased to 0.47.

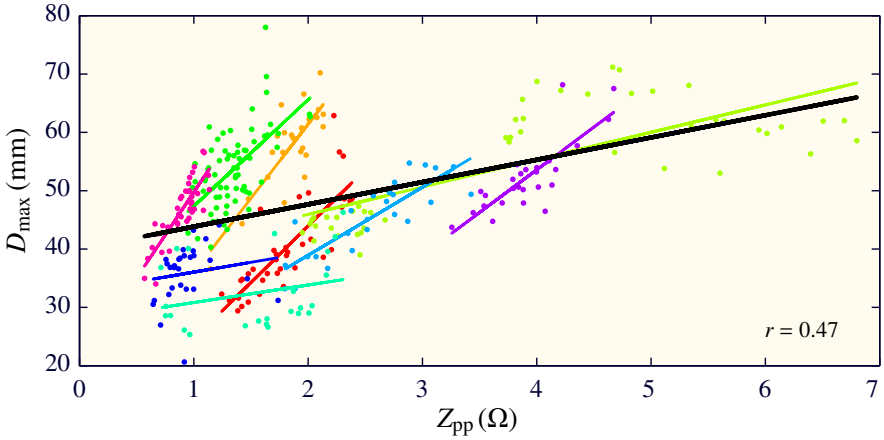

Figure 3.7: Scatterplot for chest compression series in which the single-patient-single-rescuer patent is maintained. The values and the regression line corresponding to each series are represented in a different color. The regression line fitted to all the data is depicted in black.

In Figure 3.8 the scatterplot for the set of twelve optimal and suboptimal series is presented, with a total of 390 values. For the optimal group, $D_{\max}$ was 57 (54, 63) mm, and Z_{pp} was 3.0 (2.5, 3.7) Ω. The suboptimal group had a median $D_{\max}$ of 32 (30, 34) mm, and a Z_{pp} of 0.9 (0.6, 1.5) Ω. The model fitted to the data is represented as a black line. We obtained a correlation coefficient r of 0.87.

In the discrimination analysis we evaluated the power of the TTI features to classify 5-s windows as shallow or non-shallow. Compression depths in the shallow group were 34 (31, 36) mm, and 48 (45, 53) mm in the non shallow one. The shallow group was composed of 2774 and 1174 values in the training and the test set, respectively, and the non-shallow group was composed of 4426 values for training and 1909 values for test. Table 3.1 shows the values of the features for the shallow and the non-shallow group. Mann-Whitney

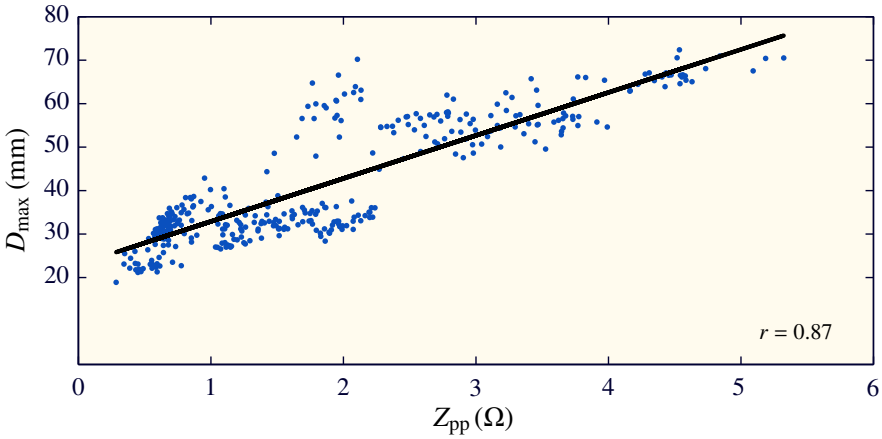

Figure 3.8: Scatterplot and regression line of D_{max} vs. Z_{pp} for the set of twelve optimal and suboptimal series. The regression line is depicted in black.

U test reported significant differences between groups for the three TTI features (p-value$<$ 0.01).

Table 3.1: Values of the three TTI features for shallow and non-shallow chest compressions.

	Feature		
Group	Z_{pp}	A	C
Shallow	1.1 (0.7, 1.5)	34 (23, 49)	2.4 (1.7, 3.2)
Non-shallow	1.5 (1.0, 2.3)	50 (33, 77)	3.4 (2.2, 5.0)

Figure 3.9 shows the probability distribution function of Z_{pp} for shallow (dark blue) and non-shallow (light blue) chest compressions. Although there were significant differences between medians, a high overlap between distributions was observed.

The logistic regression classifier showed a Se, Sp, and AUC of 90 %, 37 %, and 0.72, respectively in the training set. For the test set, Se, Sp, and AUC were 89 %, 49 %, and 0.8.

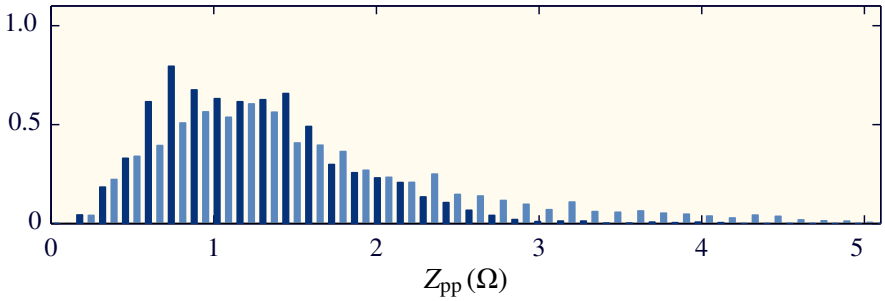

Figure 3.9: Probability distribution function of Z_{pp} for shallow (■) and non-shallow (■) chest compressions.

3.2.3 Discussion

Our study is a systematic and retrospective review of complete OHCA episodes representative of the population of patients and rescuers involved during CPR. The linear relationship between the compression depth and the features of the TTI waveform fluctuation was analyzed, and the power of the TTI to reliably discriminate shallow chest compressions quantified.

Some short communications pointed at the potential of TTI as a compression depth indicator.[24,42] Unfortunately, details on the analytical methods and the datasets used were not provided, so their results are not easily comparable to ours.

Our study included a set of episodes with a wide variety of patients and rescuers. A total of 60 patients with random physical characteristics and two to six rescuers attending each patient were considered. We used three features to characterize the fluctuation caused by the chest compressions in the TTI waveform (Z_{pp}, A, and C). The 14 424 values obtained for each feature showed very low correlation with D_{max} ($r < 0.38$ in any case). The clouds of the three scatterplots in Figure 3.5 demonstrate that the prediction of D_{max} with any of the features is highly unreliable. For instance, for any given Z_{pp} value the probability of error in the prediction of D_{max} is high because of the wide range of corresponding D_{max} values.

The large dispersion observed in Figure 3.5 was next studied by independently analyzing the episodes in order to suppress the variability introduced by different patients. The median r per episode was around 0.43 for any of the three parameters, slightly above that

obtained for the whole population. However, the variability between patients was large, with an r of $0.40\,(0.24, 0.66)$. Figure 3.6 shows the scatterplot of six distinct OHCA events where a different slope of the regression line is observed for every patient, which may reflect the individual patient-electrode characteristics. Sex, chest size, body mass, and pads position have been reported to affect the baseline TI,[58,60,88,97] and TTI amplitude fluctuations caused by ventilations have been shown to be correlated with the thoracic fat and the thoracic circumference.[79] Figure 3.6 also shows the variation in r values and in dispersion with respect to the regression line from one patient to another. When there is little dispersion and the slope is high enough, r is high, as can be observed in panels A and B. Conversely, if the dispersion is high and the slope low, then r will be low (panels C and D). Panels E and F depict episodes where two tendencies can be distinguished. This could be linked to two patterns for providing CPR by the rescuers involved in each OHCA event. In both cases a single regression model would hardly fit all the values.

The impact of several rescuers was eliminated in the series analysis shown in Figure 3.7, where the single-patient-single-rescuer pattern was maintained in every series. With a single rescuer the dispersion in each series notably decreased, resulting in an increased linearity between D_{max} and Z_{pp}, $0.81\,(0.51, 0.83)$. Nevertheless, inter-patient factors such as the chest/electrodes characteristics of the nine patients caused a low correlation, $r = 0.47$, when all the series were considered jointly, emphasizing the inability to define a confident linear fit.

In a recent study, Zhang et al. investigated the relationship between TTI changes and both compression depth and coronary perfusion pressure in a porcine model of cardiac arrest[171]. Two experts provided suboptimal (35 mm) and optimal (50 mm) chest compressions to fourteen pigs. The peak-through amplitude change of the TTI during each chest compression was averaged for every 5 s, obtaining a feature similar to our Z_{pp}. They found high correlation ($r = 0.89$) between that feature and D_{max}, and great differences in TTI amplitude between optimal and suboptimal depth groups (1.45 ± 0.37 vs. 0.47 ± 0.12, $p < 0.001$) with D_{max} (44.16 ± 4.61 vs. 29.06 ± 4.90 mm, $p < 0.001$).

Trying to replicate this experiment in humans, a set of twelve series with optimal and suboptimal chest compressions was extracted from different patients. There was a significant difference in Z_{pp} between groups (3.13 ± 0.93 vs. 1.07 ± 0.52, $p < 0.001$) with D_{max} (58.08 ± 6.40 vs. 31.35 ± 3.95 mm, $p < 0.001$) for optimal and suboptimal depth, respectively. The scatterplot obtained for D_{max} and Z_{pp} (see Figure 3.8) is very similar to the corresponding figure in the animal experiment (see Figure 2.6 in Chapter 2). Although in both cases the correlation coefficient is high (0.89 for animals and 0.87 for humans), for a given value of Z_{pp} D_{max} varied widely. For a proper interpretation of the high linearity observed, we should take into account the limitations of these analyses. On the one hand, if only optimal and suboptimal compressions are considered, a biased picture of the OHCA episodes is shown. When the complete range of compression depths is considered, the correlation coefficient r drops to 0.34, as can be observed in Figure 3.5. On the other hand, the set of patients and rescuers included was small (twelve patients/twelve rescuers and fourteen animals/two rescuers). When a greater variety was included, 60 patients and two to six rescuers, a high dispersion was observed in the scatterplot (Figure 3.5), and r decreased substantially.

Although TTI can be a good indicator for CPR quality parameters such as chest compression rate, chest compression fraction, or chest compression interruptions, in this study the TTI has proved unreliable to predict chest compression depth. Nevertheless, from a practical perspective, the power to discriminate shallow chest compressions was also analyzed. The 2005 resuscitation guidelines recommended chest compressions with depth in the range of 38–50 mm.[73] In our study 69.4 % of the chest compressions were above the recommended minimum threshold. We tried to discriminate the group of chest compressions with $D_{max} < 38$ mm from the group with $D_{max} > 43$ mm. The three TTI features showed different distributions ($p < 0.001$), but high overlap between the two classes. The logistic regression classifier revealed an AUC $= 0.71$ with the test set, which implied 86.2 % Se for detecting shallow chest compressions but 43.5 % Sp. It was thus not possible to safely identify shallow chest compressions using TTI.

3.3 Estimation of chest compression rate from TTI signal

Chest compression rate is an important quality parameter: a too low rate will not generate adequate forward blood flow, while a too fast rate may decrease depth[51,106] and not allow enough time for the heart to fill, thus decreasing the effectiveness of the compressions.[80] A recent prospective multicenter clinical trial showed that chest compression rates between 100 and 120 cpm were associated with the highest survival to hospital discharge.[81]

The TTI signal fluctuates for each compression around the patient's baseline impedance. The retrospective analysis of this signal has been proposed as a possible option for calculating CPR quality parameters for episode debriefing.[148] In fact, Codestat data review software automatically marks chest compressions by analyzing the TTI waveform.

Although the characteristics of these fluctuations are not well studied, it is accepted that they do not only reflect a real variation of the impedance of the thorax, as in the case of ventilations or circulation.[102,136] Evidence suggests that an important component of the fluctuations is an artifact generated in the electrode-skin contact.[53] As an artifact, its characteristics are influenced by many factors such as the TTI measurement system, the electrode type, the skin, the CPR performance (rate, depth, applied force, and acceleration), and the patient's chest stiffness.

During the development of this thesis work, our research group developed two automatic detectors of individual chest compressions in the TTI signal.[7,13] These methods detect chest compressions through a time-domain analysis of the amplitude and duration of the fluctuations. The ability of the algorithms to provide feedback on chest compression rate was evaluated. However, these algorithms were optimized and tested with subsets of a single database, and the TTI signals used in each study had common properties regarding the front-end for signal acquisition, the type of pads, and the rescuers' CPR performance. It is thus unclear if these algorithms are generalizable to other devices and settings.

The aim of this study was to determine the accuracy of a generic method to calculate and provide feedback on chest compression rate

for any system recording the TTI signal. The accuracy of the method in the calculation of two parameters for CPR quality debriefing, mean chest compression rate and chest compression fraction, was also evaluated. Our method does not rely on parameter optimization, and was tested on three independent OHCA databases with different characteristics to account for the variability of the TTI fluctuations and ensure that the results were generalizable.

3.3.1 Materials and methods

Data collection

Data were extracted from the three OHCA studies described in Section 3.1, compiled by different EMS systems and time periods during which different releases of international resuscitation guidelines were in effect (years 2000,[74] 2005,[73] and 2010[91]). Each database was derived from distinct monitor/defibrillators with different signal acquisition characteristics.

- Sister database, which consists of 364 episodes acquired in three European locations between 2002 and 2004, according to 2000 guidelines. Modified Heartstart 4000 defibrillators (Philips Medical Systems) were used to record the episodes. TTI was stored with a sampling frequency of 500 Hz and a bandwidth of 0–80 Hz.
- TVF&R database, comprising 623 episodes acquired by the Tualatin Valley Fire & Rescue (Oregon, USA) between 2006 and 2009, while 2005 guidelines were in effect. Heartstart MRx monitor/defibrillators (Philips Medical Systems) were used to record the episodes. TTI signal was acquired with a sampling frequency of 250 Hz and a bandwidth of 0–20 Hz.
- Oslo EMS database, which contains 370 episodes acquired in Oslo (Norway) between 2012 and 2013, according to 2010 guidelines. Lifepak 12/15 defibrillators (PhysioControl) were used to record the episodes. TTI was stored with a sampling frequency of 61 Hz and a bandwidth of 0.3–30 Hz.

All episodes contained the ECG and the TTI signals acquired through defibrillation pads. Sister and TVF&R databases included also a force signal that was acquired using an auxiliary chest pad.

We extracted the episodes that had the required signals correctly recorded and with at least 1000 chest compressions: 156/364 episodes in Sister, 136/623 in TVF&R, and 267/370 in Oslo EMS. We randomly selected sixty episodes per database for annotation and review, a sample expected to be sufficient to make clinically relevant distinctions based on our prior experience.[7,13] Table 3.2 summarizes the characteristics of the episodes extracted from each database.

Table 3.2: Characteristics of the episodes: duration (min), percentage of the episode in which the patient was intubated, chest compression fraction (CCF), percentage of the episode in which the patient had spontaneous circulation (ROSC period), and mean chest compression depth and rate per episode. All values are expressed as median (Q1, Q3). NA stands for Not Available.

	Sister ($n = 60$)	**TVF&R ($n = 60$)**	**Oslo EMS ($n = 60$)**
Duration (min)	27 (21, 34)	26 (18, 31)	29 (19, 41)
Intubation period (%)	90 (72, 97)	93 (83, 99)	91 (68, 97)
CCF (%)	67 (57, 78)	83 (78, 87)	89 (85, 92)
ROSC period (%)	0 (0, 3)	0 (0, 14)	0 (0, 8)
Compression depth (mm)	36 (29, 40)	40 (34, 43)	NA
Compression rate (cpm)	119 (111, 128)	109 (104, 116)	112 (103, 117)

Chest compression instants were annotated in the 180 episodes used in the study. For the Sister and TVF&R episodes we applied an automatic peak detector on the force signal with a fixed threshold of 2 kg. Two reviewers manually corrected the marks when necessary. For the Oslo EMS episodes we had the chest compression instants provided by the Codestat data review software. These annotations were checked independently by three reviewers and corrected, if necessary.

We discarded the signal in time intervals where the TTI was disconnected: 313 intervals in Sister (4.1 % of the time), 5 in TVF&R (0.1 %), and 137 in Oslo EMS (4.5 %). Intervals in which chest compression instants could not be reliably annotated were also discarded: 14 intervals in Sister (0.3 %), 23 in TVF&R (0.7 %), and 26 in Oslo EMS (0.3 %).

Calculation of the chest compression rate

The method was designed under the following specifications: ability to report chest compression rates between 60 and 210 cpm, minimum TTI sampling frequency of 20 Hz, and configurable feedback interval.

Chest compression rate is directly calculated in consecutive time intervals (analysis windows). We fixed the size of the analysis window to 2 s, but other window sizes could be used. For each analysis window, the gold standard for the rate was computed from the instants of the annotated chest compressions as GS (cpm) $= 60/\bar{T}$, where $\bar{T}$ is the mean time interval in seconds between consecutive compressions. Figure 3.10 shows an example in which for the selected analysis window (shaded in blue) the time intervals between compressions are $T_1 = 0.60$ s, $T_2 = 0.61$ s, and $T_3 = 0.61$ s, so the mean time interval is:

$$\bar{T} = \frac{T_1 + T_2 + T_3}{3} = 0.607 \text{ s.}$$

The gold standard in this case is GS (cpm) $= 60/\bar{T} = 98.9$ cpm.

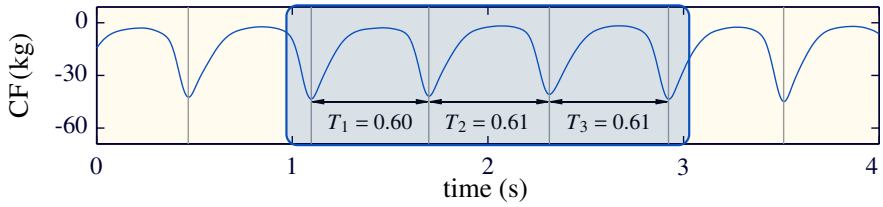

Figure 3.10: Computation of the gold-standard rate from the compressions annotated in the compression force signal (CF).

Chest compression rate for each analysis window is computed applying the following process:

- *Preprocessing:* The TTI signal is resampled to 20 Hz and filtered to suppress fluctuations out of the band of interest (60–210 cpm). Fast fluctuations and noise are suppressed using a 4th-order Butterword low-pass filter with a cut-off frequency of 3.5 Hz. The baseline of the impedance and low frequency fluctuations are removed using a 5th-order Butterword high-pass filter with a cut-off frequency of 1 Hz. Figure 3.11 illustrates the effect of

preprocessing the signal in the presence of some representative waveforms: slow TTI fluctuations induced by the ventilation of the patient (A), and spikes, probably induced by a deficient electrode-skin interface (B). For each analysis window, gold-standard rate (cpm) is shown at the top, in blue, and computed rate at the bottom, in red.

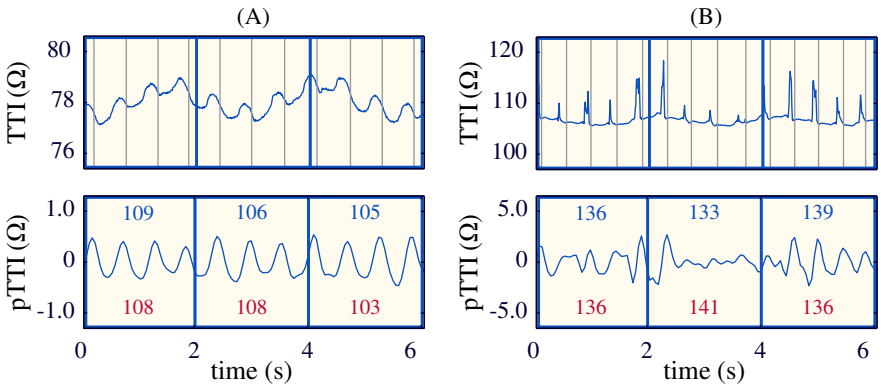

Figure 3.11: Intervals illustrating the effect of the preprocessing stage on the signal. In example A, the fluctuations induced by chest compressions are overlapped with slow fluctuations induced by ventilations. The impedance shown in example B has spike-like artifacts. Gold-standard and computed rates (cpm) are shown at the top and bottom of the second panel, respectively.

- *Energy analysis:* To decide whether each analysis window contains chest compressions, the amplitude of a sinusoidal signal with the same energy as the pTTI is computed. The decision is then made comparing this amplitude with a dynamic threshold.

  The energy of the signal is computed as follows:

$$E = \sum_{N} |\mathrm{pTTI}|^2 , \tag{3.4}$$

  where N is the number of samples of the window (in our case, $N = 40$).

Using Equation 3.5, the amplitude of a purely sinusoidal signal that has the same energy E than the real signal is computed:

$$A = \sqrt{2\frac{E}{N}} \quad (\Omega). \tag{3.5}$$

If this equivalent amplitude is below a certain threshold, the method decides that the window does not contain chest compressions, and a chest compression rate equal to 0 is reported. The threshold is initialized to $A_{\text{th}} = 0.1\,\Omega$, which corresponds to the minimum amplitude of the fluctuation to be considered. The threshold is then updated for each analysis window as a weighted average of the equivalent amplitudes of the last 5 analysis windows containing chest compressions. The value of the threshold is bounded between 0.1 and $0.35\,\Omega$. This avoids too low threshold values due to incorrect chest compression identifications or too high values due to noise in the signal. The dynamic threshold is used to account for within-episode variability of the amplitude induced by chest compressions.

- *FFT calculation:* Windows containing chest compressions are analyzed in the frequency domain to identify the dominant frequency in the band of interest. For that purpose, a Hamming window is applied and its 512-point FFT with zero-padding is computed. This provides the frequency spectrum of the pTTI signal, TTI(f).
- *Chest compression frequency identification:* Then, the dominant frequency f_0, i.e., the maximum peak of the amplitude spectrum, is identified in the band of interest (1–3.5 Hz). Depending on the TTI waveform, the dominant frequency may directly correspond to the mean chest compression frequency f_{cc} (chest compression rate in Hz) in the analysis window, as shown in the bottom panel of Figure 3.12A. In other cases, the TTI waveform presents a strong second harmonic, as in the example shown in Figure 3.12B. To correctly identify the compression frequency in these cases, if $f_0 > 2\,\text{Hz}$ the method looks for another peak of the spectrum around half the dominant frequency. If such a peak is found, its frequency is

considered the chest compression frequency of that analysis window.

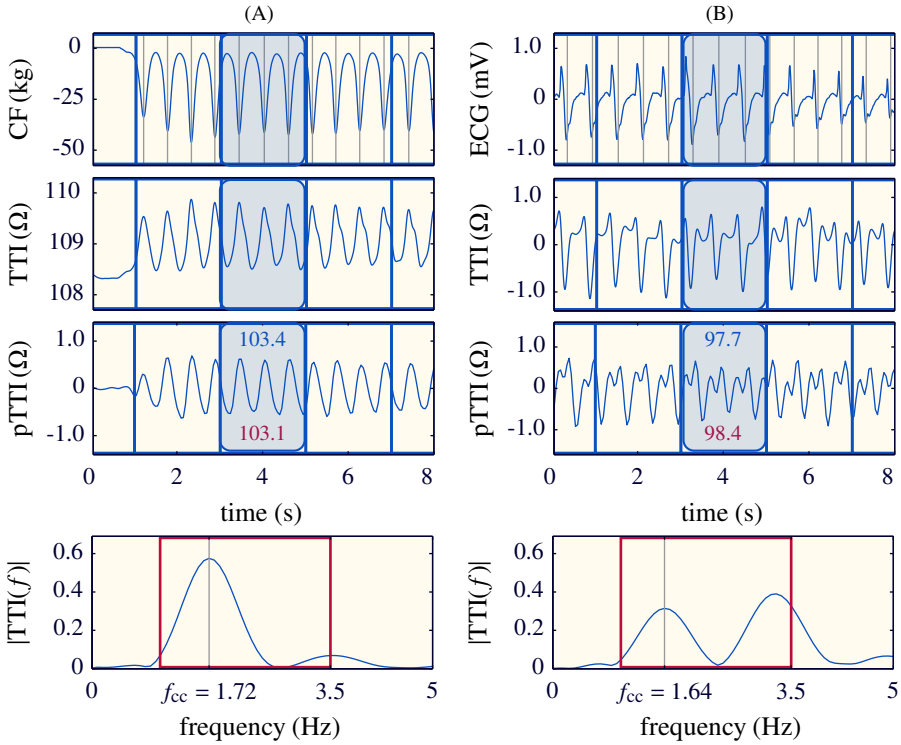

Figure 3.12: Graphical example of the method using two intervals from the TVF&R (A) and the Oslo EMS (B) databases. Gold-standard and computed rates are shown at the top and bottom of the third panel, respectively, expressed in cpm.

- *Chest compression rate calculation:* Finally, the rate of the chest compressions is computed from the f_{cc} value as:

$$\text{Chest compression rate (cpm)} = 60 \cdot f_{cc}\,(\text{Hz}).$$

Calculation of the chest compression fraction

Chest compression fraction was computed for each episode as the percentage of analysis windows that contained chest compressions. Intervals with spontaneous circulation were identified using the ECG, the force, and the TTI signal, and were excluded for the chest compression fraction calculation.

Performance evaluation and statistical analysis

Episodes were divided into non-overlapping 2-s analysis windows. Then, the performance of the method was assessed in terms of Se, i.e., the percentage of windows that did have compressions for which a chest compression rate was reported; PPV, defined as the percentage of windows that truly contained chest compressions from the total of windows for which chest compression rate was reported; and an accuracy factor (AF) that indicates the percentage of analysis windows for which chest compression rate was provided with an error below 10 % of the gold-standard rate. For the analysis windows for which chest compression rate was provided, the errors were plotted as a function of the gold-standard rate, and the 95 percentile of the unsigned error was computed.

The power of the method to provide alarms for non-adequate chest compression rates was evaluated. We adopted a tolerance of 10 cpm for the lower limit to avoid exposing the rescuer to excessive low-rate alarms, as suggested by Kramer-Johansen et al.[93] Thus, the limits used for analysis were 90–120 cpm.

Between-database comparisons were made using ANOVA for variables that passed the Lilliefors normality test, and using the Kruskal-Wallis test otherwise. Estimated and gold-standard metrics were compared using the Mann-Whitney U-test. A p-value < 0.05 was considered significant.

3.3.2 Results

Figure 3.13 shows the performance of the method for each database and for all the episodes jointly (i.e., the global results). Median (Q1, Q3) Se was 99.5 (97.4, 100.0) % , with no significant differences between databases ($p = 0.5$). Se was below 90 % in 6/60, 3/60, and 10/60 episodes for Sister, TVF&R, and Oslo EMS, respectively. Global median PPV was 98.6 (96.3, 99.5) %, and significant differences were found between databases ($p < 0.001$). PPV was below 90 % in 11, 2, and 1 episodes. The accuracy factor AF, with a median global value of 97.9 (94.7, 99.3) %, also presented significant differences between databases ($p < 0.001$). AF was below 90 % for 10, 6, and 0 episodes, respectively.

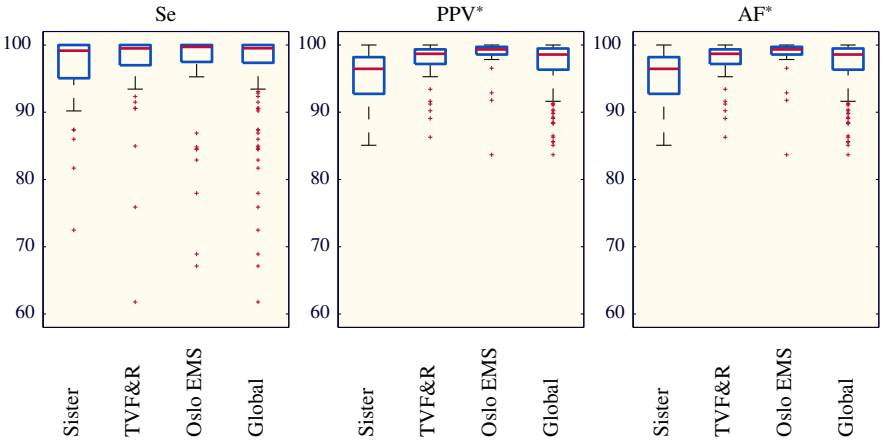

Figure 3.13: Distribution of the metrics per episode for each database and global values. The boxes show the median and interquartile ranges (IQR) and the whisker shows the last datum within the ± 1.5 IQR interval. Outliers are represented by red crosses. An asterisk (*) next to the title of the plot indicates statistically significant differences between databases in the metric.

Figure 3.14 shows a scatterplot of the errors of the estimated chest compression rates with respect to the gold-standard rate for each database. The median value of the unsigned error was 2.0, 1.9, and 1.5 cpm for Sister, TVF&R, and Oslo EMS, respectively. For 95 % of the analysis windows this error was below 13.8, 9.6, and 5.8 cpm, respectively.

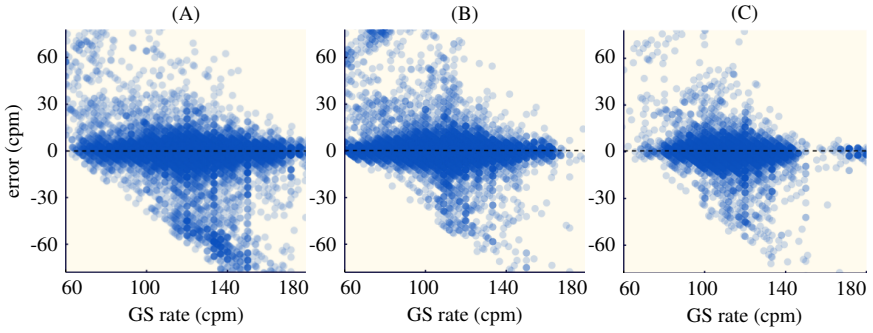

Figure 3.14: Scatterplot of the error in the estimation of chest compression rate with respect to the gold-standard rate in Sister, TVF&R, and Oslo EMS episodes, respectively.

Estimated mean chest compression rate per episode was 119 (111, 127) cpm, 110 (106, 116) cpm, and 110 (104, 117) cpm for Sister, TVF&R, and Oslo EMS, respectively. No statistical differences were found between the reference and the calculated values, and only in 1/180 episodes the error exceeded 10 %. Estimated chest compression fraction was 68 (58, 78) %, 82 (76, 86) %, and 87 (82, 91) %. No statistical differences were found for chest compression fraction either. The error in the estimation of the chest compression fraction exceeded 10% in 20/180 episodes (6, 4, and 10 for each database, respectively).

Non-adequate compression rates (below 90 cpm or above 120 cpm) were detected correctly with a median (Q1, Q3) of 99.7 (97.9, 100.0) % of the cases. Values per database were 99.2 (95.9, 100.0) %, 99.6 (98.0, 100.0) %, and 100.0 (98.1, 100.0) %, respectively. The number of episodes per database with more than 10 % of erroneous alarms were 4/60, 1/60, and 0/60, respectively.

3.3.3 Discussion

We have proposed a method for feedback on the chest compression rate based on the spectral analysis of the TTI signal. This approach is novel and has the advantages of being generalizable and not relying on algorithm training. The method was designed considering current recommendations for adequate chest compression rate,[91] and the state of the art knowledge on the characteristics of the TTI signal. Mean chest compression rate per episode and chest compression fraction can also be accurately computed applying this technique.

Performance of the method

Intervals with chest compressions were accurately detected, with a mean Se per episode of 96.3 % and a mean PPV of 97.0 %. Estimated chest compression rate was within 10 % of gold standard 95.8 % of the time. These results are comparable to those of recently published methods[7,13] based on detectors of individual chest compression instances. One of the studies[13] used 40 episodes from the Sister database. After optimization, a mean Se of 95.4 % and a mean PPV of 97.6 % per episode were reported. The method provided feedback on the chest compression rate every 5 s, and in 3.7 % and 1.3 % of the intervals the error exceeded 5 % and 10 %, respectively. The other

study[7] used 61 episodes from the TVF&R database and reported a mean Se of 97.2 % and a PPV value of 97.7 % with the 31 episodes of the test set. After adjusting the feedback intervals to 1.5 s, less than 6 % of feedback intervals had an error above 10 %. Both detection systems present the limitation of having been optimized and tested on OHCA episodes from the same database, which may share TTI characteristics. Our method does not rely on parameter optimization, and when tested on distinct databases provided similar performance in terms of Se, PPV, and accuracy.

The variability of TTI characteristics with factors including the TTI measurement front-end or the electrode type may help to explain the differences in the metrics for the three databases. Median PPV and AF were lower for Sister (96.5 % and 96.4 %, respectively), database that presented also the highest dispersion in the metrics. The Oslo EMS database presented the highest AF (99.0 %). For some of these episodes the use of a mechanical CPR device induced very regular TTI fluctuations, easier to detect by the spectral analysis. Additionally, reliance of the gold standard in the Oslo EMS database on the ECG and TTI signals may have caused overestimation of the accuracy metrics.

Figure 3.15 illustrates some of the typical errors influencing the metrics. In the third period of panel A and in the third and fourth periods of panel B, the equivalent amplitude was below the threshold as a result of a decrease in the amplitude of the fluctuations. Thus, the chest compression rate could not be identified, which lowered Se. The square waveform of panel B is probably caused by poor contact of the pads. Panels C and D show two examples of false positives during pauses in chest compressions. Fluctuations induced by patient's movement or disturbances in the skin-electrode contact (third period in panel C) and fluctuations induced by the fast ventilation of the patient (second and third periods in panel D) may be incorrectly identified as chest compressions. These kind of errors that affect PPV were more common in the Sister episodes. Finally, panels E and F show two examples of inaccuracies in chest compression rate estimation. In panel E, the TTI signal has a strong second harmonic component, which caused a reported chest compression rate twice the real one in the third period. In F, irregular fluctuations due

to noise in the TTI caused underestimated chest compression rate values, particularly in the third period.

Practical implementation

This method could be implemented in current AEDs to provide feedback on the chest compression rate. Various design alternatives could be considered. For example, chest compression rate values could be continuously presented in a display, either numerically or graphically (using a speedometer). In this scenario, the most significant errors would be those related to the accuracy of the reported values. Conversely, false chest compression rates due to TTI oscillations when the patient is being moved would have no impact, as the rescuer would know from the context to ignore feedback. Another implementation could be based on alerting the rescuer (visually, audibly, or either) only when the chest compression rate is inadequate. We reported a mean percentage of erroneous alarms per episode of 1.8 %, although for 5/180 records more than 10 % of alarms were erroneous.

These results were calculated assuming that a feedback value would be provided for each 2-s analysis window. However, the feedback interval should be adjusted to provide useful feedback without confusing the rescuer. The accuracy of the method with longer feedback intervals should be evaluated.

Metrics for debriefing

As a secondary goal, our method could also measure quality metrics per episode for debriefing. No statistically significant differences were found between the reference and the estimated mean chest compression rate and chest compression fraction for any of the databases. Traditionally compression-by-compression methods have been used to compute chest compression fraction.[82] Our frequency-domain approach is novel and has proven to be a viable alternative.

Limitations of the study

The algorithm was evaluated using episodes acquired with three distinct monitor/defibrillators. However, two of them (Heartstart 4000 and Heartstart MRX) were based on Laerdal technology, and shared some front-end characteristics. In any case, the three devices

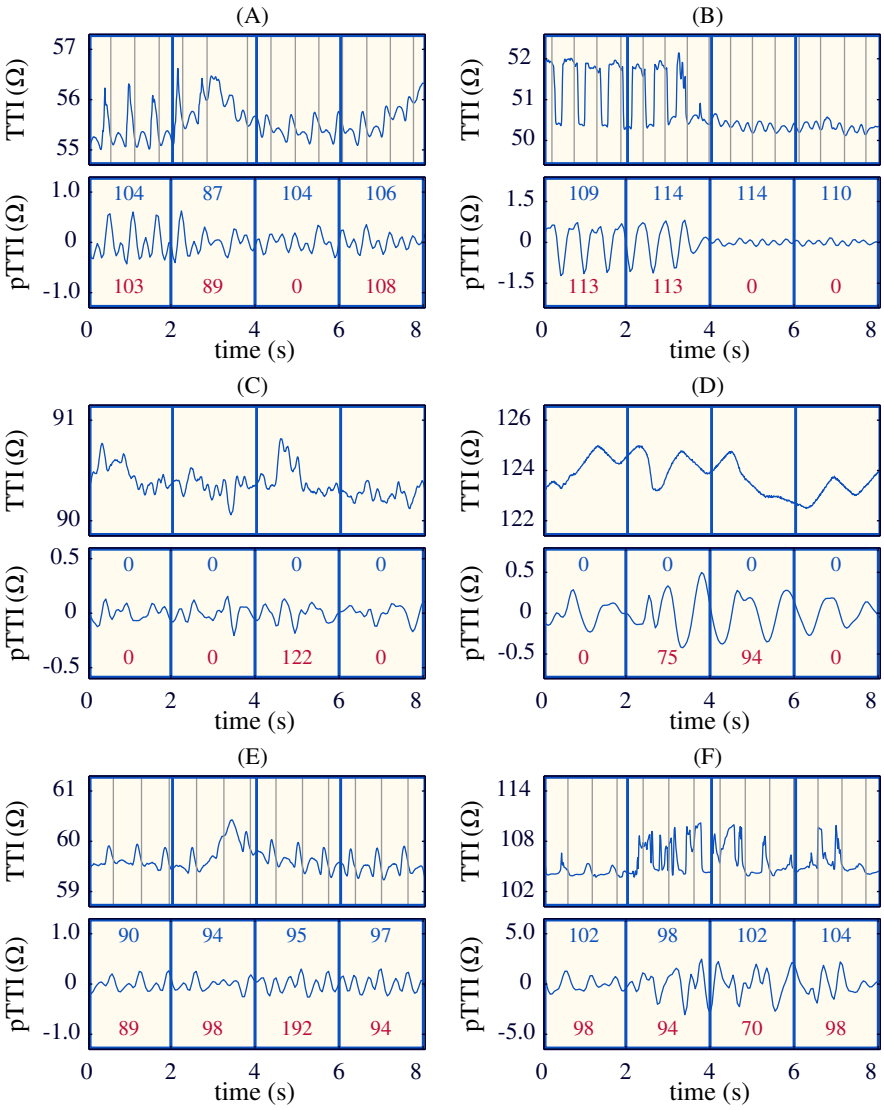

Figure 3.15: Examples of different types of errors of the method: chest compression intervals not detected (A, B), wrong chest compression rate feedback in the absence of chest compressions (C, D), inaccurate chest compression rate computation during chest compressions (E, F). Gray lines represent annotated chest compressions based on the force signal. Gold-standard rate values are shown in cpm at the top of the plots, and estimated values at the bottom.

had different TTI acquisition characteristics (sampling frequency and bandwidth), which introduced variability on the TTI fluctuations. Additionally, the three databases were collected by emergency services actively involved in resuscitation research. For some of the episodes defibrillators were used in manual mode, and in some of them feedback devices were used, so episodes may not be reflective of datasets from BLS settings. The results of this work should therefore be validated with a clinical study, integrating the algorithm into AEDs and evaluating how well it performs in a BLS system. Another issue is that parameters of the algorithm were fixed based on current recommendations for chest compression rate by resuscitation guidelines, which may change over time. However, these parameters could be easily adapted to reflect these changes. For the Oslo EMS database no independent signal, such as the force or the acceleration, was available to annotate the chest compression instants.

3.4 Summary and conclusions of the chapter

In this chapter we analyzed the potential use of the TTI signal acquired through defibrillation pads to provide feedback on chest compression quality. The characteristics of the fluctuations induced by chest compressions vary widely between episodes depending on the patient, on the front-end of the device, and on the electrodes used for signal acquisition, and even along the same episode depending on the rescuer. Despite this variability, we have successfully developed a method that accurately computes chest compression rate under a wide range of conditions without requiring parameter optimization. This could lower the barrier to implementation. In fact, Bexen cardio (Osatu S. Coop., Ermua, Spain) incorporates this technology in some of its defibrillators. In contrast, TTI features proved unreliable to predict chest compression depth and inaccurate to discriminate shallow chest compressions. The variability in TTI waveforms caused a very low correlation between TTI features and compression depth when a wide variety of patients and rescuers were included.

4 Acceleration for chest compression quality

Now I know I've got a heart,
because it's breaking.

— Frank Baum. *The Wonderful Wizard of Oz.*

The acceleration of the chest during CPR can be used to compute chest compression rate and depth and to provide feedback to the rescuers. This chapter is a compilation of two publications describing three methods to calculate compression rate and depth using exclusively the acceleration signal. In Section 4.1 the methods are described and their accuracy evaluated.[61] Then, in Section 4.2 one of the methods is analyzed in more detail, assessing the influence of the parameters of the method in the results.[143]

4.1 Methods to compute compression rate and depth from the acceleration signal

Most current real-time CPR feedback systems are based on the double integration of the acceleration to obtain chest displacement during CPR. The integration process is inherently unstable and leads to important errors unless boundary conditions are applied for each compression cycle. Commercial solutions generally use additional reference signals to identify the onset of each chest compression and establish these conditions. This section presents three methods to provide feedback on the compression rate and depth based solely on the acceleration signal.

The first method consists in applying double integration to compute the compression depth signal. This is the traditional approach, followed by most of the methods described in Chapter 2. In our proposal, integration was performed using a stable band-pass filter that approximated the trapezoidal rule while suppressing low frequencies of the signal. The second and third methods are original of this thesis work, and are characterized by not calculating the

compression depth signal: the second method computes velocity and calculates a compression rate and depth value for each compression, while the third one computes a rate and depth value for each analysis window (typically 2 s) from the spectral analysis of the acceleration signal. The accuracy of the three methods was evaluated with episodes of simulated cardiac arrest using a resuscitation manikin.

4.1.1 Experimental set-up and data collection

A Resusci Anne CPR manikin (Laerdal Medical, Norway) was equipped with a photoelectric sensor (BOD 6K-RA01-C-02, Balluff, USA) placed inside the chest to register the reference compression depth signal. This sensor is shown on the bottom right of Figure 4.1. Chest compressions were delivered in the center of the manikin's chest with a triaxial accelerometer (ADXL330, Analog Devices, USA) encased in a metal box placed beneath the rescuer's hands (see Figure 4.1). The compression depth signal and the three axes of the acceleration were digitized and recorded using a National Instruments acquisition card (USB NI 6211, USA) connected to a laptop computer, with a sampling rate of 100 Hz and a 16-bit resolution.

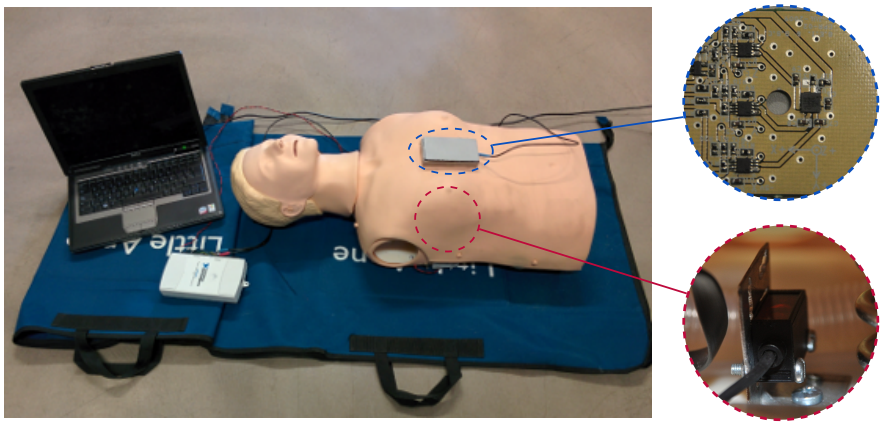

Figure 4.1: Experimental set-up: Resusci Anne manikin fitted with a photoelectric sensor (shown in the bottom circle), triaxial accelerometer encased in a metallic box positioned over the manikin's chest (shown in the top circle), acquisition card, and laptop computer.

Twenty-eight volunteers participated in the recording sessions. They were researchers, PhD candidates, and students, all of them collaborators of our research group. All participants received basic chest-compression-only CPR training and provided their written informed consent prior to participating in the recording sessions.

During these sessions they were grouped in couples. Four 10-min episodes were recorded per couple, each one with a different target compression rate (80, 100, 120, and 140 cpm), that was guided by a metronome. The target compression depth was 50 mm for all the episodes, and was guided using a custom-made computer program based on the reference depth signal recorded by the manikin's sensor. Volunteers alternated providing 2 min CPR series during each episode, each series involving thirty compressions with 5-s pauses in between. We compiled a total of 56 records.

4.1.2 Methods

In this section we describe three methods to estimate chest compression depth and chest compression rate during CPR by applying signal processing techniques exclusively to the acceleration signal.

Band pass filter (BPF)

As discussed in Chapter 2 Section 2.2.2, the system that applies the trapezoidal rule is characterized by the transfer function shown in Equation 4.1, which presents a pole in $z = 1$.

$$H_{\mathrm{TR}}(z) = \frac{T_s}{2} \cdot \frac{z+1}{z-1}, \tag{4.1}$$

where T_s is the sampling period. Analytically the filter is unstable. In practice, small low-frequency components in the input signal generate low-frequency components in the output with an amplitude that increases with time. If no detrending technique is applied to the output signal, the system could suffer an overflow.

The basis of our first approach is to approximate the integration by a stable band-pass filter. This system is the series connection of a high-pass filter and the trapezoidal rule system, which presents a low-pass

response. The purpose of the high-pass filter is to compensate the instability of the system for low frequencies.

The transfer function for the polynomial approximation of a high-pass filter of order n with a gain factor G is given by Equation 4.2:

$$H_{\mathrm{HP}}(z) = G\frac{(z-1)^n}{(z-z_{p1})(z-z_{p2})...(z-z_{pn})} = G\frac{(z-1)^n}{\prod_{i=1}^{n}(z-z_{pi})}, \quad (4.2)$$

where z_{pi} are the poles of the filter. This filter presents n zeros in $z = 1$, i.e., $f = 0$. When these two systems are put in cascade, we obtain the equivalent transfer function shown in Equation 4.3:

$$H_{\mathrm{BPF}}(z) = H_{\mathrm{HP}}(z) \cdot H_{\mathrm{TR}}(z) = G \cdot \frac{T_s}{2} \cdot \frac{(z-1)^{n-1}(z+1)}{\prod_{i=1}^{n}(z-z_{pi})}. \quad (4.3)$$

In the equivalent system, the pole of $H_{\mathrm{TR}}(z)$ and one of the zeros of $H_{\mathrm{HP}}(z)$ cancel each other, so the resulting system is inherently stable (all its poles are inside the unit circle). Figure 4.2 shows the magnitude of the frequency response of the band-pass filter, $H_{\mathrm{BPF}}(f)$, represented by a solid blue line. Note that for frequencies above 0.6 Hz the system matches the ideal response of the trapezoidal rule, depicted with a dotted red line.

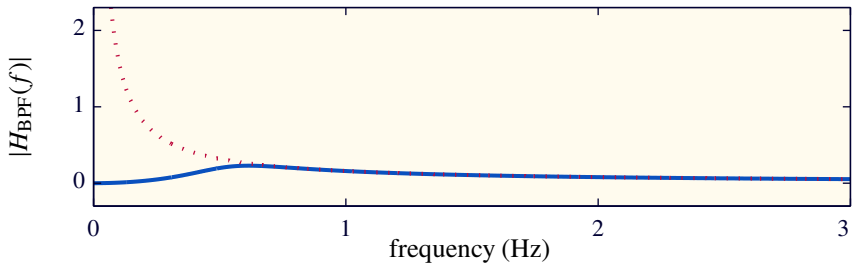

Figure 4.2: Frequency response of the band-pass filter (solid blue line) compared to the ideal frequency response of the trapezoidal rule (dotted red line).

Figure 4.3 shows an example of the computation of the compression depth signal with this method. The first step consists

on processing the acceleration signal $a(t)$ (first panel) with the band-pass filter once to obtain the velocity $v(t)$ (second panel). This process is then repeated with the velocity to obtain the compression depth signal $s(t)$ (third panel). Compared to the reference $s_r(t)$ (fourth panel), this signal has a different waveform because of the suppression of the low-frequency components and the waveform distortion caused by the filtering process. However, the depth and the rate of the chest compressions can be easily computed by applying a peak detector and measuring the peak-to-peak amplitude and the distance between the peaks, respectively. The detected compressions and their corresponding depth are depicted by vertical red lines in the third and fourth panels. In the bottom panel, the computed values are compared to the reference values (green lines) obtained from the recorded compression depth signal, $s_r(t)$.

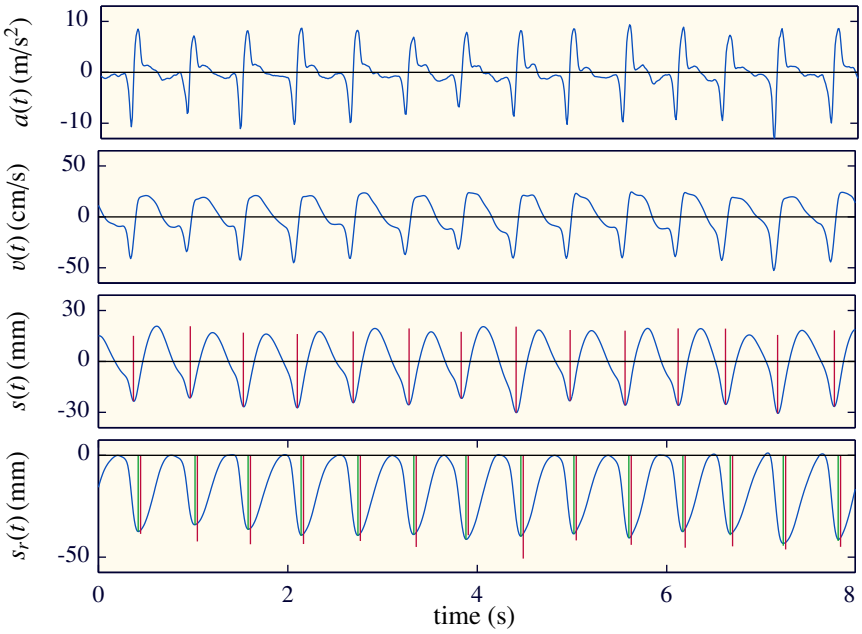

Figure 4.3: Graphical example of the BPF method, based on band-pass filtering.

Detection of zero-crossing instants in the velocity signal (ZCV)

The basic idea of this method is to calculate the compression rate and depth values directly from the velocity signal, without

computing the compression depth signal. First, the band-pass filter described in the previous section is applied to the acceleration to obtain the velocity signal. This signal is quite stable, and can be analyzed to identify the instants corresponding to the onset of each compression cycle and the points of maximum displacement of the chest, as shown in Figure 4.4. For that purpose, the zero-crossing instants of the velocity signal when it goes from positive to negative (onset of each compression, marked by red circles in the second panel of the figure) and when it goes from negative to positive (maximum displacement point, marked by black crosses) are identified. Then the compression depth corresponding to each cycle is computed as the area of the velocity signal between the onset and the maximum displacement point, filled in blue in the figure. In the bottom panel the computed values (red lines) are compared to the reference values (green lines), and drawn over the reference compression depth signal. The frequency of the chest compressions can be computed as the inverse of the interval in seconds between two zero-crossing instants from positive to negative.

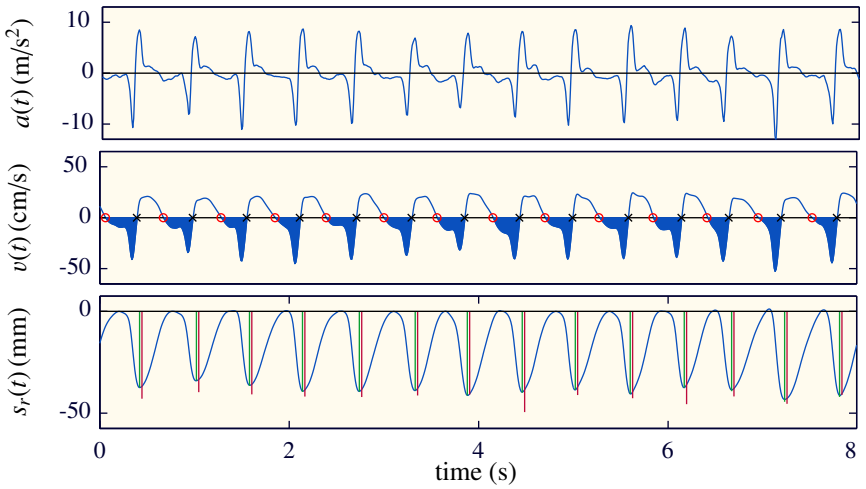

Figure 4.4: Graphical example of the ZCV method, based on the analysis of velocity.

Spectral analysis of the acceleration signal (SAA)

In this third method neither the compression depth nor the velocity signal are computed by integrating. Rather, the average

chest compression rate and depth are computed every 2 seconds by applying spectral analysis to the acceleration signal.[61]

We assume that during short intervals with continuous chest compressions, the acceleration and the displacement signals are quasi-periodic. Both signals can be modeled as a periodic acceleration and a periodic depth, with a fundamental frequency f_{cc} (Hz), which represents the mean frequency of the compressions during the interval. For each analysis interval of duration T_w, fixed in this case to 2 s, the acceleration $a(t)$ and the chest displacement $s(t)$ can be decomposed using the first N harmonics of their Fourier series representation (without DC component):

$$a(t) = \sum_{k=1}^{N} A_k \cos(2\pi k f_{cc} t + \theta_k) \tag{4.4}$$

$$s(t) = \sum_{k=1}^{N} S_k \cos(2\pi k f_{cc} t + \phi_k), \tag{4.5}$$

were A_k (m/s^2), θ_k (rad) and S_k (mm), ϕ_k (rad) are the amplitudes and phases of the k-th harmonic of the acceleration and of the depth, respectively. Since the acceleration is the second derivative of the displacement, the amplitudes and phases of $a(t)$ and $s(t)$ are related by the following equations:

$$S_k = \frac{A_k}{(2\pi k f_{cc})^2} \cdot 1000, \quad \phi_k = \theta_k + \pi, \quad \text{for} \quad k = 1, 2, \ldots, N \tag{4.6}$$

which can be used to reconstruct $s(t)$ once f_{cc}, A_k, and θ_k are obtained from the acceleration signal. The mean rate expressed in cpm and the mean peak-to-peak depth of the compressions within the analysis interval are then:

$$\text{rate (cpm)} = 60 \cdot f_{cc}\,(\text{Hz}) \tag{4.7}$$

$$\text{depth (mm)} = \max\{s(t)\} - \min\{s(t)\} \tag{4.8}$$

Based on this mathematical model feedback on the mean rate and depth for each analysis interval were obtained following these steps:

- The acceleration signal was windowed to select the analysis interval and its FFT with zero padding was computed. In the

example shown in Figure 4.5, the selected window is shaded in blue.

- The amplitude spectrum of the acceleration $|A(f)|$ was obtained from the FFT. The fundamental frequency f_{cc}, and the first three harmonics of the acceleration ($N = 3$ in equation 4.4) were identified using peak detection. Their amplitudes and phases were obtained from the FFT (middle panel of Figure 4.5).
- The equations shown in 4.6 were used to obtain the amplitudes and phases of the first three harmonics of $s(t)$.
- The displacement for the average compression cycle, i.e., one period of $s(t)$, was reconstructed applying Equation 4.5.
- Equations 4.7 and 4.8 were used to obtain the mean rate and depth for the analyzed interval.

The third panel of Figure 4.5 shows the reference compression depth signal (blue) and the reconstructed signal for the selected window (red). The reconstructed signal is periodic, so it has the same amplitude for all the compressions. This amplitude represents the average compression depth during the analysis window.

4.1.3 Performance evaluation

To evaluate the performance of each method, we calculated the error as the difference between the estimated rate and depth and the gold-standard values. To obtain the gold standard first we applied an automatic peak detector to the reference compression depth signal. For each identified peak (i.e., for each chest compression), the depth was computed as the peak-to-peak amplitude of the fluctuation (depicted by green lines in the bottom panels of Figure 4.3 and Figure 4.4). The rate was computed as the inverse of the distance in seconds between two consecutive compressions, multiplied by 60 to convert the units to cpm. These values were the gold standard for the BPF and the ZCV methods. The SAA method, however, provides one depth and one rate value every 2 s, and its gold standard was obtained as the average of the rate and depth values in the corresponding 2-s analysis window.

The distribution of the error in depth was analyzed using boxplots, while histograms and scatterplots were used to study the error in rate.

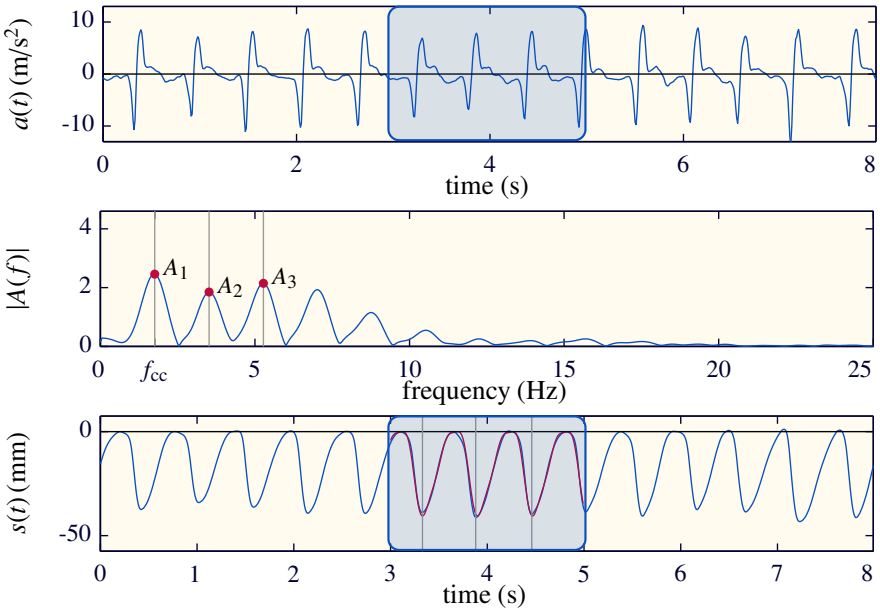

Figure 4.5: Graphical example of the SAA method, based on the spectral analysis of the acceleration.

Additionally, median and percentiles of the unsigned error (absolute and percent values) were measured. The influence of the target rate and the rescuer couple in the depth estimation was also analyzed.

As data did not pass the Lilliefors normality test, Kruskal-Wallis Analysis of Variance was used to perform between-groups comparisons. Differences in global errors by method, and for each of the methods by rate and by rescuer couple were evaluated. *P*-values < 0.05 were considered statistically significant.

4.1.4 Results

Figure 4.6 shows the boxplots of the error in the estimation of compression depth for each of the methods. On each box, the central mark is the median, and the edges of the box are the Q1 and the Q3 values. The whiskers extends to the most extreme data points not considered outliers, i.e., within the ± 1.5 IQR (inter quartile range) interval. There were statistically significant differences in the errors by method ($p < 0.001$). BPF and ZCV had a slight tendency to overestimate depth values, and the errors were smaller for SAA.

Table 4.1 shows median and percentile values for the unsigned error. Median (Q1, Q3) unsigned percent error was 5.9 (2.8, 10.3), 6.3 (2.9, 11.3), and 2.5 (1.2, 4.4) %.

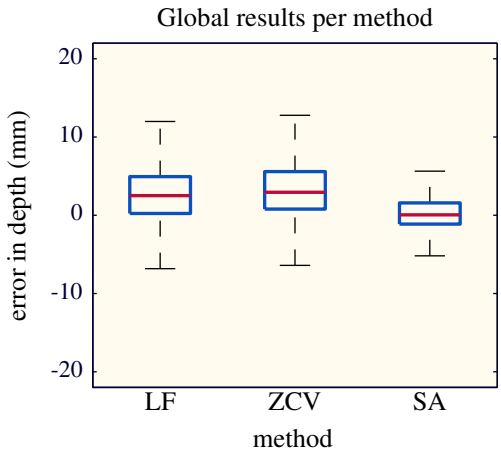

Figure 4.6: Boxplots of the global error in depth for the three methods.

Table 4.1: Global results per method. Unsigned error in depth (mm).

	Median	P_{25}	P_{75}	P_{90}	P_{95}
BPF	3.1	1.5	5.4	8.5	11.2
ZCV	3.4	1.5	6.0	9.5	12.9
SAA	1.3	0.6	2.3	4.0	5.9

Figure 4.7 shows the boxplots of the error in depth per target rate. There were significant differences in the errors per rate for the three methods (p-value < 0.001).

Finally, Figure 4.8 shows the error in depth estimation by rescuer couple. There were significant differences in the performance of each method for different couples (p-value < 0.001). Some of the couples presented higher errors in the estimation of the depth for all the methods.

With respect to rate estimation, histograms of the error in rate are shown in Figure 4.9, and Bland-Altman plots in Figure 4.10. Bland-Altman plots represent the agreement between the values

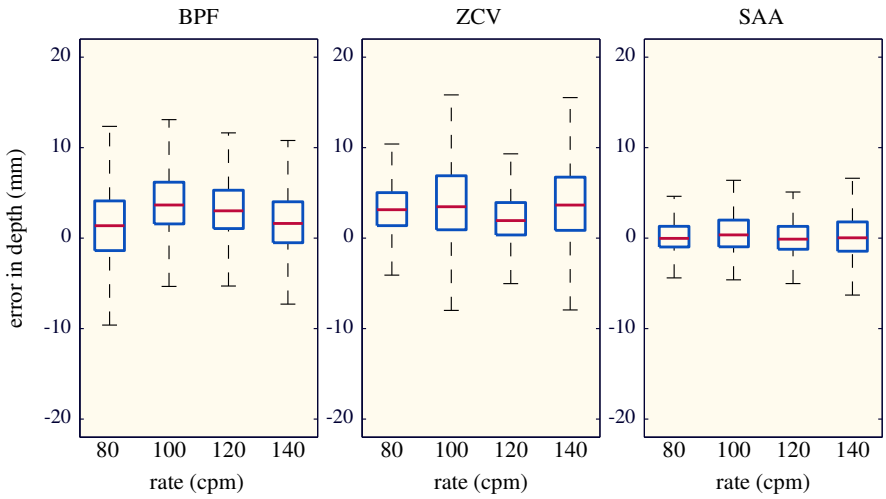

Figure 4.7: Boxplots of the error in depth for the three methods by target rate.

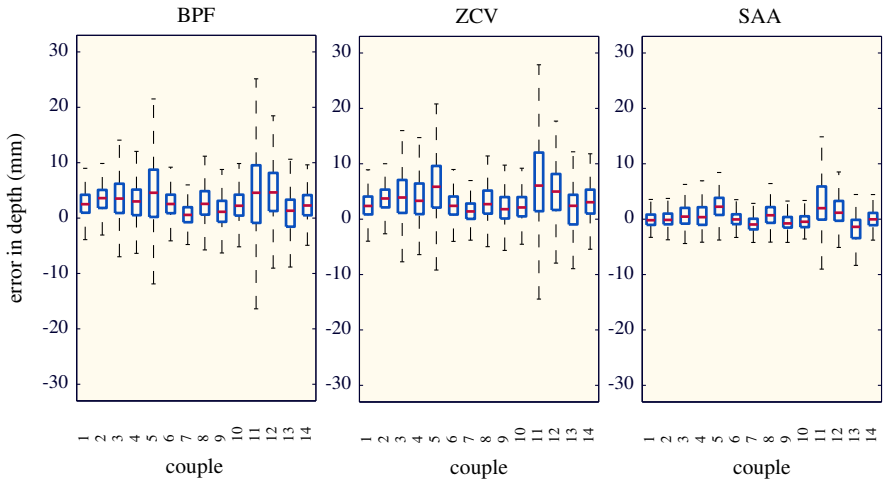

Figure 4.8: Boxplots of the error in depth for the three methods by rescuer couple.

obtained by the methods and the gold standard. The median and the 95 % limits of agreement (LOA) are depicted with dashed lines. The time-domain methods (BPF and ZCV) presented a very pronounced peak in zero in the histograms, while the errors for the SAA method followed a wider normal-like distribution. However, the BPF and ZCV methods presented some high errors (above 10 cpm), while SAA method presented lower errors and with a smaller variation by rate (see Figure 4.10). Table 4.2 shows median and percentiles of the unsigned error in rate. Median (Q1, Q3) percent error was 1.7 (0.0, 2.3) %, 0.0 (0.0, 2.0) %, and 0.9 (0.4, 1.6) % for BPF, ZCV, and SAA, respectively. SAA had the lowest 75 percentile for unsigned absolute and percent errors. However, these differences were not statistically significant (p-value = 0.43).

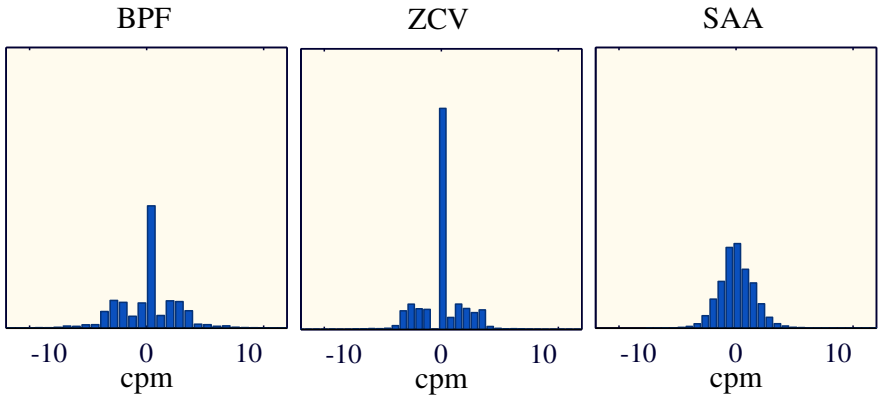

Figure 4.9: Histograms of the global error in rate for the three methods.

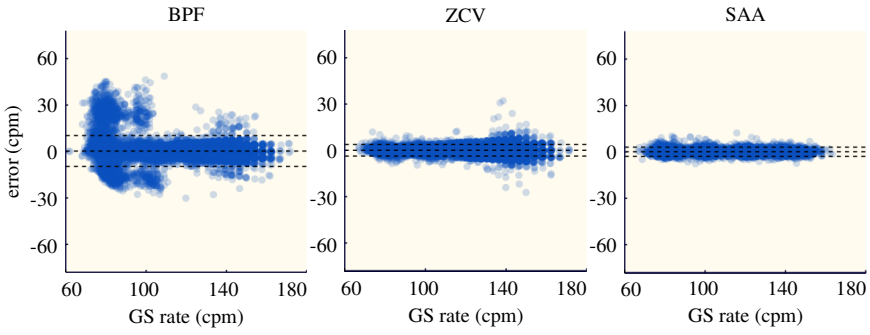

Figure 4.10: Bland-Altman plot of the rate estimation for the three methods.

Table 4.2: Global results per method. Unsigned error in rate (cpm).

	Median	P_{25}	P_{75}	P_{90}	P_{95}
BPF	1.7	0.0	3.1	4.8	8.5
ZCV	0.0	0.0	2.3	3.2	3.5
SAA	0.9	0.4	1.6	2.4	2.9

4.1.5 Discussion

This chapter presents three strategies for feedback on the rate and depth of the chest compressions by processing exclusively the acceleration signal, and assesses their accuracy in a simulated cardiac arrest scenario. Volunteers were grouped in couples and 30:2 CPR was provided on a manikin with a reliable reference compression depth signal.

BPF and ZCV methods reported important errors in the estimation of chest compression depth. In both approaches the error was above 5 mm in 25 % of the compressions, and they tended to overestimate the depth. In contrast, the SAA method was very accurate, with an error above 5 mm in only about 5 % of the cases, and it was not biased. Percent errors in depth were higher for the time domain methods: 5.9 % and 6.3 % for BPF and ZCV, respectively, compared to 2.5 % for SAA. Accuracy in the estimation of compression depth depended on the rate and on the rescuer couple ($p < 0.001$), but for any particular case the errors were smaller for the SAA method.

We used histograms and Bland-Altman plots to describe the performance regarding compression rate estimation. BPF presented high errors at low target rates, and its limits of agreement were the highest (LOA: -9.8, 10.3 cpm). The ZCV method improved this results (LOA: -3.7, 3.9 cpm), although the SAA method outperformed both time-domain methods (LOA: -3.0, 3.2 cpm). The accuracy of the time domain methods (BPF and ZCV) was strongly affected by the filter transient, particularly at the beginning of each compression series. This influence was higher for the BPF method, in which the filter was applied twice. On the contrary, the SAA method directly analyzed the acceleration without filtering, and it performed

robustly for a wide range of conditions. In any case, the percent error in rate was very low for the three methods (median of 1.7 %, 0.0 %, and 0.9 % for BPF, ZCV, and SAA, respectively).

Most current CPR feedback devices still rely on accelerometers and double integration to estimate depth. Manufacturers have conceived different solutions for the drift problem often protected by patent rights, based on either additional force or pressure sensors to detect each compression cycle (Q-CPR by Philips/Laerdal), or on advanced filtering techniques requiring reference signals (Real CPR Help technology by Zoll). TrueCPR device by PhysioControl based on triaxial electromagnetic field technology is a recent alternative to accelerometers. All these solutions lead to complex devices, limiting their widespread use in the practice, especially for bystanders.

The methods discussed in this paper are based solely on accelerometers and could lead to simpler and cheaper devices. However, they present two main limitations: they are not capable of detecting inadequate chest release between compressions and are inaccurate when CPR is applied on a patient lying on a soft surface, such as a mattress.[132] Inability to detect leaning during chest compressions is the current major drawback of our proposal, and, in general, of any attempt to derive feedback from only accelerometers. Currently accelerometer-based devices use force sensors to provide feedback on this quality parameter. That is the case of Q-CPR and of its standalone version, CPRmeter. Regarding the inaccuracy on soft surfaces, in Chapter 5 we present a solution to this problem based on the use of two accelerometers.

4.1.6 Practical considerations

In this chapter we presented three methods to provide feedback on chest compression rate and depth. The time-domain methods could be used for CPR quality assessment during training or debriefing. On the other hand, the algorithm based on the spectral analysis of the acceleration showed a very high accuracy and robustness, and it could be implemented for real-time feedback in the clinical practice.

A number of considerations should be taken into account in the process of implementing these methods. First, for the BPF method, a threshold value should be established for the detection of chest compressions in the computed compression depth signal. In this

case, fluctuations of the signal with a peak-to-peak amplitude above 20 mm were identified as chest compressions. Similarly, to detect zero-crossing instants in the ZCV method, positive and negative peaks of the velocity should be above 10 cm/s and below −10 cm/s, respectively. Finally, for the SAA method each analysis window should be classified as containing chest compressions or not. For that purpose the amplitude of a sinusoidal signal with the same energy as the acceleration in the analysis window was computed. If that equivalent amplitude was above 1.2 m/s^2, the window was considered to contain chest compressions, and the spectral analysis was performed. Otherwise, no compression depth or rate values were reported for that analysis window. This method presents a wide range of potential alternatives for implementation. The following section explores some of these alternatives and their influence on the accuracy of the method.

4.2 Parameter selection for the SAA method

In this section several alternatives for the practical implementation of the SAA method are analyzed. We first describe how some parameters of the method were fixed: the number of points of the FFT and the number of harmonics to consider in the reconstruction of the compression cycle. Then, the effect of using uniaxial or triaxial accelerations is evaluated both when the vertical axis of the accelerometer is perpendicular to the manikin's chest and when it is misaligned. Finally, we study how some other parameters related to how feedback is provided affect the results: the size of the analysis window T_w and feedback time T_f. To evaluate the influence of these variables independently of the presence of chest compressions, this analysis was performed with episodes in which compression-only CPR was provided to a manikin.

4.2.1 Experimental set-up and data collection

We used the experimental set-up described in Section 4.1.1, but with a sampling rate of 500 Hz. Twenty volunteers received basic compression-only CPR training before participating in two recording sessions: a *regular* session, in which the vertical axis of the accelerometer was perpendicular to the manikin's chest, and a *tilt*

session, in which it was misaligned by 18°, as shown in Figure 4.11. During each session the volunteers provided uninterrupted chest compressions during 60-s episodes. A total of eight episodes were registered per volunteer and session, combining different target rates (80, 100, 120, and 140 cpm) and depths (5 cm and 3 cm). A metronome was used to guide chest compression rate, and a custom-made computer program displayed the compression depth signal in real-time to guide chest compression depth. A total of 320 1-min records were obtained.

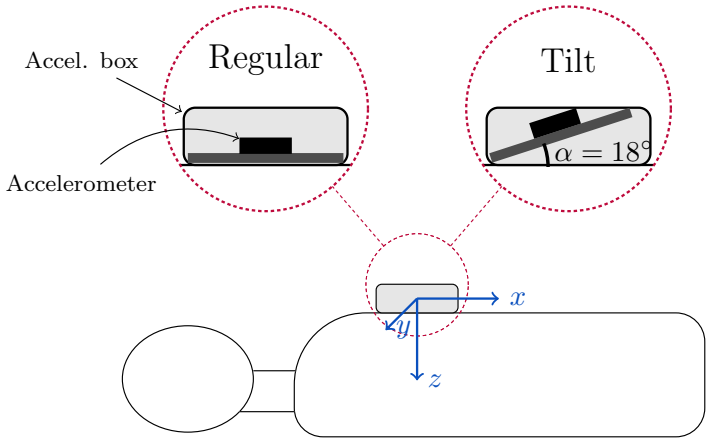

Figure 4.11: Positioning of the accelerometer within the enclosure for the regular and tilt sessions. During each recording the enclosure was kept fixed to the manikin's chest.

4.2.2 Methods

Signal preprocessing

The recorded signals were preprocessed with a third-order Butterworth low-pass filter (cut-off frequency 15 Hz) to suppress high-frequency noise, and resampled to 100 Hz. Chest compressions were automatically identified in the reference compression depth signal using a peak detector with a fixed threshold of 20 mm, and the annotations were then manually reviewed.

Estimation of mean compression rate and depth

Compression rate and depth were analyzed applying the SAA method described in Section 4.1.2. Several parameters of the method

were fixed to simplify the experiments. First, a Hamming window was used for spectral analysis because it provided an adequate trade-off between leakage and resolution. The number of points of the FFT was fixed to 2048, which for a sampling frequency of 100 Hz gives enough frequency bins to accurately resolve the chest compression frequency, f_{cc}. The number of harmonics was set to $N = 3$ because S_k rapidly decreases as the harmonic number k increases, as shown in Equation 4.6. This was confirmed by analyzing the average power spectral density (PSD) of the triaxial acceleration and the compression depth signal. For example, Figure 4.12 shows the PSD analysis of the regular session with a target depth of 5 cm and a target rate of 100 cpm. Harmonics higher than the 3rd ($k > 3$) are visible in the acceleration but negligible in the compression depth signal.

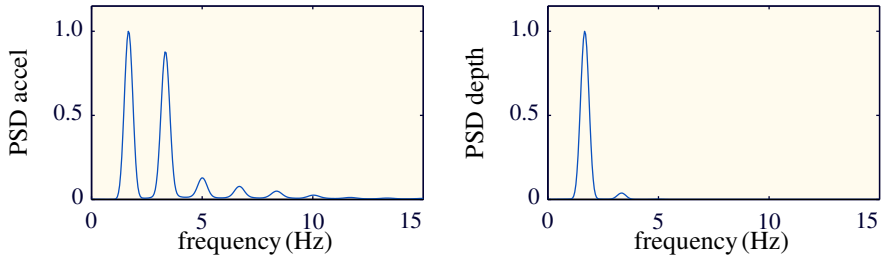

Figure 4.12: Normalized average PSD of the recorded acceleration and compression depth for the regular session with a target depth of 5 cm and a rate of 100 cpm. The DC component was removed from the compression depth signal before the spectral analysis.

We assumed that feedback would be given at the end of each analysis window. The frequency with which feedback is given to the rescuer can be set independently of the duration of the analysis window T_w. For that purpose, consecutive analysis intervals can be partially overlapped; the displacement of the window will correspond to the feedback time T_f. For example, a window size of 3 s, $T_w = 3$ s could be used to provide feedback each second, $T_f = 1$ s, with an overlap of 2 s between consecutive analysis windows.

Performance evaluation

For each analysis window, the rate and depth feedback values obtained by the method were compared to those obtained from the distance sensor placed inside the manikin.

Initially, records were divided into non-overlapping consecutive analysis intervals of duration T_w. Thus, feedback time was equal to the window duration, i.e., $T_f = T_w$. Errors in rate and depth were obtained for every analysis window. To analyze the effect of the relative position of the accelerometer and the manikin's chest, two different accelerations were considered: a uniaxial acceleration (vertical axis), and a triaxial acceleration, obtained by composing the three orthogonal axes. The root mean square error (RMSE) of all feedbacks in a session (regular or tilt) was computed for uniaxial and triaxial accelerations as a function of the duration of the analysis window, T_w.

Then, for window sizes of 2 s, 3 s, 4 s, and 5 s, the influence of feedback time T_f was analyzed. RMSE for rate and depth estimation when using the triaxial acceleration were computed for the regular and for the tilt session.

Finally, the mean rate and depth per record were analyzed for the different targeted CPR test conditions. The distributions of the mean rate and depth did not pass the Kolmogorov-Smirnov normality test and are presented as median (5–95 percentiles). Mann-Whitney U test was used to compare the median values obtained from the gold standard and from the method for triaxial acceleration with $T_w = T_f = 3$ s. Differences were considered significant for p-values < 0.05.

4.2.3 Results

The dataset comprised 320 episodes with a total of 35 312 compressions. Figure 4.13 shows the RMSE as a function of T_w. For T_w between 2 s and 5 s the RMSE for rate and depth were below 1.5 cpm and 2 mm, respectively, except for the uniaxial acceleration in the tilt session in which the RMSE for depth was always above 4 mm.

Figure 4.14 shows the influence of changing feedback time by overlapping analysis windows. Errors do not significantly change

with feedback time. Finally, Table 4.3 compares the mean rate and depth per episode obtained from the gold standard and from the triaxial acceleration when $T_f = T_w = 3\,\text{s}$. There were no significant differences between the method and the gold standard for any of the CPR target conditions.

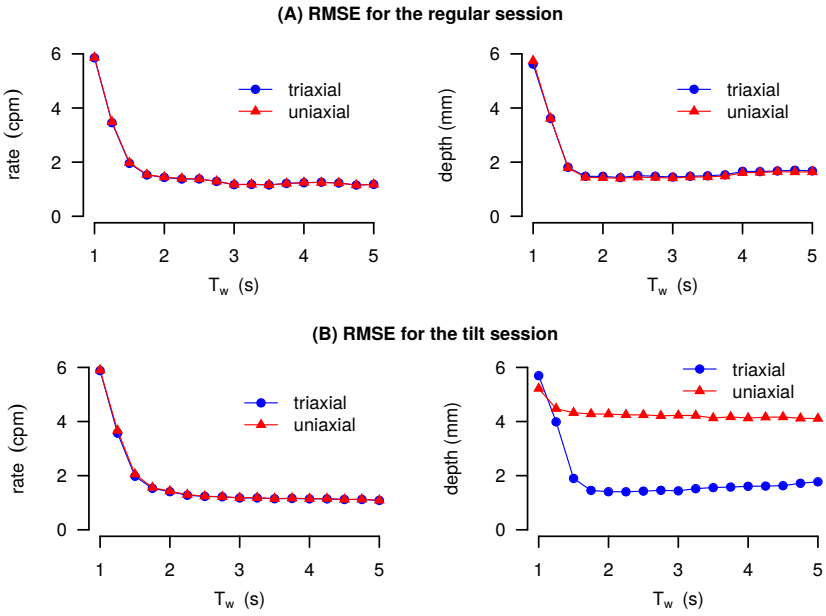

Figure 4.13: RMSE in mean rate and depth for the regular session (top) and the tilt session (bottom), as a function of the duration of the analysis interval. Results for uniaxial and triaxial accelerations are compared. All calculations were done for non-overlapping analysis intervals.

4.2.4 Discussion

We tested the algorithm in a manikin platform for a wide range of controlled conditions: different rescuers, target depths and rates, and changes in the relative position of the device and the chest.

Misalignment between the device and the chest was tested for two reasons. First, although the device is usually in contact with the patient's chest, the sternum may not be completely horizontal due to anatomical considerations. Second, other suitable positions of the

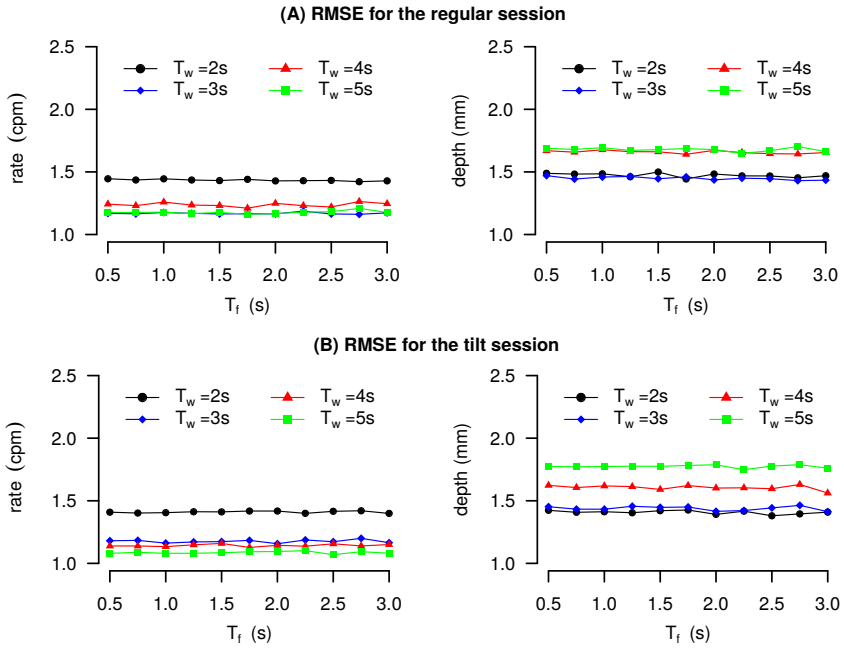

Figure 4.14: RMSE in rate and depth with the triaxial acceleration for different feedback times (T_f) and different durations of the analysis interval (T_w). The top and bottom panels show the results for the regular and the tilt sessions, respectively.

Table 4.3: Median (P_5–P_{95}) of the mean rate and depth per record for the regular and tilt sessions with $T_w = 3$ s. No significant differences were observed for any of the CPR target conditions between values obtained from the reference (CD signal) and from the acceleration (Accel. signal).

	Regular session		Tilt session	
Target	**CD signal**	**Accel. signal**	**CD signal**	**Accel. signal**
Rate[a]				
80 cpm	81 (77–85)	81 (78–85)	80 (78–84)	80 (78–84)
100 cpm	100 (98–102)	100 (97–102)	100 (97–105)	100 (96–105)
120 cpm	121 (117–124)	120 (118–124)	120 (117–124)	120 (117–124)
140 cpm	140 (134–142)	140 (135–142)	140 (135–143)	140 (135–143)
Depth[b]				
30 mm	30 (28–33)	30 (27–34)	30 (28–33)	30 (27–33)
50 mm	50 (45–54)	50 (46–55)	52 (49–55)	53 (49–57)

[a]40 records per session, [b]80 records per session.

device could be envisioned, such as on top of the hand or fixed to the wrist of the rescuer. In those situations tilt may vary during chest compressions.

For analysis intervals in the 2–5 s range RMSE in rate and depth estimation were below 1.5 cpm and 2 mm respectively when triaxial acceleration was used, which guarantees a very accurate feedback. However, in the tilt session using the uniaxial acceleration the RMSE for the depth raised unacceptably (> 4 mm).

Increasing the frequency with which feedback is given did not compromise the accuracy of the method (see Figure 4.14). The possibility to independently control the analysis interval and feedback frequency makes the method very flexible. However, this process increases the computational demands of the method, because for an equal analysis interval the method is applied more often.

4.3 Summary and conclusions of the chapter

In this chapter we described three methods to estimate compression rate and depth from the acceleration signal. The SAA method stands out because of the high accuracy it presents in a wide range of conditions. This novel method directly obtains the mean compression rate and depth of each analysis window without calculating the compression depth signal. It depends only on the spectral components of the acceleration between the first and third harmonics, i.e., on the components between 1–9 Hz for the compression rates found in practice (60–180 cpm). Consequently the method is unaffected by DC drifts, baseline oscillations, or high frequency noise components of the acceleration.

The method could be implemented in commercial devices to provide audible or visual alarms to the rescuers when compression rate or depth do not meet the recommendations. It is protected by industrial property rights.[140] The patent describes the method and some possible embodiments, based on two basic approaches: a stand-alone device that measures acceleration and provides feedback on its own, and a dependent device that works connected to a defibrillator.

Bexen cardio (Osatu S. Coop, Ermua, Spain) has developed a prototype of the dependent device. This prototype measures triaxial acceleration and sends it to the defibrillator, where it is processed to provide feedback to the rescuer.

5 Challenges in feedback devices based on acceleration

"Would you tell me, please, which way I ought to go from here?" "That depends on a good deal on where you want to get to," said the Cat.

— Lewis Carroll. *Alice's Adventures in Wonderland.*

Feedback devices based on the acceleration signal present certain limitations that should be investigated. This chapter compiles three studies that analyzed the behavior of the feedback method based on the spectral analysis of the acceleration signal (SAA method, described in Chapter 4) in three challenging situations: (1) when chest compressions are provided to a patient placed on a soft surface;[141] (2) when the feedback device is fixed to the rescuer's back of the hand, to the wrist, or to the forearm, instead of being placed between the chest of the patient and the rescuer's hand;[142] (3) when CPR is performed in a moving vehicle, particularly in a long-distance train.[63,64] In this last scenario, the performance of two commercial feedback devices, CPRmeter and TrueCPR, was also analyzed.

Section 5.1 describes the general experimental set-up used in the three studies. Then, Section 5.2 presents a solution for accurate feedback on soft surfaces using two accelerometers. Section 5.3 evaluates the performance of the SAA method when the accelerometer is placed in different positions. Finally, Section 5.4 analyzes the reliability and accuracy of the SAA method, CPRmeter, and TrueCPR, in a moving long-distance train. Most of the results described in this section have been presented at international conferences[63,64,141,142] or published in indexed journals.[139]

5.1 Experimental set-up

A Resusci Anne CPR manikin (Laerdal Medical) was equipped with a resistive sensor (SP1-4, Celesco, USA) placed inside the chest of the manikin to measure the reference chest displacement signal,

as shown in Figure 5.1 (top). This sensor replaced the photoelectric sensor used in the studies described in Chapter 4, because its linear response facilitated the calibration process.

Chest compressions were provided in the center of the manikin's chest. Compression rate was guided using a metronome, and compression depth by a custom-made computer program based on the reference compression depth signal. Additionally, in some of the experiments, described in Section 5.2, a second accelerometer encased in a metallic box was placed beneath the manikin's back. For other measurements, described in Section 5.4, either CPRmeter (Laerdal Medical) or TrueCPR (PhysioControl) commercial devices were placed between the rescuer's hands and the chest of the manikin, as shown in Figure 5.1 (bottom). The devices used for each study are specified in the corresponding section.

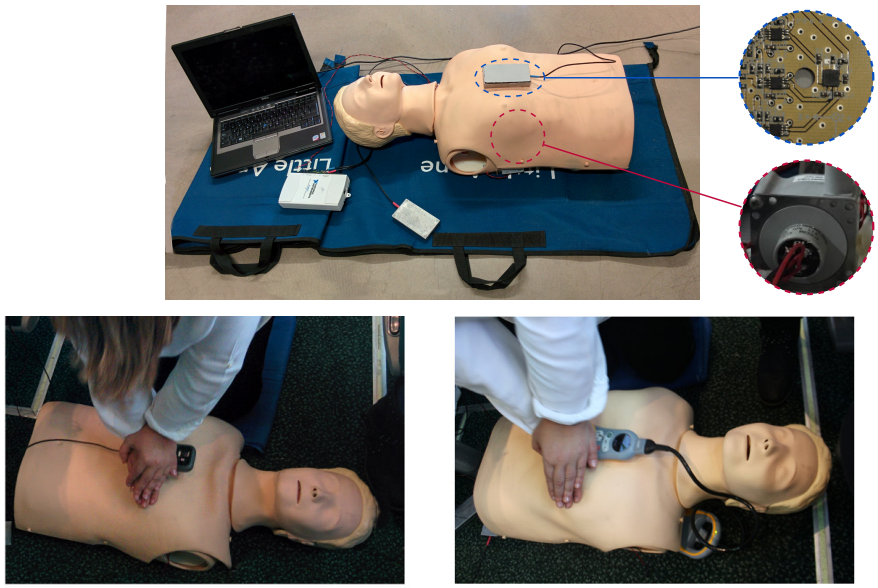

Figure 5.1: Experimental set-up: Resusci Anne manikin fitted with a resistive sensor, two triaxial accelerometers, acquisition card, and laptop computer (top). Placement of CPRmeter (bottom left) and TrueCPR (bottom right) during the measurements.

The reference compression depth signal and the accelerations were digitized using a data acquisition card (USB NI-6211, National

Instruments) connected to a laptop computer, with 16-bit resolution. A custom-made Matlab program controlled the acquisition process.

5.2 CPR feedback on soft surfaces

When cardiac arrest occurs in hospital, the patient is usually lying on a soft surface such as a bed. Mattresses tend to deform and move downwards during CPR, thus reducing the efficiency of chest compressions.[131,155] The work required to perform CPR increases in proportion with the distance traveled by the rescuer's hands, so the compression of the mattress increases workload, and consequently also rescuer fatigue.[117]

Resuscitation guidelines recommend providing CPR on firm surfaces when possible.[91] Transferring the patient to the floor would ensure a firm surface, but it cannot always be done safely and promptly. Another alternative would be the use of backboards, which can be placed beneath the patient during CPR to increase the area over which the compression force is spread and reduce the amount of mattress compression. However, it is not clear if the use of backboards alone improves compression depth.[8,132,133]

The deformation of the mattress during CPR is variable, dependent on factors such as target depth, patient weight, type of mattress, and the use of a backboard.[117] This makes it difficult for rescuers to assess whether they are providing chest compressions with an adequate depth.[155] The use of monitoring and feedback devices during CPR can help rescuers to improve chest compression quality. However, devices that do not take into account the underlying mattress will overestimate compression depth. Accelerometer-based devices measure chest displacement. When chest compressions are provided on a mattress, they sense the sum of the chest compression (sternal-spinal displacement) plus the mattress deflection.[30,115] Assuming that chest displacement corresponds to chest compression, these devices will incorrectly coach the rescuers, potentially causing too shallow chest compressions.

In this section we present a solution to provide feedback on chest compression depth and rate when CPR is performed on soft surfaces based on applying the SAA method described in Chapter 4 to two accelerometers. One is placed on the chest of the patient

and measures chest displacement (sternal-spinal displacement plus mattress deflection), while the other is placed on the back of the patient and measures mattress deflection. The difference between the depths calculated by the SAA method applied to each of the accelerometers will correspond to the chest compression depth, that is, the sternal-spinal displacement.

5.2.1 Data collection

We placed weights inside the sensorized manikin described in Section 5.1 to increase its weight up to 20 kg. This provided a more realistic simulation of a human torso lying on a mattress. Lighter bodies sink less into the mattress and thus have more potential for mattress deformation. The manikin was placed on a mattress (light gray in Figure 5.2), with or without a backboard beneath its back (represented by a dark gray rectangle in the figure). Two mattresses were tested, foam and sprung, with a thickness of 9 cm and 10 cm respectively. During CPR, one accelerometer was placed on the center of the manikin's chest and another one beneath the manikin's back.

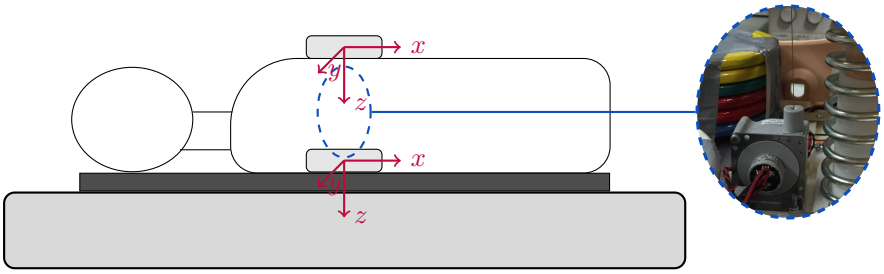

Figure 5.2: Experimental set-up. A resuscitation manikin fitted with a displacement sensor and loaded with weights (see right side of the figure) was placed on a mattress, with or without a backboard beneath its back (represented by a dark gray rectangle). A triaxial accelerometer was placed on the chest of the manikin and another one beneath its back.

Eight rescuers grouped in couples participated in the data collection. Twelve 3-min episodes per couple were acquired. Each episode comprised a first minute of continuous chest compressions and two minutes of series of 30 compressions with 5-s pauses in between. Target compression depth was always 5 cm. Episodes were

recorded for three different target rates (80, 100, and 120 cpm), for each of the two mattresses with and without the blackboard. A total of 48 records were compiled, with a sampling frequency of 250 Hz.

5.2.2 Data analysis and performance evaluation

Episodes were divided into 2-s analysis intervals. For each interval, we applied the SAA method to the chest acceleration to compute chest displacement, d_{chest}, and to the back acceleration to obtain mattress displacement, d_{mat}. Then chest compression depth was calculated as the difference between both values: $d_{\text{cc}} = d_{\text{chest}} - d_{\text{mat}}$. Chest compression rate was calculated from the fundamental frequency of the chest acceleration, as described in Chapter 4. Depth and rate values were compared to those obtained from the reference compression depth signal, d_{ref} and r_{ref}, respectively. The distribution of the error was analyzed using boxplots and Bland-Altman plots. Values are presented as median (Q_1, Q_3). Wilcoxon rank sum test and Kruskal-Wallis test were used to perform between-groups comparisons, and p-values< 0.05 were considered significant.

5.2.3 Results

Table 5.1 shows the computed chest and mattress displacement, the reference chest compression depth, and the unsigned error in the estimation of the chest compression for the different mattress/backboard combinations. Mattress compression was significantly higher for the sprung mattress ($p < 0.001$) and for both mattresses it was significantly reduced with the use of backboard ($p = 0.002$ and $p < 0.001$ for foam and sprung, respectively). The error in depth estimation depended on the type of mattress used and on the target compression rate ($p < 0.001$).

Median unsigned error in rate estimation was $0.9\,(0.4, 1.6)$ cpm, and its 95th percentile was 2.9 cpm. No statistically significant differences were found in errors in rate for the different test conditions.

Figure 5.3 shows the distribution of the error in depth depending on the mattress/backboard combination (left) and the global distribution of the error in rate, depicting the 95 % limits of agreement (-3.3 and 3.4 cpm) with dashed lines (right).

Table 5.1: Computed chest and mattress displacement (d_{chest} and d_{mat}), reference chest compression depth (d_{ref}) and unsigned error in the estimation of the chest-sternal displacement using the SAA method with two accelerometers, for different mattress/backboard combinations.

	Parameter			
Mattress type	d_{chest} (mm)	d_{mat} (mm)	d_{ref} (mm)	error (mm)
Foam				
backboard	56 (52, 59)	7 (6, 7)	49 (45, 52)	3 (2, 4)
no backboard	57 (52, 60)	10 (10, 11)	46 (42, 49)	2 (1, 3)
Sprung				
backboard	70 (62, 80)	24 (22, 28)	46 (40, 52)	2 (1, 3)
no backboard	83 (78, 89)	37 (35, 40)	46 (43, 50)	2 (1, 3)
Global	62 (55, 79)	17 (8, 32)	47 (43, 50)	2 (1, 4)

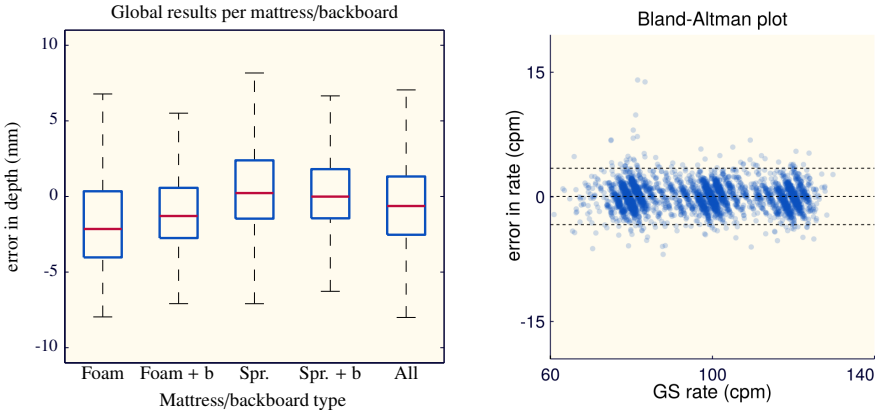

Figure 5.3: Distribution of the error in depth depending on the mattress/backboard combination (left) and global distribution of the error in rate (right). Tested mattresses were foam and sprung (Spr.) The use of a backboard is indicated with + *b* in the boxplot. In the Bland-Altman plot, dashed lines represent the median of the errors (0 cpm) and the 95 % limits of agreement (−3.3 and 3.4 cpm).

5.2.4 Discussion

In this section we proposed a method to provide accurate feedback on chest compression depth and rate when CPR is provided on soft surfaces. The method is based on applying spectral analysis of the acceleration (SAA) to the signals acquired by two accelerometers placed on the chest and beneath the back of the patient, in order to compute chest and mattress displacement, respectively. Chest compression, that is, chest-sternal displacement, can then be obtained as the difference between these two values.

We evaluated the accuracy of this method in a simulated cardiac arrest scenario, using a resuscitation manikin. This allowed testing different conditions: different mattresses with and without using a backboard, and different compression rates. Global median (Q_1, Q_3) mattress compression was 17 (8, 32) mm. A back accelerometer is therefore required to compensate mattress deflection and avoid an important overestimation in chest compression depth. When a backboard was used, mattress compression was significantly reduced, as expected (see Table 5.1). Accuracy in the computation of chest compression depth was high for all the test conditions, with a global median unsigned error of 2 (1, 4) mm. Unsigned errors in rate were also low, with a global median of 0.9 (0.4, 1.6) cpm.

Aase et al. suggested in 2002[1] the use of two accelerometers to estimate chest compression depth in moving environments. One accelerometer measured chest acceleration and the other one floor acceleration. Both accelerations were subtracted prior to applying the algorithm to compute chest compression depth. Nishisaki et al. (2009)[115] and Oh et al. (2012)[121] used two accelerometers to estimate chest compression depth when CPR was performed on a mattress. In all these studies depth was estimated by applying double integration to the acceleration, and thus it was necessary to apply different techniques to avoid the integration instability problem. The main difficulty consists on synchronizing the two acceleration signals prior to subtracting them; small synchronization errors could lead to important errors in depth estimation. For this reason, to date, none of these solutions has been implemented to provide feedback on soft surfaces.

The solution we proposed does not require a fine synchronization of both acceleration signals. Only one d_{chest} and one d_{mat} values are computed for each 2-s window. Even if the two windows were not perfectly aligned, the error in the subtraction of both computed distances would be small. This method could be technically implemented using two equal devices, one of them placed on the chest and another one on the back of the patient. Each device would apply the spectral analysis method to compute displacement, obtaining one depth and one rate value every two seconds. These values could be wirelessly sent to a central device, such as a tablet or a smartphone. This device would subtract depth values to compute chest compression depth, d_{cc}, and provide feedback to the rescuer on chest compression depth and rate. This solution is illustrated in Figure 5.4.

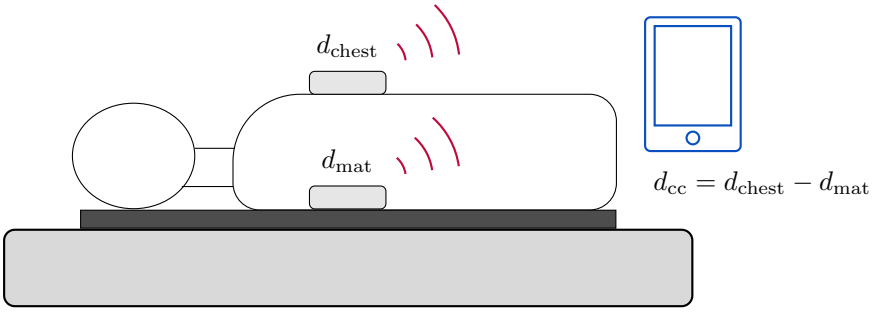

Figure 5.4: Technical solution proposed to provide accurate feedback on chest compression depth and rate when CPR is performed on soft surfaces.

5.3 Alternative placements for CPR feedback devices

Current commercial feedback devices are designed to be positioned between the chest of the patient and the rescuer's hands during CPR. However, as mentioned in Chapter 2, the prolonged pressure of the device may cause soft-tissue damage to the patient[27] or to the rescuer, along with wrist discomfort.[130,170]

The aim of this study was to evaluate the accuracy of the SAA method for the calculation of chest compression depth and rate when the device was placed in alternative positions that reduce discomfort and that follow the movement of the chest during CPR: the rescuer's

back of the hand, the wrist, and the forearm. We compared these results with those obtained when the accelerometer was placed on the traditional positioning, that is, between the patient's chest and the heel of the rescuer's hands.

5.3.1 Data collection

We used the experimental set-up described in Section 5.1. Ten rescuers provided continuous chest compressions during one-minute episodes at different target rates (80, 100, and 120 cpm) and depths (35 and 50 mm), with an accelerometer placed in four different positions: on the manikin's chest, encased in a metallic box; on the back of the rescuer's hand; on the wrist; and fixed to the forearm, 12 cm above the wrist. In the three last positions, the accelerometer was fixed using an elastic band, as shown in Figure 5.5. Before the recording sessions, rescuers received training in chest-compression only CPR and provided chest compressions to the manikin with the accelerometer placed beneath their hands. They were not given specific instructions on CPR technique for other placements of the accelerometer. A total of 240 1-min episodes were acquired, 60 per position, with a sampling frequency of 1000 Hz.

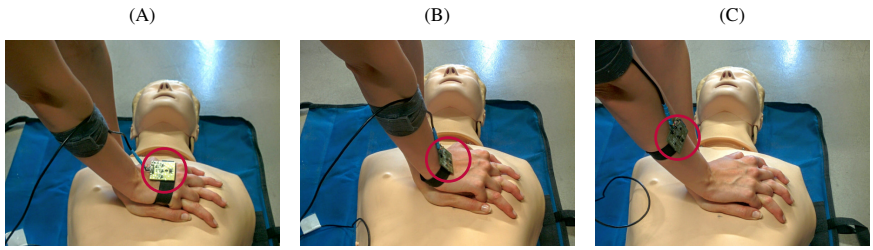

Figure 5.5: Accelerometer (inside the red circle) fixed with an elastic band to the rescuer's back of the hand (A), to the wrist (B), and to the forearm (C).

5.3.2 Data analysis and performance evaluation

Episodes were divided into non-overlapping 2-s analysis intervals. The SAA method was applied to each interval to compute chest compression depth and rate. These values were then compared to those obtained from the reference compression depth signal. The

distribution of the error in depth and rate was analyzed using boxplots and Bland-Altman plots, respectively. Values are presented as median (Q_1, Q_3). Kruskal-Wallis test was used to perform between-groups comparisons, and $p < 0.05$ were considered significant.

5.3.3 Results

Figure 5.6 shows boxplots of the error in depth estimation for the different accelerometer positions. There were statistically significant differences in errors between positions ($p < 0.001$). For each position, there were also statistically significant differences per rescuer ($p < 0.001$). Figure 5.7 shows boxplots of the error in depth estimation depending on the rescuer.

There were statistically significant differences for different target rates in the four positions ($p < 0.001$). With regard to target depth, there were only statistically significant differences in errors in depth estimation when the accelerometer was placed on the chest of the patient or on the rescuer's forearm ($p < 0.001$ in both cases). In the back of the hand and in the wrist no differences were found depending on target depth ($p = 0.6$ and $p = 0.5$, respectively).

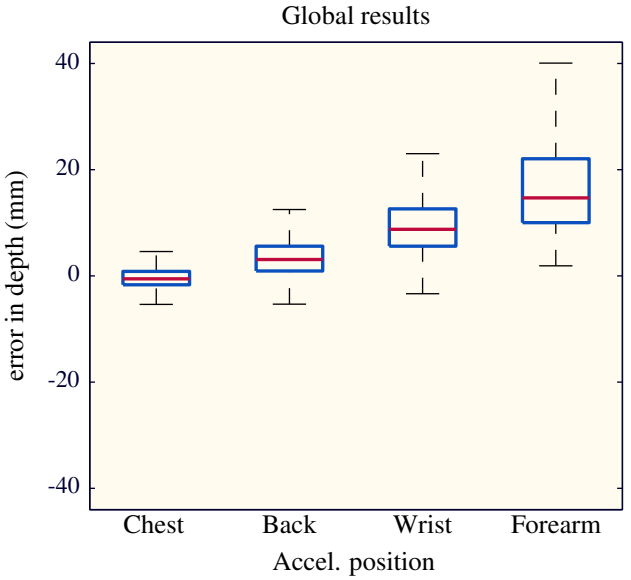

Figure 5.6: Boxplots of the global error in depth for the different accelerometer positions.

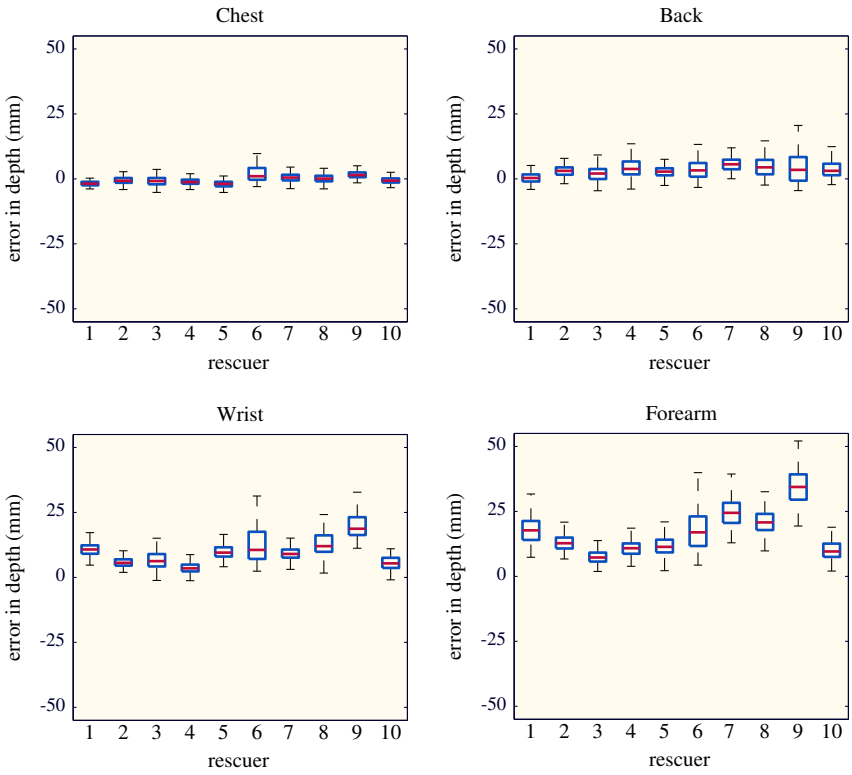

Figure 5.7: Boxplots of the error in depth by rescuer for each of the accelerometer positions.

With respect to rate, no statistically significant differences were found in errors depending on acceleration positioning ($p = 0.9$), target rate ($p = 0.06$), rescuer ($p = 0.3$), or target depth ($p = 0.7$). Figure 5.8 shows a Bland-Altman plot of the global error in rate estimation. Ninety-five percent limits of agreement were -3.4 and 3.4 cpm.

Table 5.2 shows the median (Q_1, Q_3) and the 95th percentiles of the unsigned error in depth and rate for the different positions.

5.3.4 Discussion

In this section we evaluated how placing the accelerometer in positions other than the chest of the patient would affect the accuracy of the SAA method for chest compression depth and rate calculation.

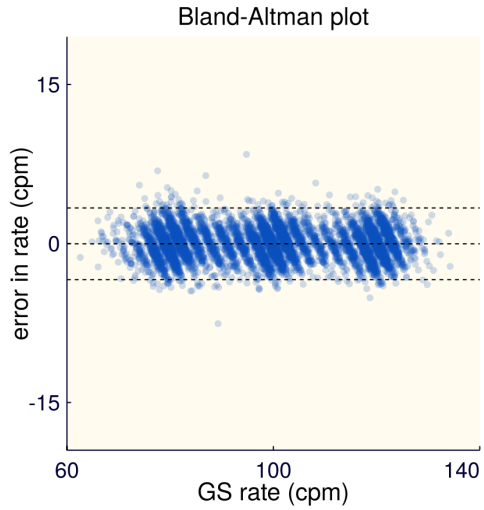

Figure 5.8: Bland-Altman plot of the error in rate, depicting the median (0 cpm) and the 95 % limits of agreement (−3.4 and 3.4 cpm) with dashed lines.

Table 5.2: Unsigned error in depth and rate calculation for different accelerometer positions.

	Depth (mm)		Rate (cpm)	
Position	Mdn (Q_1, Q_3)	P_{95}	Mdn (Q_1, Q_3)	P_{95}
Chest	1.4 (0.7, 2.3)	4.4	0.9 (0.4, 1.5)	2.7
Back	3.2 (1.5, 5.6)	10.3	0.9 (0.4, 1.5)	2.7
Wrist	8.8 (5.6, 12.6)	21.1	0.9 (0.4, 1.5)	2.6
Forearm	14.7 (10.0, 22.1)	36.7	0.9 (0.4, 1.5)	2.8

We analyzed the errors when the accelerometer was fixed to the rescuer's back of the hand, wrist, or forearm.

Chest compression rate was accurately computed in any of the evaluated positions, with 95 % limits of agreement of -3.4 and 3.4 cpm. No statistically significant differences in errors were found between positions ($p = 0.9$).

For depth, in contrast, errors increased with the distance between the chest of the patient and the accelerometer, and there was a tendency to overestimate compression depth (see Figure 5.6). The SAA method composes the three axes of the acceleration and computes compression depth assuming that the measured acceleration is perpendicular to the chest, and thus generates downward movement. However, when the accelerometer is not fixed to the chest of the patient, this may not be true. Fixed to the wrist or to the forearm, the sensor is subjected to swinging movements not reflected on chest displacement. Additionally, some rescuers tended to separate the hands from the chest during chest release, which may be the cause of the slight overestimation in depth when the accelerometer was placed on the back of the hand. Errors were different for different rescuers (see Figure 5.7), depending on their CPR technique.

Errors in depth estimation when the accelerometer was fixed to the wrist or to the forearm were too high to consider implementation (median above 8 mm). On the back of the hand, however, errors were admissible, with a median (Q_1, Q_3) of $3\,(2, 6)$ mm, and this position could be used in the practice. Instructing the rescuers to minimize movements of the hands with respect to the chest could have reduced errors. This supports the development of new devices that could be fixed to the back of the rescuer's hand, reducing discomfort and risks of injury, while other embodiments such as watches or bracelets should be avoided. Smartphones with software implementations of feedback algorithms could also be used fixed to the back of the rescuer's hand. Smartphones are widely available, and they already comprise accelerometers and processing means. Studies have shown that smartphone applications can provide cognitive aids that help to improve the performance of doctors[103] and laypeople[28,50] during simulated medical emergencies.

5.4 CPR feedback in a moving long-distance train

Early bystander CPR and early defibrillation are key to increase the chances of survival from sudden cardiac arrest. Public access defibrillation programs aim to make defibrillation accessible to the community by deploying AEDs in public places. Currently, AEDs are widespread in public transportation settings, particularly in airports and in bus, metro, and train stations where the density of passengers per year is high.[26,85,125,145] They are also being deployed on board transportation means such as aircraft, cruise ships, and long distance trains,[56,123] in which the long time between collapse and the access to emergency medical services makes an immediate in-situ intervention necessary.

CPR feedback devices are increasingly being used to improve CPR quality. However, devices based on accelerometers may provide erroneous feedback when they are used in moving environments, as they would sense the acceleration of the vehicle along with that of the chest compressions. Devices based on magnetic fields, on the other hand, could suffer from electromagnetic or radio frequency interferences if they are used near electrical equipment.

The aim of this study was twofold. First, we wanted to assess the feasibility of computing chest compression depth and rate by applying the SAA method to the acceleration signal when CPR is provided in a long-distance train. Second, in this same scenario, we wanted to evaluate the reliability and accuracy of two standalone commercial feedback devices: CPRmeter, based on acceleration, and TrueCPR, based on electromagnetic fields. CPRmeter's user manual warns that if the device is used in moving environments, it may provide inaccurate feedback in chest compression depth. TrueCPR's manual alerts of potential interferences when the device is used in close proximity to equipment emitting strong electromagnetic fields, but, no information is given in relation to its use in trains. There are no studies analyzing the performance of these devices in a moving long-distance train, so the results of this study could be of interest.

5.4.1 Data collection

We used the experimental set-up described in Section 5.1, with an accelerometer, CPRmeter, or TrueCPR placed on the chest of the manikin during chest compressions.

In the records acquired to evaluate the SAA method or CPRmeter, a couple of rescuers alternated providing CPR for 3 min. The first minute consisted of continuous chest compressions, while the other two minutes consisted of series of 30 chest compressions with 5-s pauses in between. The information acquired by the accelerometer was processed with the SAA method to provide a depth and rate value for each 2-s interval. For CPRmeter, a commercial program (QCPR v3, Laerdal Medical, Norway) was used to extract the acquired compression depth signal to a readable format, and then the depth and rate of each compression were computed by applying a peak detector.

For TrueCPR, the instantaneous compression depth signal measured by the device was not accessible. The program TrueCPR report generator (PhysioControl, USA) allows generating a report that summarizes some CPR quality parameters per record, including median compression rate and depth. The device was turned off after each series of ten compressions to create a new file, and for each file a report was generated. Reported median rate and depth values for each series of ten compressions constituted a data point.

Data collection was performed in two settings: in the laboratory (baseline measurements), and in a long-distance train.

Baseline measurements

Baseline measurements were performed by ten rescuers, with a target rate of 100 cpm and target depths of 50 mm and 35 mm. For the SAA method and CPRmeter rescuers were grouped in couples. Each couple generated two records, one per target depth. A total of ten 3-min records were obtained in each case, which yielded 900 depth and rate values for the SAA method (one for each 2-s interval) and 2477 for CPRmeter (one per chest compression).

For TrueCPR each rescuer generated ten data points. Target depth was 50 mm for five data points and 35 mm for the other five. A total of 100 data points were acquired for TrueCPR.

Long-distance train measurements

Measurements were performed in the four-car Alvia S-120 train, during the route Bilbao-Zaragoza-Bilbao operated by the railway company Renfe. This train has distributed traction and comprises eight asynchronous motors, two per car. The train contains two driver's cabs, where the control and driving equipment is installed. The units can be powered at 3000 V DC (conventional) or 25 000 V with 50 Hz alternate current (high velocity). The experiment was performed in the first-class cars, in the areas indicated in Figure 5.9. These areas were selected because of the availability of space to place the equipment and comfortably perform the measurements. The manikin was placed over the synthetic carpeting that covered the floor of the car. A member of the company traveled with the researchers to ensure the safety of the measurements and to minimize disturbance to other travelers and members of the staff.

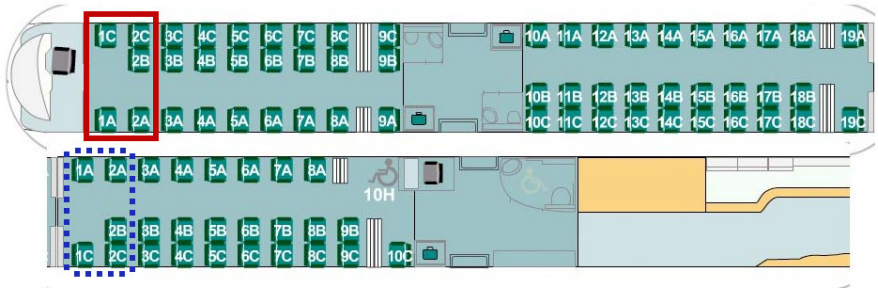

Figure 5.9: Distribution of the first-class seats in the Alvia S-120 train. During the outward journey, experiments were performed in the area indicated with a red solid line, and during the inward journey, in the area marked with a blue dotted line. These areas were selected because of the availability of space to comfortably place the manikin on the floor without disturbing the rest of the passengers.

Four rescuers grouped in two couples participated in the measurements. Chest compressions were provided with a target rate of 100 cpm and target depths of 50 and 35 mm. The train departed from Bilbao and stopped in eight stations during the journey. Table 5.3 shows the duration of the trip to each station, the average velocity, and the number of records acquired, together with a letter that identifies the couple performing CPR in each case. For

the SAA method and CPRmeter, 2A indicates that two 3-min records were acquired with CPR performed by couple A. For TrueCPR, 20A indicates that 20 data points corresponding to 20 series of ten chest compressions were acquired with CPR provided by couple A. The number of records and data points was always even; half of them had a target rate of 35 mm and the other half, of 50 mm. A total of 48 3-min records were registered for the SAA method, 32 for CPRmeter, and 200 data points were obtained for TrueCPR, considering both the outward and the inward journey. Half of the records were acquired in each direction.

Table 5.3: Characteristics of the journey: stations in which the train stopped, duration and average velocity for each interval, and number of episodes acquired for each device. The number of episodes is indicated with a number and a letter identifying the couple that performed CPR.

Station	Dur. (min)	Vel. (km/h)	Episodes		
			SAA	CPRmeter	TrueCPR
Miranda de Ebro	93	67	8A + 8B	4A + 4B	40A + 40B
Haro	16	74	2A + 2B	2A + 2B	-
Logroño	40	74	4A + 4B	2A + 2B	20A + 20B
Calahorra	31	94	4A + 4B	2A + 2B	20A + 20B
Alfaro	13	103	2A + 2B	2A + 2B	-
Castejón de Ebro	6	53	-	-	-
Tudela de Navarra	11	89	-	2A + 2B	-
Zaragoza Delicias	43	102	4A + 4B	2A + 2B	20A + 20B

5.4.2 Data analysis and performance evaluation

The reliability of CPRmeter and TrueCPR to provide feedback was analyzed by evaluating the number of episodes in which they provided feedback to the rescuer during the whole record. Additionally, the accuracy of the three methods was evaluated by measuring the errors in depth and rate estimation. Errors were computed as the difference between values obtained from each of the feedback methods and from the reference compression depth signal.

For the SAA method one depth and rate value were obtained for each 2-s interval, for CPRmeter one value for each chest compression, and for TrueCPR one value for each series of ten chest compressions. Wilcoxon rank sum test was used to perform between-groups comparisons, and p-values< 0.05 were considered significant.

5.4.3 Results

Feedback reliability

During baseline measurements, both CPRmeter and TrueCPR provided visual feedback the whole time in all the acquired episodes.

In the long-distance train, CPRmeter also provided feedback for all the acquired episodes. In contrast, TrueCPR failed to provide feedback in all the episodes. During the outward journey it showed an alert indicating that the back pad was at an incorrect distance from the chest pad (see Figure 5.10A), and it did not provide feedback for any of the compressions. Even if we tried to adjust the position of the pads, the alert persisted. During the inward journey, in some cases it did provide feedback for the first two or three compressions, but then it showed an alert indicating that electronic noise was interfering with the device (see Figure 5.10B).

(A) (B)

Figure 5.10: Alerts displayed by TrueCPR during the long-distance train measurements. (A) shows an alert indicating that the distance between the back pad and the chest pad is incorrect, and that the back pad should be repositioned. (B) indicates that electronic noise is interfering with the device.

Accuracy on depth and rate estimation

Even if TrueCPR did not provide feedback during the records, it did store CPR information on the device. In this section we evaluate the accuracy on depth and rate estimation of the SAA method, CPRmeter, and TrueCPR. Figure 5.11 shows boxplots of the error in compression depth estimation for the three feedback systems. There were statistically significant differences in errors during baseline and in the train only for TrueCPR ($p = 0.14$, $p = 0.18$, and $p < 0.001$ for SAA, CPRmeter, and TrueCPR, respectively).

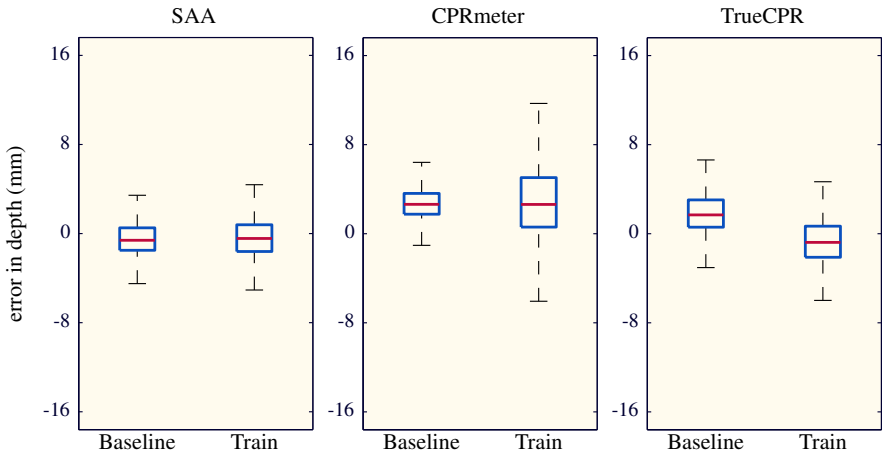

Figure 5.11: Boxplots of the error in depth estimation for the three feedback systems (SAA, CPRmeter, and TrueCPR) during baseline measurements and in the train.

Figure 5.12 shows Bland-Altman plots of the error in rate estimation. The 95 % limits of agreement for baseline and train measurements, depicted with dashed black lines in Figure 5.12, were (−2.4, 2.6 cpm) and (−3.0, 3.2 cpm) for SAA; (−2.7, 2.8 cpm) and (−3.4, 3.5 cpm) for CPRmeter; and (−1.6, 2.2 cpm) and (−2.5, 2.9 cpm) for TrueCPR. There were no statistically differences in errors in rate estimation during baseline measurements and in the train ($p = 0.7$, $p = 0.8$, and $p = 0.2$ for SAA, CPRmeter, and TrueCPR, respectively).

Finally, Table 5.4 shows the median (Q_1, Q_3) and 95th percentile of the unsigned error in depth and rate estimation for each of the feedback systems.

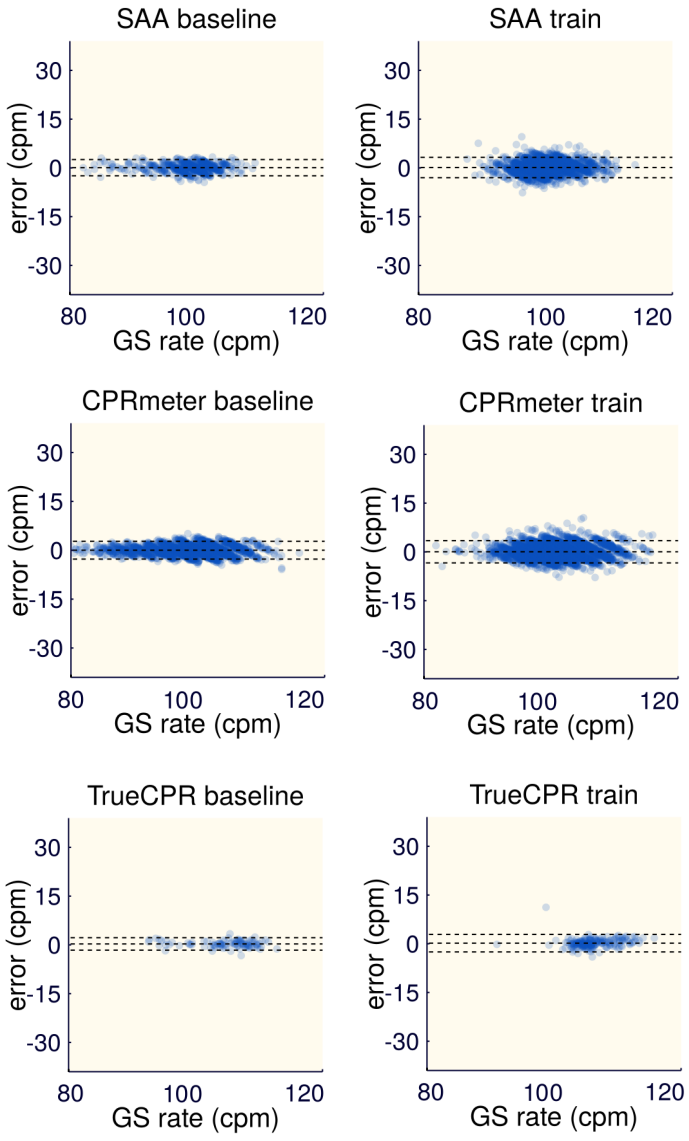

Figure 5.12: Bland-Altman plots of rate estimation for the three feedback methods during baseline measurements and in the train. Median and 95 % limits of agreement are depicted with dashed black lines.

Table 5.4: Unsigned error in depth and rate calculation for different feedback systems (SAA, CPRmeter, and TrueCPR) both during baseline measurements and in a long-distance train.

Method		Depth (mm)		Rate (cpm)	
		Mdn (Q_1, Q_3)	P_{95}	Mdn (Q_1, Q_3)	P_{95}
SAA	Baseline	1.2 (0.6, 1.9)	3.3	0.9 (0.4, 1.5)	2.5
	Train	1.3 (0.6, 2.3)	4.8	0.9 (0.4, 1.7)	3.2
CPRmeter	Baseline	2.6 (1.8, 3.6)	6.1	0.8 (0.6, 1.5)	2.7
	Train	3.1 (1.5, 5.4)	11.6	1.3 (0.7, 2.0)	3.2
TrueCPR	Baseline	2.2 (1.1, 3.5)	6.1	0.7 (0.4, 1.1)	1.9
	Train	1.5 (0.7, 2.5)	4.6	0.7 (0.4, 1.3)	2.2

5.4.4 Discussion

Environmental conditions in a moving train severely affected TrueCPR, as the device failed to provide feedback to the rescuer. However, it did store CPR performance information, and depth and rate were accurately computed. Thus, if changes were applied to the user interface to avoid excessive alerts, it could be used in a moving train. CPRmeter did provide feedback during all the measurements.

For SAA and CPRmeter, errors in depth estimation tended to be larger in the train compared to the baseline measurements, although the differences were not statistically significant. The SAA method provided the lowest unsigned errors in depth estimation, even in the train. Accelerations generated during chest compressions are in the range of 1–10 Hz. Frequency components of the acceleration out of the range of interest were not taken into account by the method, and they did not influence its performance. With respect to rate estimation, the three methods were very accurate; 95th percentile of the unsigned error was below 3.5 cpm in all cases.

5.5 Summary and conclusions of the chapter

In this chapter we analyzed the behavior of the SAA method in three challenging scenarios. First, we proposed an adaptation of the method consisting in the use of two accelerometers to account for

mattress deflection when CPR is performed on soft surfaces. The method was accurate both in rate and in depth estimation. Then, we evaluated the effect of placing the accelerometer on the rescuer's back of the hand, fixed to the wrist, or to the forearm. For depth estimation, errors increased with the distance between the chest of the patient and the accelerometer, but on the back of the hand errors were still acceptable. This position would reduce discomfort and risks of injury during chest compressions, both for the rescuer and for the patient. Finally, we studied the behavior of the SAA method and of two commercial devices in a long-distance train. TrueCPR was affected by environmental conditions and could require user interface modifications to be used in this scenario. However, the three devices were accurate in chest compression rate and depth calculation.

6 Conclusions

Prince John: "Have you finished?"
Sir Robin of Locksley: "I'm only just beginning."

— The Adventures of Robin Hood

This chapter summarizes the main findings and contributions of this thesis work, several parts of which have been published in indexed journals (A1–A5), patented (P1), or presented at international conferences (C4–C10). The chapter concludes with a brief description of the future research lines opened by this work.

Main contributions of the thesis work

The objective of this thesis work was to develop new methods to provide feedback on the quality of chest compressions (compression rate and depth) based on the TTI signal acquired through defibrillation pads or on the chest acceleration signal. Its main contributions are those presented as intermediate goals in the introduction (Chapter 1), and respond to the main challenges described in the background (Chapter 2).

- *Feedback on chest compression quality using the TTI signal.* We analyzed the relationship between three morphologic features of the TTI and compression depth during cardiac arrest episodes. The characteristics of the fluctuations induced by chest compressions varied widely between episodes, and along each episode depending on the rescuer. When a wide variety of patients and rescuers were included, there was a very low correlation between TTI features and compression depth. Consequently, TTI could not be used to identify too shallow chest compressions. However, the instants of the chest compressions could be reliably identified on the TTI. We developed a new method to calculate and provide feedback on chest compression rate for any system recording the TTI

signal. This method provided a high accuracy under different device's front-ends and a wide range of conditions without requiring parameter optimization. Bexen cardio's new line of defibrillators implements this method for feedback on chest compression rate.

- *Feedback on chest compression quality using the chest acceleration signal.* We developed three methods to provide feedback on the compression rate and depth based solely on the acceleration signal. The accuracy of the methods was evaluated with episodes of simulated cardiac arrest using a resuscitation manikin. One of the methods, based on the spectral analysis of the acceleration, presented a particularly high accuracy in a wide range of conditions. This method is very novel, and it does not infringe any existing patent. Bexen cardio has developed a prototype of a feedback device implementing this method, which will be marketed next year.
- *Performance of feedback systems in challenging scenarios.* We evaluated the performance of feedback systems in three challenging scenarios: when CPR is performed on a soft surface; when the feedback device is fixed to the rescuer's back of the hand, wrist, or forearm, instead of being placed on the chest of the patient; and when CPR is performed in a moving long-distance train. The proposed solution could be reliably used on a soft surface. Regarding positioning, feedback could be provided with an accelerometer placed on the rescuer's back of the hand, but when it was fixed to the wrist or to the forearm, the errors were too large. Feedback devices based on accelerometers provided reliable feedback when used in a long-distance train. These results could allow extending the scenarios of application of feedback devices.

Financial support

This thesis work was financially supported by a predoctoral research grant (F1), by government-funded research projects (F2 and F6), by institutional and governmental programs to support science and research (F3 and F4), and by a collaboration project with Bexen cardio, Osatu S. Coop (F5).

F1 *Ayuda para la formación de personal investigador.*
Ref: BFI-2011-166
Basque Government Department of Education, Universities and Research.
January 2012 – December 2015

F2 *Optimización del intervalo hands-off en la resucitación cardiaca.* Ref: TEC2009-10460
Spanish Ministry of Science and Innovation
January 2010 – December 2012
Financing: 34 400 €

F3 *Ayuda a las Unidades de Formación e Investigación en la UPV/EHU.* Ref: UFI11/16
University of the Basque Country
January 2012 – December 2014
Financing: 75 624 €

F4 *Ayudas para apoyar las actividades de grupos de investigación del sistema universitario vasco.*
Basque Government
January 2013 – December 2015
Financing: 62 900 €

F5 *Nuevos hitos en la desfibrilación cardiaca.* Ref: PT10181
Bexen cardio, Osatu S. Coop.
January 2013 – December 2015
Financing: 60 000 €

F6 *Estudio del origen, naturaleza y reducción de la interferencia debida a la resucitación cardiopulmonar en el contexto de la desfibrilación cardiaca.* Ref: TEC2012-31144
Spanish Ministry of Economy and Competitiveness
January 2013 – December 2015
Financing: 33 930 €

Publications

In this section the contributions published in indexed journals, patented, and presented at international conferences in relation to this thesis work are cited.

- Two publications in indexed journals and five communications at international conferences related to the use of the TTI signal to evaluate the depth and rate of the chest compressions (A1, A2, C1–C5).
- Two publications in indexed journals, a European patent, and a communication at an international conference related to the development of methods to estimate compression depth and rate using exclusively the acceleration signal (A3, A4, P1, C6).
- A publication in an indexed journal and two communications at international conferences related to the accuracy of methods and devices to provide feedback on the depth and rate of the chest compressions in a long-distance train (A5, C7, C8).
- Two communications at international conferences related to the estimation of the depth and rate of the chest compressions when CPR is performed on soft surfaces (C9) and when the accelerometer is positioned on the rescuer's back of the hand or forearm (C10).

Indexed journals

A1 Alonso E, **González-Otero DM**, Aramendi E, Ruiz de Gauna S, Ruiz J, Ayala U, Russell JK, and Daya M. Can thoracic impedance monitor the depth of chest compressions during out-of-hospital cardiopulmonary resuscitation? *Resuscitation* 2014;85(5);637–643.

A2 **González-Otero DM**, Ruiz de Gauna S, Ruiz J, Daya MD, Wik L, Russell JK, Kramer-Johansen J, Eftestøl T, Alonso E, and Ayala U. Chest compression rate feedback based on transthoracic impedance. *Resuscitation* 2015;93;82–88.

A3 **González-Otero** DM, Ruiz J, Ruiz de Gauna S, Irusta U, Ayala U, and Alonso E. A new method for feedback on the quality of chest compressions during cardiopulmonary resuscitation. *BioMed research international*;2014: Article ID 865967.

A4 Ruiz de Gauna S, **González-Otero** DM, Ruiz J, and Russell JK. Feedback on the rate and depth of chest compressions during cardiopulmonary resuscitation using only accelerometers. *PLOS ONE*. Under Review.

A5 Ruiz J, **González-Otero** DM, Ruiz de Gauna S, and Russell JK. Feasibility of CPR feedback systems in a moving long-distance train. *Resuscitation*. In Preparation.

Patents

P1 Ruiz J, **González-Otero DM**, Ruiz de Gauna S, Irusta U, Aramendi E, Alonso E, and Ayala U. Device and method to assist in performing chest compressions during cardiopulmonary resuscitation. *European Patent* EP 2883496 A1. 2013.

International conferences

C1 **González-Otero DM**, Ruiz de Gauna S, Ruiz J, Ayala U, and Alonso E. Automatic detection of chest compression pauses using the transthoracic impedance signal. In *Computing in Cardiology (CinC), 2012*;21–24. September 2012. Krakov, Poland.

C2 Ruiz de Gauna S, **González-Otero DM**, Ruiz J, Ayala U, Alonso E, Eftestøl T, and Kramer-Johansen J. Is rhythm analysis during chest compression pauses for ventilation feasible? In *Resuscitation 2012*;e8. October 2012. Vienna, Austria.

C3 **González-Otero DM**, Alonso E, Ruiz J Aramendi E, Ruiz de Gauna S, Ayala U, Kramer-Johansen J, and Eftestøl T. A simple impedance-based method for ventilation detection during cardiopulmonary resuscitation. In *Computing in Cardiology (CinC), 2013*;807–810. September 2013. Zaragoza, Spain.

C4 Alonso E, **González-Otero DM**, Aramendi E, Ruiz de Gauna S, Ruiz J, Ayala U, and Russell JK. Study on the linear relation between chest compression depth and the fluctuation caused in the thoracic impedance acquired by defibrillation pads. In *Computing in Cardiology (CinC), 2013*;803–806. September 2013. Zaragoza, Spain.

C5 **González-Otero DM**, Alonso E, Ruiz J, Ruiz de Gauna, S, Aramendi E, Ayala U, Russell JK, and Daya, M. Comparison of time and frequency domain methods for the feedback on chest compression rate. In *Computing in Cardiology (CinC), 2014*;1101–1104. September 2014. Cambridge, Massachusetts.

C6 Ruiz de Gauna S, **González-Otero DM**, Ruiz J, Chicote B, and Vidales N. Alternatives to estimate the compression depth from the acceleration signal during cardiopulmonary resuscitation. In *Computing in Cardiology (CinC), 2015*. September 2015. Nice, France.

C7 **González-Otero DM**, Ruiz de Gauna S, Ruiz J, Chicote B, and Plaza S. Feasibility of compression depth estimation from the acceleration signal during cardiopulmonary resuscitation in long-distance trains. In *Computing in Cardiology (CinC), 2015*. September 2015. Nice, France.

C8 **González-Otero DM**, Ruiz de Gauna S, Ruiz J, Chicote B, Rivero R, and Russell JK. Accurate feedback of chest compression depth and rate on a manikin in a moving train. In *Resuscitation 2015*. October 2015. Prague, Czech Republic.

C9 Ruiz de Gauna S, **González-Otero DM**, Ruiz J, Chicote B, Pelayo S and Russell JK. Accurate measurement of chest compression depth when CPR is performed on soft surfaces. In *Resuscitation 2015*. October 2015. Prague, Czech Republic.

C10 Ruiz de Gauna S, **González-Otero DM**, Ruiz J, Chicote B, Ruiz J, and Russell JK. Estimation of the chest compression depth using an accelerometer positioned on the rescuer's back of the hand or forearm. In *Resuscitation 2015*. October 2015. Prague, Czech Republic.

Future lines of research

New methods to provide feedback on chest compression rate and depth during CPR have been successfully proposed in this thesis work. Further testing could be performed on these methods, and further studies could be carried out to improve and extend the proposed solutions.

- *Performance of the acceleration-based method method with cardiac arrest data.* The methods to estimate chest compression rate and depth from the acceleration were developed and tested with data obtained in a simulated cardiac arrest scenario, with a sensorized resuscitation manikin. The method based on the spectral analysis of the acceleration (SAA), which provided the best results, should be tested retrospectively with cardiac arrest data. This would provide a wide range of acceleration waveforms, and would allow analyzing the effect in accuracy of more irregular waveforms due to rescuer's fatigue.

- *Performance of the acceleration-based method in different trains and routes.* In this thesis work we analyzed the performance of three feedback methods, CPRmeter, TrueCPR, and SAA, in a long-distance train. It would be interesting to extend this study to include different trains with different average velocities and distinct levels of vibration. In order to simplify the measurement protocol for the SAA method, an additive model could be used. That is, it could be assumed that the acceleration recorded when CPR is performed in a moving train corresponds to the addition of the acceleration that would have been recorded if CPR had been performed in static conditions and the accelerations of the train. In that case, a database of accelerations of different trains in different routes could be acquired and combined with the records acquired in the laboratory for an extensive testing of the method.

- *Extraction of information about chest release from the acceleration signal.* The methods proposed in this thesis work provide information about the rate and depth of the chest compressions. Some commercial devices provide also information about adequate chest release between compressions, which is important to optimize blood flow. For that purpose they integrate force sensors (CPRmeter) or use triaxial magnetic fields (TrueCPR). No current device provides information about chest release using solely the acceleration signal. A feasibility analysis of the possibility of obtaining information about chest release by applying signal processing techniques to the acceleration signal should be performed.

Bibliography

[1] Aase SO and Myklebust H. Compression depth estimation for CPR quality assessment using DSP on accelerometer signals. *IEEE Transactions on Biomedical Engineering* 2002;49(3); 263–268.

[2] Abella BS, Alvarado JP, Myklebust H, et al. Quality of cardiopulmonary resuscitation during in-hospital cardiac arrest. *JAMA: the Journal of the American Medical Association* 2005;293(3); 305–310.

[3] Abella BS, Edelson DP, Kim S, et al. CPR quality improvement during in-hospital cardiac arrest using a real-time audiovisual feedback system. *Resuscitation* 2007;73(1); 54–61.

[4] Allison RD, Holmes EL, and Nyboer J. Volumetric dynamics of respiration as measured by electrical impedance plethysmography. *Journal of Applied Physiology* 1964;19(1); 166–173.

[5] Alonso E. Thoracic impedance for cardiopulmonary resuscitation quality assessment and for circulation detection. Ph.D. thesis, University of the Basque Country (UPV/EHU) 2014.

[6] Alonso E, González-Otero DM, Aramendi E, et al. Can thoracic impedance monitor the depth of chest compressions during out-of-hospital cardiopulmonary resuscitation? *Resuscitation* 2014;85(5); 637–643.

[7] Alonso E, Ruiz J, Aramendi E, et al. Reliability and accuracy of the thoracic impedance signal for measuring cardiopulmonary resuscitation quality metrics. *Resuscitation* 2015;88(0); 28–34.

[8] Andersen L, Isbye D, and Rasmussen L. Increasing compression depth during manikin CPR using a simple backboard. *Acta Anaesthesiologica Scandinavica* 2007;51(6); 747–750.

[9] Aramendi E, Ayala U, Irusta U, and Alonso E. Use of the transthoracic impedance to determine CPR quality parameters. *Resuscitation* 2010; 81(2); S52.

[10] Aramendi E, Ayala U, Irusta U, Alonso E, Eftestøl T, and Kramer-Johansen J. Suppression of the cardiopulmonary resuscitation artefacts using the instantaneous chest compression rate extracted from the thoracic impedance. *Resuscitation* 2012;83(6); 692–698.

[11] Atwood C, Eisenberg MS, Herlitz J, and Rea TD. Incidence of EMS-treated out-of-hospital cardiac arrest in Europe. *Resuscitation* 2005; 67(1); 75–80.

[12] Aufderheide TP, Pirrallo RG, Yannopoulos D, et al. Incomplete chest wall decompression: a clinical evaluation of CPR performance by EMS personnel and assessment of alternative manual chest compression-decompression techniques. *Resuscitation* 2005;64(3); 353–362.

[13] Ayala U, Eftestøl T, Alonso E, et al. Automatic detection of chest compressions for the assessment of CPR-quality parameters. *Resuscitation* 2014;85(7); 957–963.

[14] Babbs CF, Kemeny AE, Quan W, and Freeman G. A new paradigm for human resuscitation research using intelligent devices. *Resuscitation* 2008;77(3); 306–315.

[15] Bahr J, Klingler H, Panzer W, Rode H, and Kettler D. Skills of lay people in checking the carotid pulse. *Resuscitation* 1997;35(1); 23–26.

[16] Baker L, Hill D, and Pate T. Comparison of several pulse-pressure techniques for monitoring stroke volume. *Medical and Biological Engineering* 1974;12(1); 81–89.

[17] Bankman IN, Gruben KG, Halperin HR, Popel AS, Guerci AD, and Tsitlik JE. Identification of dynamic mechanical parameters of the human chest during manual cadiopulmonary resuscitation. *IEEE Transactions on Biomedical Engineering* 1990;37(2); 211–217.

[18] Banville I, Marx R, Brown D, and Nova R. Alerting users of CPR feedback device of detected magnetic interference. 2013. US Patent App. 13/598 508.

[19] Beckers SK, Skorning MH, Fries M, et al. CPREzy™ improves performance of external chest compressions in simulated cardiac arrest. *Resuscitation* 2007;72(1); 100–107.

[20] Berdowski J, Berg RA, Tijssen JG, and Koster RW. Global incidences of out-of-hospital cardiac arrest and survival rates: Systematic review of 67 prospective studies. *Resuscitation* 2010;81(11); 1479–1487.

[21] Bissing JW and Kerber RE. Effect of shaving the chest of hirsute subjects on transthoracic impedance to self-adhesive defibrillation electrode pads. *The American Journal of Cardiology* 2000;86(5); 587–589.

[22] Bossaert L. Fibrillation and defibrillation of the heart. *British Journal of Anaesthesia* 1997;79(2); 203–213.

[23] Boyle AJ, Wilson AM, Connelly K, McGuigan L, Wilson J, and Whitbourn R. Improvement in timing and effectiveness of external cardiac compressions with a new non-invasive device: the CPR-Ezy. *Resuscitation* 2002;54(1); 63–67.

[24] Brody D, Di Maio R, Crawford P, Navarro C, and Anderson J. The impedance cardiogram amplitude as an indicator of cardiopulmonary resuscitation efficacy in a porcine model of cardiac arrest. *Journal of the American College of Cardiology* 2011;14(57); E1134.

[25] Caffrey S. Feasibility of public access to defibrillation. *Current Opinion in Critical Care* 2002;8(3); 195–198.

[26] Caffrey SL, Willoughby PJ, Pepe PE, and Becker LB. Public use of automated external defibrillators. *New England Journal of Medicine* 2002;347(16); 1242–1247.

[27] Cho G. Skin and soft tissue damage caused by use of feedback-sensor during chest compressions. *Resuscitation* 2009;5(80); 600.

[28] Choa M, Park I, Chung HS, Yoo SK, Shim H, and Kim S. The effectiveness of cardiopulmonary resuscitation instruction: animation versus dispatcher through a cellular phone. *Resuscitation* 2008;77(1); 87–94.

[29] Chugh SS, Jui J, Gunson K, et al. Current burden of sudden cardiac death: multiple source surveillance versus retrospective death certificate-based review in a large U.S. community. *Journal of the American College of Cardiology* 2004;44(6); 1268–1275.

[30] Cloete G, Dellimore K, Scheffer C, Smuts M, and Wallis L. The impact of backboard size and orientation on sternum-to-spine compression depth and compression stiffness in a manikin study of CPR using two mattress types. *Resuscitation* 2011;82(8); 1064–1070.

[31] Colwell CB and Soriya G. Basic Life Support. In Vincent JL and Hall JB, editors, Encyclopedia of Intensive Care Medicine. Springer 2012; pages 285–288.

[32] Cromie NA, Allen JD, Navarro C, Turner C, Anderson JM, and Adgey AAJ. Assessment of the impedance cardiogram recorded by an automated external defibrillator during clinical cardiac arrest. *Critical Care Medicine* 2010;38(2); 510–517.

[33] Cromie NA, Allen JD, Turner C, Anderson JM, and Adgey AAJ. The impedance cardiogram recorded through two electrocardiogram/defibrillator pads as a determinant of cardiac arrest during experimental studies. *Critical Care Medicine* 2008;36(5); 1578–1584.

[34] Cummins RO, Chamberlain DA, Abramson NS, et al. Recommended guidelines for uniform reporting of data from out-of-hospital cardiac arrest: the Utstein style. A statement for health professionals from a task force of the American Heart Association, the European Resuscitation Council, the Heart and Stroke Foundation of Canada, and the Australian Resuscitation Council. *Circulation* 1991;84(2); 960.

[35] Cummins RO, Eisenberg MS, Hallstrom AP, and Litwin PE. Survival of out-of-hospital cardiac arrest with early initiation of cardiopulmonary resuscitation. *The American Journal of Emergency Medicine* 1985;3(2); 114–119.

[36] Cummins RO, Ornato JP, Thies WH, Pepe PE, et al. Improving survival from sudden cardiac arrest: the "chain of survival" concept. *Circulation* 1991;83(5); 1832–1847.

[37] Cummins RO and Thies W. Automated external defibrillators and the Advanced Cardiac Life Support Program: a new initiative from the American Heart Association. *The American Journal of Emergency Medicine* 1991;9; 91–93.

[38] Dahl E. Implementation of automated external defibrillators on German merchant ships. *Journal of Travel Medicine* 2011;18(4); 229–230.

[39] de Luna AB, Coumel P, and Leclercq JF. Ambulatory sudden cardiac death: mechanisms of production of fatal arrhythmia on the basis of data from 157 cases. *American Heart Journal* 1989;117(1); 151–159.

[40] Deakin C, McLaren R, Petley G, Clewlow F, and Dalrymple-Hay M. A comparison of transthoracic impedance using standard defibrillation paddles and self-adhesive defibrillation pads. *Resuscitation* 1998;39(1); 43–46.

[41] Di Maio R, Howe A, Crawford P, et al. Measurement of depth, thrust and thoracic impedance during mechanical cardiopulmonary resuscitation: is thoracic impedance a potential indicator of effective external cardiac massage in a porcine model of cardiac arrest? *Circulation* 2011;124(21 Supplement); A196.

[42] Di Maio R, Howe A, McCanny P, et al. Is the impedance cardiogram a potential indicator of effective external cardiac massage in a human

model? A study to establish if there is a linear correlation between the impedance cardiogram and depth in a cardiac arrest setting. *Circulation* 2012;126(21 Supplement); A94.

[43] Di Maio RC, Navarro C, Cromie N, Anderson J, and Adgey A. The impedance cardiogram is an indicator of CPR effectiveness for out-of-hospital cardiac arrest victims. *European Heart Journal, Supplement* 2010;12; F123.

[44] Eberle B, Dick WF, Schneider T, Wisser G, Doetsch S, and Tzanova I. Checking the carotid pulse check: diagnostic accuracy of first responders in patients with and without a pulse. *Resuscitation* 1996; 33(2); 107–116.

[45] Edelson DP, Abella BS, Kramer-Johansen J, et al. Effects of compression depth and pre-shock pauses predict defibrillation failure during cardiac arrest. *Resuscitation* 2006;71(2); 137–145.

[46] Edelson DP, Eilevstjønn J, Weidman EK, Retzer E, Hoek TLV, and Abella BS. Capnography and chest-wall impedance algorithms for ventilation detection during cardiopulmonary resuscitation. *Resuscitation* 2010;81(3); 317–322.

[47] Eftestøl T, Sunde K, and Steen PA. Effects of interrupting precordial compressions on the calculated probability of defibrillation success during out-of-hospital cardiac arrest. *Circulation* 2002;105(19); 2270–2273.

[48] Eisenberg M and White RD. The unacceptable disparity in cardiac arrest survival among American communities. *Annals of Emergency Medicine* 2009;54(2); 258–260.

[49] Elding C, Baskett P, and Hughes A. The study of the effectiveness of chest compressions using the CPR-plus. *Resuscitation* 1998;36(3); 169–173.

[50] Ertl L and Christ F. Significant improvement of the quality of bystander first aid using an expert system with a mobile multimedia device. *Resuscitation* 2007;74(2); 286–295.

[51] Field RA, Soar J, Davies RP, Akhtar N, and Perkins GD. The impact of chest compression rates on quality of chest compressions - A manikin study. *Resuscitation* 2012;83(3); 360–364.

[52] Firoozabadi R, Helfenbein E, and Babaeizadeh S. Accuracy of detecting chest compression rate from the thoracic impedance data recorded through chest pads. *Circulation* 2012;126; A253.

[53] Fitzgibbon E, Berger R, Tsitlik J, and Halperin HR. Determination of the noise source in the electrocardiogram during cardiopulmonary resuscitation. *Critical Care Medicine* 2002;30(4); S148–S153.

[54] Fossan H and Myklebust H. System for measuring and using parameters during chest compression for cardio-pulmonary resuscitation or a simulation thereof 2009. EP Patent 1 057 451.

[55] Fried DA, Leary M, Smith DA, et al. The prevalence of chest compression leaning during in-hospital cardiopulmonary resuscitation. *Resuscitation* 2011;82(8); 1019–1024.

[56] Fukuike S, Otomo Y, et al. Cardiac arrest cases and automated external defibrillator use in railroad stations in Tokyo. *International Journal of Clinical Medicine* 2014;5(20); 1328.

[57] Gallagher EJ, Lombardi G, and Gennis P. Effectiveness of bystander cardiopulmonary resuscitation and survival following out-of-hospital cardiac arrest. *JAMA: the Journal of the American Medical Association* 1995;274(24); 1922–1925.

[58] Garcia L and Kerber R. Transthoracic defibrillation: does electrode adhesive pad position alter transthoracic impedance? *Resuscitation* 1998;37(3); 139–143.

[59] Geddes L, Hoff H, Mello A, and Palmer C. Continuous measurement of ventricular stroke volume by electrical impedance. *Cardiovascular Research Center Bulletin* 1966;4(4); 118–131.

[60] Geddes L and Valentinuzzi M. Temporal changes in electrode impedance while recording the electrocardiogram with dry electrodes. *Annals of Biomedical Engineering* 1973;1(3); 356–367.

[61] González-Otero DM, Ruiz JM, Ruiz de Gauna S, Irusta U, Ayala U, and Alonso E. A new method for feedback on the quality of chest compressions during cardiopulmonary resuscitation. *BioMed research international* 2014;2014. Article ID 865967.

[62] González-Otero DM, Ruiz de Gauna S, Ruiz JM, Ayala U, and Alonso E. Automatic detection of chest compression pauses using the transthoracic impedance signal. In Computing in Cardiology (CinC), 2012. IEEE, pages 21–24.

[63] González-Otero DM, Ruiz de Gauna S, Ruiz JM, Chicote B, and Plaza S. Feasibility of compression depth estimation from the acceleration signal during cardiopulmonary resuscitation in long-distance trains. In Computing in Cardiology (CinC), 2015. IEEE.

[64] González-Otero DM, Ruiz de Gauna S, Ruiz JM, Chicote B, Rivero R, and Russell JK. Accurate feedback of chest compression depth and rate on a manikin in a moving train. In Resuscitation, 2015. European Resuscitation Council.

[65] González-Otero DM, Ruiz de Gauna S, Ruiz JM, et al. Chest compression rate feedback based on transthoracic impedance. *Resuscitation* 2015;93; 82–88.

[66] Goodwin T. In-flight medical emergencies: an overview. *BMJ: British Medical Journal* 2000;321(7272); 1338.

[67] Gruben KG, Guerci A, Halperin H, Popel A, and Tsitlik J. Sternal force-displacement relationship during cardiopulmonary resuscitation. *Journal of Biomechanical Engineering* 1993;115(2); 195–201.

[68] Gruben KG, Romlein J, Halperin HR, and Tsitlik JE. System for mechanical measurements during cardiopulmonary resuscitation in humans. *IEEE Transactions on Biomedical Engineering* 1990;37(2); 204–210.

[69] Gruber J, Stumpf D, Zapletal B, Neuhold S, and Fischer H. Real-time feedback systems in CPR. *Trends in Anaesthesia and Critical Care* 2012; 2(6); 287–294.

[70] Gupta AK. Respiration rate measurement based on impedance pneumography. Technical Report, Texas Instruments Inc. 2011.

[71] Halperin HR. Mechanisms of forward flow during external chest compression. In Paradir NA, Halperin HR, Kern KB, Wenzel V, and Chamberlain D, editors, Cardiac Arrest: science and practice of resuscitation medicine. Cambridge University Press, Cambridge 2007; pages 326–346.

[72] Hamilton L, Beard J, and Kory R. Impedance measurement of tidal volume and ventilation. *Journal of Applied Physiology* 1965;20(3); 565–568.

[73] Handley AJ, Koster R, Monsieurs K, et al. European Resuscitation Council guidelines for resuscitation 2005. Section 2. Adult basic life support and use of automated external defibrillators. *Resuscitation* 2005;67(suppl 1); S7–S23.

[74] Handley AJ, Monsieurs KG, Bossaert LL, and European Resuscitation Council Guidelines. European Resuscitation Council guidelines 2000 for adult basic life support. A statement from the Basic Life Support

and Automated External Defibrillation Working Group and approved by the Executive Committee of the European Resuscitation Council. *Resuscitation* 2001;48(3); 199–205.

[75] Hazinski MF and Field JM. 2010 American Heart Association guidelines for cardiopulmonary resuscitation and emergency cardiovascular care science. *Circulation* 2010;122(Suppl); S639–S946.

[76] Herlitz J, Bång A, Gunnarsson J, et al. Factors associated with survival to hospital discharge among patients hospitalised alive after out of hospital cardiac arrest: change in outcome over 20 years in the community of Göteborg, Sweden. *Heart* 2003;89(1); 25–30.

[77] Hollenberg J, Herlitz J, Lindqvist J, et al. Improved survival after out-of-hospital cardiac arrest is associated with an increase in proportion of emergency crew-witnessed cases and bystander cardiopulmonary resuscitation. *Circulation* 2008;118(4); 389–396.

[78] Howe AJ, Di Maio R, Crawford P, et al. The impedance cardiogram as an indicator of chest compression efficacy during cardiopulmonary resuscitation in a porcine model: correlation with physiological parameters and comparison with compression depth and thrust. *Circulation* 2011;124(21 Supplement); A54.

[79] Hull E, Irie T, Heemstra H, and Wildevuur R. Transthoracic electrical impedance: artifacts associated with electrode movement. *Resuscitation* 1978;6(2); 115–124.

[80] Idris AH, Guffey D, Aufderheide TP, et al. The relationship between chest compression rates and outcomes from cardiac arrest. *Circulation* 2012;125(24); 3004–3012.

[81] Idris AH, Guffey D, Pepe PE, et al. Chest compression rates and survival following out-of-Hospital cardiac arrest. *Critical Care Medicine* 2015;43(4); 840–848.

[82] Iyanaga M, Gray R, Stephens SW, et al. Comparison of methods for the determination of cardiopulmonary resuscitation chest compression fraction. *Resuscitation* 2012;83(5); 568–571.

[83] Jermyn BD. Response interval comparison between urban fire departments and ambulance services. *Prehospital Emergency Care* 1999;3(1); 15–18.

[84] Johnston PW, Imam Z, Dempsey G, Anderson J, and Adgey AA. The transthoracic impedance cardiogram is a potential haemodynamic

sensor for an automated external defibrillator. *European Heart Journal* 1998;19(12); 1879–1888.

[85] Kanz KG, Kay MV, Biberthaler P, et al. Susceptibility of automated external defibrillators to train overhead lines and metro third rails. *Resuscitation* 2004;62(2); 189–198.

[86] Kerber RE, Becker LB, Bourland JD, et al. Automatic external defibrillators for public access defibrillation: recommendations for specifying and reporting arrhythmia analysis algorithm performance, incorporating new waveforms, and enhancing safety. A statement for health professionals from the American Heart Association Task Force on Automatic External Defibrillation, subcommittee on AED Safety and Efficacy. *Circulation* 1997;95(6); 1677–1682.

[87] Kerber RE, Deakin CD, and Tacker Jr WA. Transthoracic defibrillation. In Paradir NA, Halperin HR, Kern KB, Wenzel V, and Chamberlain D, editors, Cardiac Arrest: science and practice of resuscitation medicine. Cambridge University Press, Cambridge 2007;pages 470–481.

[88] Kerber RE, Grayzel J, Hoyt R, Marcus M, and Kennedy J. Transthoracic resistance in human defibrillation. Influence of body weight, chest size, serial shocks, paddle size and paddle contact pressure. *Circulation* 1981;63(3); 676–682.

[89] Kerber RE, Kouba C, Martins J, et al. Advance prediction of transthoracic impedance in human defibrillation and cardioversion: importance of impedance in determining the success of low-energy shocks. *Circulation* 1984;70(2); 303–308.

[90] Kerber RE, Martins J, Kienzle M, et al. Energy, current, and success in defibrillation and cardioversion: clinical studies using an automated impedance-based method of energy adjustment. *Circulation* 1988; 77(5); 1038–1046.

[91] Koster RW, Baubin MA, Bossaert LL, et al. European Resuscitation Council guidelines for Resuscitation 2010. Section 2. Adult basic life support and use of automated external defibrillators. *Resuscitation* 2010;81(10); 1277–1292.

[92] Koster RW, Chamberlain D, and L AD. Automated external defibrillators. In Paradir NA, Halperin HR, Kern KB, Wenzel V, and Chamberlain D, editors, Cardiac Arrest: science and practice of resuscitation medicine. Cambridge University Press, Cambridge 2007; pages 482–495.

[93] Kramer-Johansen J, Edelson DP, Losert H, Köhler K, and Abella BS. Uniform reporting of measured quality of cardiopulmonary resuscitation (CPR). *Resuscitation* 2007;74(3); 406–417.

[94] Kramer-Johansen J, Eilevstjønn J, Olasveengen TM, Tomlinson AE, Dorph E, and Steen PA. Transthoracic impedance changes as a tool to detect malpositioned tracheal tubes. *Resuscitation* 2008;76(1); 11–16.

[95] Kramer-Johansen J, Myklebust H, Wik L, et al. Quality of out-of-hospital cardiopulmonary resuscitation with real time automated feedback: a prospective interventional study. *Resuscitation* 2006;71(3); 283–292.

[96] Kramer-Johansen J, Wik L, and Steen PA. Advanced cardiac life support before and after tracheal intubation - direct measurements of quality. *Resuscitation* 2006;68(1); 61–69.

[97] Krasteva V, Matveev M, Mudrov N, and Prokopova R. Transthoracic impedance study with large self-adhesive electrodes in two conventional positions for defibrillation. *Physiological measurement* 2006;27(10); 1009–1022.

[98] Lababidi Z, Ehmke D, Durnin RE, Leaverton PE, and Lauer RM. The first derivative thoracic impedance cardiogram. *Circulation* 1970;41(4); 651–658.

[99] Larsen MP, Eisenberg MS, Cummins RO, and Hallstrom AP. Predicting survival from out-of-hospital cardiac arrest: a graphic model. *Annals of Emergency Medicine* 1993;22(11); 1652–1658.

[100] Li Y, Ristagno G, Yu T, Bisera J, Weil MH, and Tang W. A comparison of defibrillation efficacy between different impedance compensation techniques in high impedance porcine model. *Resuscitation* 2009; 80(11); 1312–1317.

[101] Losert H, Risdal M, Sterz F, et al. Thoracic impedance changes measured via defibrillator pads can monitor ventilation in critically ill patients and during cardiopulmonary resuscitation. *Critical Care Medicine* 2006;34(9); 2399–2405.

[102] Losert H, Risdal M, Sterz F, et al. Thoracic-impedance changes measured via defibrillator pads can monitor signs of circulation. *Resuscitation* 2007;73(2); 221–228.

[103] Low D, Clark N, Soar J, et al. A randomised control trial to determine if use of the iResus© application on a smart phone improves the

performance of an advanced life support provider in a simulated medical emergency. *Anaesthesia* 2011;66(4); 255–262.

[104] Malmivuo J and Plonsey R. Impedance plethysmography. In Bioelectromagnetism: principles and applications of bioelectric and biomagnetic fields. Oxford university press 1995;pages 405–434.

[105] Meaney PA, Bobrow BJ, Mancini ME, et al. Cardiopulmonary resuscitation quality: improving cardiac resuscitation outcomes both inside and outside the hospital: a consensus statement from the American Heart Association. *Circulation* 2013;128(4); 417–435.

[106] Monsieurs KG, De Regge M, Vansteelandt K, et al. Excessive chest compression rate is associated with insufficient compression depth in prehospital cardiac arrest. *Resuscitation* 2012;83(11); 1319–1323.

[107] Morrison LJ, Nichol G, Rea TD, et al. Rationale, development and implementation of the Resuscitation Outcomes Consortium epistry - Cardiac arrest. *Resuscitation* 2008;78(2); 161–169.

[108] Myerburg RJ and Castellanos A. Emerging paradigms of the epidemiology and demographics of sudden cardiac arrest. *Heart Rhythm* 2006;3(2); 235–239.

[109] Myklebust H and Fossan H. System for measuring and using parameters during chest compression in a life-saving situation or a practice situation, and also application thereof. 2001. US Patent 6 306 107.

[110] Navarro C, Cromie N, Maio RD, and Anderson J. Use of the impedance cardiogram in public access defibrillators as an indicator of cardiopulmonary resuscitation effectiveness. In Computing in Cardiology, 2011. IEEE, pages 601–604.

[111] Neumar RW, Nolan JP, Adrie C, et al. Post-cardiac arrest syndrome: epidemiology, pathophysiology, treatment, and prognostication. A consensus statement from the International Liaison Committee on Resuscitation (American Heart Association, Australian and New Zealand Council on Resuscitation, European Resuscitation Council, Heart and Stroke Foundation of Canada, InterAmerican Heart Foundation, Resuscitation Council of Asia, and the Resuscitation Council of Southern Africa); the American Heart Association Emergency Cardiovascular Care Committee; the Council on Cardiovascular Surgery and Anesthesia; the Council on Cardiopulmonary, Perioperative, and Critical Care; the Council on Clinical Cardiology; and the Stroke Council. *Circulation* 2008;118(23); 2452–2483.

[112] Nichol G and Baker D. The epidemiology of sudden death. In Paradir NA, Halperin HR, Kern KB, Wenzel V, and Chamberlain D, editors, Cardiac Arrest: Science and Practice of Resuscitation Medicine. Cambridge University Press, Cambridge 2007;pages 26–50.

[113] Nichol G, Thomas E, Callaway CW, et al. Regional variation in out-of-hospital cardiac arrest incidence and outcome. *JAMA: the Journal of the American Medical Association* 2008;300(12); 1423–1431.

[114] Niles D, Nysaether J, Sutton R, et al. Leaning is common during in-hospital pediatric CPR, and decreased with automated corrective feedback. *Resuscitation* 2009;80(5); 553–557.

[115] Nishisaki A, Nysaether J, Sutton R, et al. Effect of mattress deflection on CPR quality assessment for older children and adolescents. *Resuscitation* 2009;80(5); 540–545.

[116] Noordergraaf GJ, Drinkwaard BW, van Berkom PF, et al. The quality of chest compressions by trained personnel: the effect of feedback, via the CPREzy, in a randomized controlled trial using a manikin model. *Resuscitation* 2006;69(2); 241–252.

[117] Noordergraaf GJ, Paulussen IW, Venema A, et al. The impact of compliant surfaces on in-hospital chest compressions: effects of common mattresses and a backboard. *Resuscitation* 2009;80(5); 546–552.

[118] Nysaether J and Eilevstjønn J. Method for accurate determining of CPR chest compression depth in real time 2009. EP Patent App. EP20 080 250 519.

[119] Nysaether J and Eilevstjønn J. System and method for increased accuracy in determining CPR chest compression depth in real time 2013. US Patent 8 465 292.

[120] Nysaether JB, Dorph E, Rafoss I, Steen P, et al. Manikins with human-like chest properties - a new tool for chest compression research. *IEEE Transactions on Biomedical Engineering* 2008;55(11); 2643–2650.

[121] Oh J, Song Y, Kang B, et al. The use of dual accelerometers improves measurement of chest compression depth. *Resuscitation* 2012;83(4); 500–504.

[122] Oldenburg M, Baur X, and Schlaich C. Implementation of automated external defibrillators on merchant ships. *Journal of Travel Medicine* 2011;18(4); 233–238.

[123] O'Rourke MF, Donaldson E, and Geddes JS. An airline cardiac arrest program. *Circulation* 1997;96(9); 2849–2853.

[124] Page RL, Hamdan MH, and McKenas DK. Defibrillation aboard a commercial aircraft. *Circulation* 1998;97(15); 1429–1430.

[125] Page RL, Joglar JA, Kowal RC, et al. Use of automated external defibrillators by a US airline. *New England Journal of Medicine* 2000; 343(17); 1210–1216.

[126] Palazzolo J, Berger R, Halperin H, and Sherman D. Method of determining depth of compressions during cardio-pulmonary resuscitation 2004. US Patent 6 827 695.

[127] Palazzolo J, Berger R, Halperin H, and Sherman D. Devices for determining depth of chest compressions during CPR 2006. US Patent 7 118 542.

[128] Paradir NA, Halperin HR, Kern KB, Wenzel V, and Chamberlain D, editors. Cardiac Arrest: science and practice of resuscitation medicine. Cambridge University Press, Cambridge 2007.

[129] Pellis T, Bisera J, Tang W, and Weil MH. Expanding automatic external defibrillators to include automated detection of cardiac, respiratory, and cardiorespiratory arrest. *Critical Care Medicine* 2002;30(4); S176–S178.

[130] Perkins GD, Augré C, Rogers H, Allan M, and Thickett DR. CPREzy™: an evaluation during simulated cardiac arrest on a hospital bed. *Resuscitation* 2005;64(1); 103–108.

[131] Perkins GD, Benny R, Giles S, Gao F, and Tweed MJ. Do different mattresses affect the quality of cardiopulmonary resuscitation? *Intensive Care Medicine* 2003;29(12); 2330–2335.

[132] Perkins GD, Kocierz L, Smith SC, McCulloch RA, and Davies RP. Compression feedback devices over estimate chest compression depth when performed on a bed. *Resuscitation* 2009;80(1); 79–82.

[133] Perkins GD, Smith CM, Augre C, et al. Effects of a backboard, bed height, and operator position on compression depth during simulated resuscitation. *Intensive Care Medicine* 2006;32(10); 1632–1635.

[134] Pozner CN, Almozlino A, Elmer J, Poole S, McNamara D, and Barash D. Cardiopulmonary resuscitation feedback improves the quality of chest compression provided by hospital health care professionals. *The American Journal of Emergency Medicine* 2011;29(6); 618–625.

[135] Risdal M, Aase SO, Kramer-Johansen J, and Eftestol T. Automatic identification of return of spontaneous circulation during cardiopulmonary resuscitation. *IEEE Transactions on Biomedical Engineering* 2008;55(1); 60–68.

[136] Risdal M, Aase SO, Stavland M, and Eftestøl T. Impedance-based ventilation detection during cardiopulmonary resuscitation. *IEEE Transactions on Biomedical Engineering* 2007;54(12); 2237–2245.

[137] Roberts K, Srinivasan V, Niles DE, et al. Does change in thoracic impedance measured via defibrillator electrode pads accurately detect ventilation breaths in children? *Resuscitation* 2010;81(11); 1544–1549.

[138] Ruiz J, Alonso E, Aramendi E, et al. Reliable extraction of the circulation component in the thoracic impedance measured by defibrillation pads. *Resuscitation* 2013;84(10); 1345–1352.

[139] Ruiz JM, González-Otero D, Ruiz de Gauna S, and Russell J. Feasibility of CPR feedback systems in a moving long-distance train. *Resuscitation* 2015;In Preparation.

[140] Ruiz JM, González-Otero DM, Ruiz de Gauna S, et al. Device and method to assist in performing chest compressions during cardiopulmonary resuscitation. 2013. EP Patent 2883496 A1.

[141] Ruiz de Gauna S, González-Otero DM, Ruiz JM, Chicote B, Pelayo S, and Russell JK. Accurate measurement of chest compression depth when CPR is performed on soft surfaces. In Resuscitation, 2015. European Resuscitation Council.

[142] Ruiz de Gauna S, González-Otero DM, Ruiz JM, Chicote B, Ruiz J, and Russell JK. Estimation of the chest compression depth using an accelerometer positioned on the rescuer's back of the hand or forearm. In Resuscitation, 2015. European Resuscitation Council.

[143] Ruiz de Gauna S, González-Otero DM, Ruiz JM, and Russell JK. Feedback on the rate and depth of chest compressions during cardiopulmonary resuscitation using only accelerometers. *PLOS one* 2015;Under Review.

[144] Ruiz de Gauna S, González-Otero DM, Ruiz JM, et al. Is rhythm analysis during chest compression pauses for ventilation feasible? *Resuscitation* 2012;83; e8.

[145] Sasaki M, Iwami T, Kitamura T, et al. Incidence and outcome of out-of-hospital cardiac arrest with public-access defibrillation - A descriptive

epidemiological study in a large urban community. *Circulation Journal* 2011;75(12); 2821–2826.

[146] Shuster M, Kloeck W, Stapleton ER, Christensen UJ, and Braslow A. CPR training. In Paradir NA, Halperin HR, Kern KB, Wenzel V, and Chamberlain D, editors, Cardiac Arrest. Cambridge University Press, second edition edition 2007;pages 1258–1277.

[147] Skorning M, Beckers SK, Brokmann JC, et al. New visual feedback device improves performance of chest compressions by professionals in simulated cardiac arrest. *Resuscitation* 2010;81(1); 53–58.

[148] Stecher FS, Olsen JA, Stickney RE, and Wik L. Transthoracic impedance used to evaluate performance of cardiopulmonary resuscitation during out of hospital cardiac arrest. *Resuscitation* 2008; 79(3); 432–437.

[149] Sunde K, Pytte M, Jacobsen D, et al. Implementation of a standardised treatment protocol for post resuscitation care after out-of-hospital cardiac arrest. *Resuscitation* 2007;73(1); 29–39.

[150] Tang WW and Tong W. Measuring impedance in congestive heart failure: current options and clinical applications. *American Heart Journal* 2009;157(3); 402–411.

[151] Thomas SH, Stone CK, Austin PE, March JA, and Brinkley S. Utilization of a pressure-sensing monitor to improve in-flight chest compressions. *The American Journal of Emergency Medicine* 1995;13(2); 155–157.

[152] Tibballs J and Weeranatna C. The influence of time on the accuracy of healthcare personnel to diagnose paediatric cardiac arrest by pulse palpation. *Resuscitation* 2010;81(6); 671–675.

[153] Tomlinson AE, Nysaether J, Kramer-Johansen J, Steen P, and Dorph E. Compression force-depth relationship during out-of-hospital cardiopulmonary resuscitation. *Resuscitation* 2007;72(3); 364–370.

[154] Tsitlik JE, Weisfeldt ML, Chandra N, Effron MB, Halperin HR, and Levin HR. Elastic properties of the human chest during cardiopulmonary resuscitation. *Critical Care Medicine* 1983;11(9); 685–692.

[155] Tweed M, Tweed C, and Perkins GD. The effect of differing support surfaces on the efficacy of chest compressions using a resuscitation manikin model. *Resuscitation* 2001;51(2); 179–183.

[156] Valenzuela TD, Roe DJ, Cretin S, Spaite DW, and Larsen MP. Estimating effectiveness of cardiac arrest interventions: a logistic regression survival model. *Circulation* 1997;96(10); 3308–3313.

[157] Valenzuela TD, Roe DJ, Nichol G, Clark LL, Spaite DW, and Hardman RG. Outcomes of rapid defibrillation by security officers after cardiac arrest in casinos. *The New England Journal of Medicine* 2000;343(17); 1206–1209.

[158] van Berkom PF, Noordergraaf GJ, Scheffer GJ, and Noordergraaf A. Does use of the CPREzy™ involve more work than CPR without feedback? *Resuscitation* 2008;78(1); 66–70.

[159] Waalewijn RA, de Vos R, Tijssen JG, and Koster RW. Survival models for out-of-hospital cardiopulmonary resuscitation from the perspectives of the bystander, the first responder, and the paramedic. *Resuscitation* 2001;51(2); 113–122.

[160] Waalewijn RA, Nijpels MA, Tijssen JG, and Koster RW. Prevention of deterioration of ventricular fibrillation by basic life support during out-of-hospital cardiac arrest. *Resuscitation* 2002;54(1); 31–36.

[161] Weisfeldt ML. A three phase temporal model for cardiopulmonary resuscitation following cardiac arrest. *Transactions of the American Clinical and Climatological Association* 2004;115; 115–122.

[162] Weisfeldt ML and Becker LB. Resuscitation after cardiac arrest: a 3-phase time-sensitive model. *JAMA: the Journal of the American Medical Association* 2002;288(23); 3035–3038.

[163] Weisfeldt ML, Kerber RE, McGoldrick RP, et al. Public access defibrillation. A statement for healthcare professionals from the American Heart Association Task Force on Automatic External Defibrillation. *Circulation* 1995;92(9); 2763.

[164] Wenzel V. Advanced life support. In Bierens JJLM, editor, Drowning. Springer Berlin Heidelberg 2014;pages 635–639.

[165] White RD, Asplin BR, Bugliosi TF, and Hankins DG. High discharge survival rate after out-of-hospital ventricular fibrillation with rapid defibrillation by police and paramedics. *Annals of Emergency Medicine* 1996;28(5); 480–485.

[166] Wik L, Kramer-Johansen J, Myklebust H, et al. Quality of cardiopulmonary resuscitation during out-of-hospital cardiac arrest. *JAMA: the Journal of the American Medical Association* 2005;293(3); 299–304.

[167] Wissenberg M, Lippert FK, Folke F, et al. Association of national initiatives to improve cardiac arrest management with rates of bystander intervention and patient survival after out-of-hospital cardiac arrest. *JAMA: the Journal of the American Medical Association* 2013;310(13); 1377–1384.

[168] Yannopoulos D, McKnite S, Aufderheide TP, et al. Effects of incomplete chest wall decompression during cardiopulmonary resuscitation on coronary and cerebral perfusion pressures in a porcine model of cardiac arrest. *Resuscitation* 2005;64(3); 363–372.

[169] Yeung J, Meeks R, Edelson D, Gao F, Soar J, and Perkins GD. The use of CPR feedback/prompt devices during training and CPR performance: a systematic review. *Resuscitation* 2009;80(7); 743–751.

[170] Zapletal B, Greif R, Stumpf D, et al. Comparing three CPR feedback devices and standard BLS in a single rescuer scenario: a randomised simulation study. *Resuscitation* 2014;85(4); 560–566.

[171] Zhang H, Yang Z, Huang Z, et al. Transthoracic impedance for the monitoring of quality of manual chest compression during cardiopulmonary resuscitation. *Resuscitation* 2012;83(10); 1281–1286.

RESUMEN DE LA TESIS

Resumen

Introducción, antecedentes y objetivos

La parada cardiorrespiratoria (PCR) se caracteriza por el cese brusco e inesperado de la circulación sanguínea y de la respiración espontánea. Es una de las urgencias médicas más graves, ya que si no se actúa con rapidez conduce a la muerte del paciente en pocos minutos. La incidencia exacta de la PCR extra hospitalaria es desconocida, y las estimaciones varían ampliamente dependiendo de los criterios de inclusión. Sin embargo, datos obtenidos de 37 países europeos indican que se sitúa en valores de alrededor de 38 casos por cada 100 000 habitantes. Estos datos predicen un número de PCRs muy importante, alrededor de 190 000 casos al año solamente en Europa. La tasa de supervivencia a la PCR es muy baja, inferior al 10 % en poblaciones no especialmente protegidas. La importancia de esta urgencia médica hace que en cada país se establezcan consejos nacionales de resucitación, que a su vez se asocian con criterios regionales. Así surge en Europa el European Resuscitation Council (ERC), en Estados Unidos la American Heart Association (AHA) y otros organismos para distintas regiones de los cinco continentes. La misión de estos consejos es proporcionar recomendaciones para todas las intervenciones en el ámbito de la resucitación, desde los aspectos formativos del personal mínimamente entrenado hasta los cuidados más avanzados proporcionados por personal médico especializado. En 1992 nace el International Liasion Committe on Resuscitation (ILCOR), cuya misión es coordinar todos los consejos regionales. Una de las principales acciones de los consejos de resucitación consiste en la edición cada 5 años de unas guías de resucitación que recogen el consenso de la comunidad científica en todos los aspectos relacionados con la PCR.

Para describir las acciones que unen al paciente de una PCR extra hospitalaria con la supervivencia, a principios de los 90 la AHA estableció la metáfora de la cadena de supervivencia.

Esta cadena consta de cuatro eslabones:

- Identificación de la PCR y aviso al sistema de emergencias.
- Reanimación cardiopulmonar (RCP) básica precoz.
- Desfibrilación precoz.
- Soporte vital avanzado precoz y cuidados posteriores a la resucitación.

El eslabón fundamental para este trabajo de tesis es el segundo. La RCP consiste en realizar compresiones torácicas y opcionalmente ventilaciones sobre el paciente. Las compresiones permiten proporcionar un mínimo flujo de sangre oxigenada a los órganos vitales. Se ha demostrado que la RCP permite duplicar o triplicar la supervivencia a una PCR. Las guías de resucitación enfatizan la importancia de la calidad de las compresiones torácicas para que estas sean efectivas. Cuatro factores determinan la calidad de la RCP: una frecuencia de las compresiones de entre 100 y 120 compresiones por minuto (cpm); una profundidad de entre 5 y 6 cpm; minimizar las interrupciones en las compresiones; y permitir la recuperación total del pecho entre compresiones. Existen evidencias claras de que la calidad de las compresiones está ligada con la probabilidad de supervivencia del paciente. Sin embargo, varios estudios demuestran que tanto rescatadores legos como bien entrenados tienen dificultades para proporcionar RCP de calidad. Por este motivo, las guías de resucitación recomiendan el uso de dispositivos que permitan guiar y en su caso corregir al rescatador durante la RCP. Se ha demostrado que estos dispositivos de *feedback* mejoran la calidad de las compresiones torácicas durante la RCP.

La desfibrilación es otro eslabón clave de la cadena, ya que es la única terapia efectiva para revertir una PCR. Consiste en el suministro de una corriente eléctrica al músculo cardiaco para tratar de restaurar un ritmo efectivo en el bombeo de sangre. Existen diversos equipos electromédicos con capacidad de desfibrilación. El personal médico o paramédico especializado habitualmente utiliza monitores-desfibriladores. Estos dispositivos permiten mostrar en pantalla diversas señales biomédicas del paciente como son su electrocardiograma (ECG), impedancia transtorácica (ITT), señal de capnografía (concentración de CO_2 en los gases respiratorios), o señal de pulsioximetría (saturación de oxígeno en sangre). Es el médico el que las interpreta y decide el tratamiento más adecuado en cada caso. En el polo opuesto se sitúa el desfibrilador externo automático (DEA). Dado que el tiempo hasta que se produce la desfibrilación es clave para la supervivencia ante una PCR, en 1995 la AHA estableció el concepto de desfibrilación de acceso público. Con ello se recomienda que la desfibrilación se haga accesible al público general a través del DEA. Este equipo puede ser utilizado por personal mínimamente

entrenado, ya que guía al paciente durante la resucitación y analiza el ritmo cardiaco del paciente de forma automática. Cuando detecta un ritmo desfibrilable, propone al rescatador el suministro de la descarga eléctrica. En la actualidad los programas de desfibrilación de acceso público se han extendido a multitud de ubicaciones, como aeropuertos, estaciones de tren o metro, centros deportivos o centros escolares. Con respecto a medios de transporte, desde hace años se han desplegado AEDs en aviones y barcos, y más recientemente se están instalando en trenes de larga distancia.

Los desfibriladores miden la ITT a través de los parches de desfibrilación. La ITT representa la resistencia del tórax al paso de corriente. Esta señal presenta un valor base de alrededor del centenar de ohmios, aunque puede variar significativamente entre individuos. Además, tanto las ventilaciones como las compresiones torácicas inducen variaciones en la señal. Las ventilaciones o respiraciones inducen fluctuaciones con amplitudes entre 0.2 y 3 Ω. Las compresiones torácicas, por otro lado, generan interferencias con amplitudes entre 0.15 y varios ohmios. Esta señal ha sido utilizada en los últimos años de forma *offline* para analizar la calidad de la RCP en programas de mejora de los servicios de emergencias. Así, la aplicación Codestat data review software (PhysioControl) incorpora un detector de compresiones torácicas basado fundamentalmente en el análisis de la señal ITT. A partir de la detección de las compresiones, este programa permite calcular métricas de calidad como son su frecuencia media o la fracción del tiempo durante el que se han realizado compresiones. Diversos trabajos han estudiado la relación entre la profundidad de las compresiones y la amplitud de las interferencias que generan sobre la ITT, con resultados contradictorios. Además, en el año 2012 se publicó un estudio experimental con cerdos, en el que de forma manual se proporcionaban compresiones torácicas óptimas (50 mm de profundidad) o sub-óptimas (35 mm) a los animales. El análisis de los datos proporcionó buenos índices de correlación entre la profundidad de las compresiones y la amplitud de las interferencias generadas. Parecía que la amplitud de las interferencias en la señal de ITT podía ser una buena medida indirecta de la profundidad de las compresiones.

En definitiva, al comenzar este trabajo de tesis no se había explorado la posibilidad de utilizar la señal de ITT para proporcionar *feedback* en tiempo real sobre la frecuencia de las compresiones, y existían expectativas positivas de que la amplitud de las fluctuaciones sobre la señal de ITT proporcionara información útil sobre la profundidad de las compresiones.

Desde hace 10 años se han desarrollado sistemas comerciales de *feedback* sobre la frecuencia y profundidad de las compresiones torácicas basados en la señal de aceleración. Se puede calcular el desplazamiento como la segunda integral de la aceleración. Aunque existen diversos métodos para obtener la integral de una señal trabajando en el dominio discreto, el más

utilizado es la regla del trapecio. Esta regla puede implementarse mediante un filtro lineal que, aplicado a la señal de aceleración, proporciona la señal de velocidad. Aplicando de nuevo el filtro a la señal de velocidad, se obtiene la señal de desplazamiento o, en nuestro caso, la señal de profundidad de la compresión. El problema es que este sistema es inestable. Pequeñas componentes continuas en la señal de aceleración hacen que al integrar se vaya acumulando un valor creciente que se superpone a la verdadera velocidad. Para evitar la acumulación de errores se puede integrar la señal de aceleración compresión a compresión, estableciendo condiciones de contorno al principio de cada compresión. La solución que se suele aplicar consiste en utilizar señales auxiliares, como pueden ser la señal de fuerza o presión o la propia señal de ITT o el ECG, que permitan delimitar cada ciclo de compresión. Estas soluciones están protegidas industrialmente mediante patentes. Como resultado, hoy en día los sistemas de *feedback* comerciales basados en la aceleración están en manos fundamentalmente de dos multinacionales del sector (Zoll y Philips). Hace pocos años otra multinacional del sector, PhysioControl, presentó un nuevo sistema de *feedback* basado en la generación de campos magnéticos tridimensionales.

En este contexto el principal objetivo de este trabajo de tesis consistía en el estudio de nuevas estrategias para obtener sistemas de *feedback* sobre la calidad de las compresiones torácicas durante la RCP a partir de la señal de ITT y de la señal de aceleración. Este objetivo general puede estructurarse en tres objetivos intermedios:

- Análisis de la capacidad de la señal de ITT para proporcionar en tiempo real *feedback* sobre la frecuencia y profundidad de las compresiones torácicas en humanos.
- Estimación de la profundidad y frecuencia de las compresiones torácicas trabajando exclusivamente con la señal de aceleración, sin usar ninguna señal de referencia.
- Estudio del comportamiento de un sistema de feedback basado exclusivamente en la aceleración cuando se utiliza en condiciones desfavorables, como puede ser que el paciente se encuentre sobre un colchón, que el dispositivo no se sitúe directamente sobre el pecho del paciente o que este se encuentre en un tren en movimiento.

Calidad de las compresiones torácicas a partir de la señal de ITT

El objetivo de este estudio era analizar la capacidad de la señal de ITT para proporcionar *feedback* en tiempo real sobre la frecuencia y profundidad de las compresiones torácicas. Se realizó en dos partes. En la primera se estudió la relación entre la profundidad de las compresiones y diversas

características morfológicas de las fluctuaciones que las compresiones inducen en la señal de ITT. En la segunda se diseñó un nuevo método para obtener en tiempo real la frecuencia de las compresiones a partir de la señal de ITT.

El primer trabajo se desarrolló conjuntamente con el autor de otra tesis doctoral realizada en nuestro grupo de investigación y presentada hace un año. Se realizó un estudio retrospectivo utilizando episodios reales de resucitación de la base de registros Tualatin Valley Fire & Rescue (TVF&R). Esta base incorpora la señal de profundidad obtenida mediante el dispositivo Q-CPR meter de Philips, basado en la señal de aceleración y en la señal de fuerza. Se estudiaron 60 registros completos con más de 100 000 compresiones torácicas. Las fluctuaciones inducidas por las compresiones en la TTI fueron caracterizadas mediante tres características morfológicas. Para cada compresión se calcularon las tres características de la fluctuación en la señal de ITT y la verdadera profundidad sobre la señal de profundidad, y se estudió la relación lineal entre las características y la profundidad. De los resultados de este estudio se concluye que la señal de ITT no aporta información útil sobre la profundidad de las compresiones. La correlación entre la verdadera profundidad y las características morfológicas de la señal de ITT es muy baja. Cuando se analizan bloques de compresiones de un único rescatador sobre un único paciente pueden obtenerse correlaciones elevadas, pero cuando se contemplan todos los pacientes y rescatadores la correlación disminuye de forma drástica. También se analizó la capacidad de las características morfológicas para identificar compresiones de profundidad baja, y la conclusión es que su capacidad predictiva es muy baja, e imposible de aprovechar en la práctica.

El segundo trabajo se realizó utilizando registros de resucitación extraídos de tres bases de datos de paradas cardiorrespiratorias en humanos: la base SISTER, la base TVF&R y la base Oslo EMS. Se seleccionaron 60 episodios completos de cada base. La idea era diseñar un método para estimar en tiempo real la frecuencia de las compresiones procesando la señal de ITT. Se pretendía que el método fuera independiente de los diversos factores que pueden afectar a la forma de onda de las fluctuaciones inducidas por las compresiones en la señal de ITT, como pueden ser el paciente, el tipo de parches de desfibrilación, el rescatador, el equipo con el que se adquiere la señal de ITT y características de esta señal como la frecuencia de muestreo y la resolución. Se diseñó un nuevo método que estimaba la frecuencia de las compresiones mediante el análisis de la señal de ITT en el dominio de la frecuencia. Los resultados globales para las tres bases de registros presentaron una capacidad para detectar intervalos con compresiones, o sensibilidad media, del 96 %, una capacidad para no detectar compresiones cuando realmente no las hay, o valor predictivo positivo medio, del 97 %

y un factor de precisión medio del 6 %. Dados los buenos resultados, se concluyó que el método era susceptible de ser aplicado en situaciones reales.

Calidad de las compresiones torácicas a partir de la señal de aceleración

El objetivo de este estudio consistía en diseñar tres nuevos métodos para calcular la profundidad y la frecuencia de las compresiones a partir exclusivamente de la señal de aceleración.

Para caracterizar la precisión de cada método se usaron registros obtenidos de un entorno de RCP simulado basado en un maniquí de resucitación, Resusci Anne (Laerdal Medical). El maniquí se dotó de un sensor de desplazamiento fotoeléctrico, colocado en el interior del pecho, para obtener la señal de profundidad de la compresión. Además, se utilizó un acelerómetro triaxial colocado sobre el pecho del maniquí para registrar la aceleración. Las señales de profundidad y aceleración fueron digitalizadas mediante una tarjeta de adquisición y un ordenador portátil. En las sesiones de grabación de registros de RCP participaron 28 voluntarios agrupados por parejas. Cada pareja realizó 4 registros de 10 minutos de duración, proporcionando compresiones con una frecuencia de 80, 100, 120 y 140 cpm guiada por un metrónomo. La profundidad objetivo fue de 50 mm en todos los registros. Como guía para la profundidad, en el ordenador se mostraba gráficamente en tiempo real la señal de referencia de la profundidad obtenida del dispositivo fotoeléctrico. Se obtuvieron un total de 48 registros de 10 minutos, a los que se aplicaron los tres métodos de estimación de profundidad y frecuencia.

El primer método se basa en la obtención de la señal de profundidad a través del filtrado lineal de la señal de aceleración. El sistema lineal que implementa la regla del trapecio tiene una característica paso bajo con ganancia infinita para la componente continua. Para compensar la inestabilidad del sistema, este se ha combinado con un filtro paso alto. De este modo se obtiene un sistema paso banda estable, cuya característica frecuencial coincide con la de la regla del trapecio en la banda de frecuencias de interés. Sin embargo, este método introduce una cierta distorsión de la señal, y en el 25 % de los casos el error sin signo de la profundidad fue superior a los 5.4 mm. Este método no es lo suficientemente preciso como para ser implementado en la práctica.

El segundo método consiste en calcular la señal de velocidad aplicando el filtro paso banda anteriormente descrito a la señal de aceleración. A continuación, se detectan los pasos por cero de la señal de velocidad para delimitar cada ciclo de compresión. La profundidad de cada compresión se obtiene integrando la velocidad desde el inicio de la compresión (paso

por cero de positivo a negativo) hasta el instante de profundidad máxima (paso por cero de negativo a positivo). En este caso, para el 25 % de las compresiones el error sin signo de la profundidad fue superior a 6 mm. Por tanto, los errores cometidos por el segundo método son también demasiado elevados, y no se recomienda su implementación práctica.

El tercer método sigue una estrategia totalmente distinta a la de los dos primeros. En este caso se calculan la profundidad y frecuencia media de las compresiones cada 2 segundos a partir del análisis espectral de la señal de aceleración (AEA). El método se basa en el hecho de que, durante las compresiones, para intervalos cortos de tiempo (2 segundos), las señales de aceleración y profundidad tienen una característica marcadamente periódica. A partir del análisis espectral de intervalos de 2 s de la señal de aceleración se obtienen el módulo y la fase de sus tres primeros armónicos. A continuación, se utilizan estos valores para calcular el módulo y la fase de los tres primeros armónicos de la señal de profundidad. Con estos datos, utilizando la expresión de la descomposición en serie de Fourier, se reconstruye un ciclo de la señal, y se calcula la profundidad de la compresión. El percentil 75 del error sin signo para la estimación de la profundidad y de la frecuencia con este método fue de 2.3 mm y 1.6 cpm, respectivamente. La precisión de este método es considerablemente superior a la de los dos métodos basados en el dominio del tiempo. Además el método AEA es muy novedoso, no incumple ninguna patente de su ámbito y por tanto es susceptible de ser implementado en la práctica y de ser protegido industrialmente.

Retos de los sistemas de feedback basados en la aceleración

En este apartado se recogen tres estudios realizados para analizar la posibilidad de utilizar el algoritmo AEA en situaciones en las que los sistemas de *feedback* basados en la aceleración presentan dificultades de uso.

El primer estudio hace referencia a la utilización del sistema de *feedback* en un paciente que reposa sobre una superficie blanda, como podría ser un colchón. En este caso, la aceleración aplicada sobre el pecho del paciente provoca la compresión del pecho, pero también la del colchón. La profundidad calculada aplicando el algoritmo AEA a la aceleración sería la suma de ambas compresiones. La solución aportada consiste en colocar dos acelerómetros, uno sobre el pecho del paciente y otro entre su espalda y el colchón. La profundidad del pecho se calcularía como la resta de la profundidad obtenida a partir de la aceleración del pecho y la obtenida de la aceleración en la espalda. La precisión de cálculo se ha evaluado utilizando registros de RCP simulada obtenidos de un maniquí de resucitación. El sistema experimental utilizado es muy similar al descrito en la sección

anterior, pero en este caso se ha situado otro acelerómetro bajo la espalda del maniquí, se ha sustituido el sensor de desplazamiento fotoeléctrico por otro resistivo, más fácil de calibrar, y se ha situado el maniquí sobre un colchón. Se han adquirido registros utilizando dos tipos de colchón, de espuma y de muelles, con y sin situar una tabla bajo la espalda del maniquí para reducir la compresión del colchón. El error sin signo en el cálculo de la profundidad presentó en todos los casos un percentil 75 menor de 4 mm. Además, los límites de confianza del 95 % para los errores en frecuencia fueron siempre menores de 3.5 cpm. Por tanto, se concluyó que el método AEA es lo suficientemente preciso para se utilizado para el cálculo de la frecuencia y profundidad de las compresiones sobre una superficie blanda. Esta solución se podría implementar en la práctica utilizando dos dispositivos con comunicación inalámbrica y un smartphone. Se colocaría un dispositivo sobre el pecho y otro bajo la espalda del paciente. Cada dispositivo calcularía la profundidad y la frecuencia cada 2 s aplicando el método AEA, y transmitiría estos valores al *smartphone*. El *smartphone* se encargaría de calcular la profundidad real de las compresiones torácicas restando los dos valores de profundidad y de proporcionar *feedback* al rescatador.

El segundo estudio se centra en la posibilidad de utilizar el algoritmo AEA en un dispositivo que no se coloque entre la palma del rescatador y el pecho del paciente. Los dispositivos comerciales pueden provocar incomodidad e incluso daño tanto en el paciente como en el rescatador. Por este motivo se ha estudiado la posibilidad de colocar el dispositivo en el dorso de la mano, en la muñeca o en el antebrazo del rescatador. El estudio se realizó con registros experimentales obtenidos sobre el maniquí de resucitación. Los resultados obtenidos revelan que puede utilizarse sobre el dorso de la mano, siempre y cuando el rescatador no separe las manos del pecho del paciente durante las compresiones. Sin embargo, los errores cometidos cuando el dispositivo se sitúa en la muñeca o en el antebrazo son excesivamente elevados. Esto se debe a que en estas posiciones, el dispositivo está sujeto a movimientos que no se traducen en la compresión del pecho, como pueden ser balanceos o movimientos laterales. Por este motivo, la profundidad calculada a partir de las aceleraciones en estas posiciones sobrestima de forma importante la verdadera profundidad de compresión del pecho.

El tercer estudio analiza la posibilidad de utilizar el algoritmo AEA en un tren de larga distancia en movimiento. El uso de sistemas de *feedback* basados en aceleración está desaconsejado en vehículos en movimiento; en esta situación el dispositivo registraría la aceleración debida al movimiento del vehículo junto con la del pecho durante las compresiones, lo que podría dar lugar a errores importantes en el cálculo de la profundidad. Sin embargo, debido al creciente despliegue de programas de desfibrilación

de acceso público en trenes de larga distancia, se ha decidido estudiar la precisión del algoritmo AEA en este escenario. Se ha aprovechado para analizar también el comportamiento de dos dispositivos comerciales: el dispositivo basado en la aceleración CPRmeter (Laerdal Medical) y el basado en un campo magnético triaxial TrueCPR (PhysioControl). El sistema experimental utilizado es similar al de los trabajos anteriores, pero en este caso se ha utilizado el maniquí de resucitación en el tren de larga distancia Bilbao-Zaragoza-Bilbao. Se ha seleccionado este trayecto porque presenta intervalos con diferentes velocidades medias y diversas características de trazado. El dispositivo CPRmeter proporcionó *feedback* al rescatador en todas las pruebas. Tanto el algoritmo AEA como el dispositivo CPRmeter fueron precisos en el cálculo de la frecuencia y la profundidad de las compresiones, aunque los errores cometidos fueron superiores a los que presentaban en condiciones de laboratorio. Por tanto, ambos métodos pueden usarse para proporcionar *feedback* al rescatador de forma fiable en las condiciones ensayadas. El dispositivo TrueCPR no fue capaz de proporcionar *feedback* al rescatador durante ninguna de las pruebas; mostraba alertas indicando que el dispositivo no estaba bien colocado o que sufría interfencias electromagnéticas. Sin embargo, sí almacenó información sobre la profundidad y la frecuencia de las compresiones, que habían sido calculadas con gran precisión. Por tanto, si se realizaran cambios en la interfaz de usuario, el dispositivo también podría usarse en este escenario.

Conclusiones

En este trabajo de tesis se ha estudiado de forma detallada la posibilidad de obtener *feedback* en tiempo real sobre la profundidad y frecuencia de las compresiones torácicas durante la RCP a partir de la señal de ITT y a partir de la señal de aceleración. Con respecto a la señal de ITT se ha demostrado que no permite obtener información útil sobre la profundidad, pero se ha desarrollado un método novedoso para obtener de forma fiable *feedback* en tiempo real de la frecuencia de las compresiones. Este método ha sido implementado en los equipos de la empresa Bexen cardio, única empresa de nuestro país que diseña, fabrica y comercializa equipos de desfibrilación. Con respecto a la aceleración, se ha diseñado un nuevo algoritmo que estima la frecuencia y profundidad de las compresiones. Por su novedad, ha sido objeto de una patente europea que explota la empresa Bexen cardio. En la actualidad la empresa dispone ya de un dispositivo que puede ser utilizado conectado a sus equipos de desfibrilación. En un futuro próximo lo implementará como un dispositivo independiente.

A nivel científico, los trabajos realizados durante el desarrollo de esta tesis doctoral han dado lugar a cinco publicaciones en revistas internacionales indexadas y siete comunicaciones en conferencias internacionales.